9G51-F

OBSERVATION OF SEA SURFACE TEMPERATURE PATTERNS AND THEIR SYNOPTIC CHANGES THROUGH OPTIMAL PROCESSING OF NIMBUS II DATA

James R. Greaves
James H. Willand
David T. Chang

FINAL REPORT
CONTRACT NO. NASW-1651
September 1968

ALLIED RESEARCH ASSOCIATES, INC.
Virginia Road, Concord, Massachusetts 01742

Prepared For

HEADQUARTERS
NATIONAL AERONAUTICS AND SPACE ADMINISTRATION
OFFICE OF NATURAL RESOURCES PROGRAMS
WASHINGTON, D.C. 20546

9G51-F

OBSERVATION OF SEA SURFACE TEMPERATURE PATTERNS AND THEIR SYNOPTIC CHANGES THROUGH OPTIMAL PROCESSING OF NIMBUS II DATA

James R. Greaves
James H. Willand
David T. Chang

FINAL REPORT
CONTRACT NO. NASW - 1651
September 1968

ALLIED RESEARCH ASSOCIATES, INC.
Virginia Road, Concord, Massachusetts 01742

Prepared For

HEADQUARTERS
NATIONAL AERONAUTICS AND SPACE ADMINISTRATION
OFFICE OF NATURAL RESOURCES PROGRAMS
WASHINGTON, D.C. 20546

FOREWORD

This report, by the Geophysics and Aerospace Division of Allied Research Associates, Inc., Concord, Massachusetts, presents the results of a study of optimal processing of Nimbus II data for the observation of sea surface temperature patterns and their synoptic changes. These studies were performed for the Earth Resources Survey Program of the National Aeronautics and Space Administration under Contract NASW-1651. The Spacecraft Oceanography Project of the U.S. Naval Oceanographic Office was requested by NASA to act as monitor for this contract.

A separate publication, Bibliography on the Use of Satellites for Oceanographic Observations, was published in April of 1968 under this same contract.

Section 4 of this report was prepared by Mr. Willand, who was primarily responsible for the programming efforts during this study. Mr. Chang conducted the studies of manned observations from spacecraft, which are presented in Section 8.

The authors wish to acknowledge the assistance of Mr. William Bandeen of the NASA, Goddard Space Flight Center in obtaining the basic Nimbus data reduction programs. We also wish to acknowledge the kind assistance and cooperation of Mr. Joe Johns of the National Space Science Data Center in the development and operation of the modified programs. Mr. Larry McMillan of Allied Research Associates, Inc. is primarily responsible for the development of the Digital Color Printer used extensively in this study.

ABSTRACT

This report presents the results of a study of the optimal processing of satellite data for the observation of sea surface temperature patterns and their synoptic changes. Nimbus II data are used extensively. A two-phase approach is taken, using multi-spectral low resolution data for the development of data processing techniques, and single spectral region high resolution data for the actual observation of sea surface temperature patterns. Particular emphasis is placed on the Gulf Stream region. Individual topics discussed in this report include the following:

1. Modifications of the Nimbus data reduction programs to permit immediate mapping of only clear-sky data.
2. Development of techniques for day and nighttime automated cloud discrimination.
3. Preparation of recommendations on optimum data processing and analysis methods for routine operational measurement of sea surface temperature patterns on a near real-time basis.
4. Feasibility and parametric design studies with regard to sea surface temperature observations from manned satellites.
5. Development of a time history of Gulf Stream meander movement.

It was determined that for the optimal detection of cloud contamination in daytime cases (including high thin cirrus), a combination of visible and water vapor absorption radiation data should be used. For the Nimbus data, a 15% albedo threshold and a 237°K temperature threshold (in the water vapor absorption band) were established. Further refinement of threshold levels and cloud radiation characteristics can and should be accomplished using observations from manned spacecraft. For nighttime data, only the water vapor absorption data is available for cloud discrimination, although temperature limits may be placed on the IR data themselves. Computer programs were written to automatically apply these threshold criteria, and to map single or multiple pass clear sky data. An application of Monte Carlo statistical programs utilizing a world-wide cloud data bank revealed that observation of rapidly changing transient oceanographic phenomena may not be feasible under certain climatic conditions. Graphs are presented for the Gulf Stream area relating area coverage and the probability of obtaining that coverage as a function of the number of passes.

Gulf Stream menader movements for the month of October 1966 as determined from the Nimbus II HRIR (High Resolution Infrared) data were somewhat slower than anticipated, but are believed to be accurate. Near-shore meanders seemed to move at a rate of about 8 n. mi. per day while those larger meanders toward the northeast moved more slowly at about 4 to 5 n. mi. per day.

Because it is beyond the present state-of-the-art to automatically include atmospheric attenuation effects on any large scale basis, it is recommended that only the temperature gradient information be used in conjunction with conventional shipboard measurements. For rapid interpretation of resultant sea surface temperature maps in research applications, automatically generated color coded analyses are recommended.

TABLE OF CONTENTS

TABLE OF CONTENTS (cont)

TABLE OF CONTENTS (cont)

LIST OF FIGURES

LIST OF TABLES

1. INTRODUCTION

1.1 The Importance of Sea Surface Temperature Data

The temperature of the ocean's surface is the one oceanographic parameter most readily measured from a space platform. As such, its measurement will be a primary goal in the first flights of any program of Earth Resources Survey from space (Newell, 1968). This emphasis on sea surface temperature is well placed in that nearly all of man's sea-oriented activities, including fisheries, civil applications, and the military rely to some extent upon knowledge of the sea surface temperature patterns and their variation with time.

Fisheries

Correlations between water temperature and the behavior and occurrence of fish have been found (Hela, 1962). Particularly important is the location and estimation of intensity of upwelling which brings cold nutrient-rich bottom water to the ocean's surface. Important fishing grounds for pelagic fish are often found at the confluence or divergence of oceanic currents. From the surface temperatures, the pelagic fish population and their migrations may also be inferred. Fisheries already use analyses and forecasts of surface temperature for the prediction of spawning times, their location, and for estimation of the survival rate of the larvae (Wolff, 1965).

Civil Applications

In recent years the problem of sea-air interaction has gained increasing attention because of its importance in the better understanding of both the oceanic and the atmospheric circulations and their relation to weather prediction. The long-term prediction aspect of sea surface temperature has been emphasized by Namias, (1963) and others. The synoptic analyses and forecasts of sea surface temperature are finding greater use in synoptic meteorology through inclusion of heat exchange effects in forecasting models. Furthermore, sea surface temperature is required in the estimation of changes of surface air properties over the ocean, in wave forecasting for shipping, and in prediction of visibility, fog probability, and icing conditions. Various investigators (Fisher, 1958) have demonstrated direct correlations between the sea surface temperature and such meteorological phenomena as the growth and travel of hurricanes, and extratropical cyclonic development.

Military

In publishing the results of its 1965 meetings, the Panel on Oceanography of the President's Science Advisory Committee made the following statement; "The importance to Anti-Submarine Warfare of a continuing, effective program to study and characterize the ocean environment in which its equipment is designed to operate cannot be overstated." (Panel on Oceanography, 1966). One such property of the ocean environment is the sea surface temperature. It is used as an input to mathematical models for the prediction of the subsurface temperature structure, which in turn greatly affects the propagation of sound.

1.2 Benefits of Satellite Systems

The obvious advantage of satellite monitoring of surface temperatures is the vastly increased coverage available, both in space and in time. For fisheries this could mean the discovery of new fishing areas, and the ability to proceed directly to a fishing area, thereby eliminating many hours of fruitless searching. Assuming that space oceanography will be able to provide the data essential to the world-wide regulation of fisheries, it has been estimated that the potential economic benefits to the United States by 1975 would be $75 to $215 million (General Electric, 1967). As might be expected, the economic benefits which could result from improved long-range forecasting of marine weather systems are enormous. Apart from such sea-related activities as shipping, or the prediction of fog and icing conditions, the National Academy of Sciences has estimated that the potential benefits to farming, construction, recreation, etc. would exceed $2 billion (N.A.S., 1965). For the military, the real-time aspects of satellite measurement programs would be the most important. A satellite carrying infrared sensors in a sun synchronous orbit would provide twice-daily global coverage of the world's oceans. To accumulate a sufficient data base to generate meaningful sea surface temperature (SST) analyses, the Fleet Numerical Weather Facility (FNWF) in Monterey, California currently must average 3-1/2 days of conventional surface ship data (Wolff, 1965a). The melding of these surface ship data with satellite temperature measurements would represent a significant step toward the real-time mapping of sea surface temperature patterns on a global scale.

1.3 Philosophy of Present Study

The optimal sea surface temperature measurement platform would be a near-polar orbiting sun synchronous satellite with a cross track scanning high resolution (better than 6 mi.) multi-spectral radiometer. Recommended spectral regions include a clean atmospheric window, a visible albedo channel, and a clean water vapor absorption band. The presence of the visible and water vapor bands would make possible the immediate flagging of cloud contaminated temperature data for day and nighttime passes (see Section 5). For the present study, which involved both the development of optimal data processing techniques and oceanographic studies per se, no such system was available. The most applicable data were those obtained by the Nimbus II radiometers.

The Nimbus II single channel High Resolution Infrared Radiometer (HRIR) operated in the 3.5 to 4.1μm window region. The spatial resolution is approximately 5 n.mi. at the subpoint. Because of contamination by reflected solar radiation, these data are generally usable only at night. The HRIR data have the spatial resolution required for meaningful surface temperature analyses, but because of the single spectral region, they provide no means for the automatic discrimination of cloud contamination.

The five channel Medium Resolution Infrared Radiometer (MRIR) operated in the following spectral regions:

Channel 1	6.4 to 6.9μm	water vapor absorption
Channel 2	10 to 11μm	atmospheric window
Channel 3	14 to 16μm	CO_2 absorption
Channel 4	5 to 30μm	long wavelength infrared
Channel 5	.2 to 4.0μm	visible.

The spatial resolution of all MRIR channels is approximately 30 n.mi. at the subpoint. The MRIR data are thus of such low resolution that they preclude observation of detailed surface patterns. They do, however, permit the development and application of cloud discrimination techniques. As a result, the two broad areas of data processing and data applications had to be treated separately.

In developing data processing techniques, the MRIR data were used. Day and nighttime cloud discrimination as well as composite mapping programs were developed for the Nimbus data, although little oceanographic interpretation was made of the resultant analyses. The HRIR data were used to develop a time history

of the Gulf Stream for the month of October, 1966. In the development of these cases, the experience of the researcher in distinguishing cloud forms in the HRIR analog data had to be relied upon to indicate cloud contamination. This can certainly not be considered an optimal data processing technique. The details and the results of these and other aspects of the present study are given in Sections 3 through 8. The following section presents a brief review of the results of previous investigations.

2. PREVIOUS STUDIES

The work which had been done prior to the current study may be divided into two phases. Phase I was largely the experimental stage, looking into the feasibility of using satellite data for sea surface temperature measurement, and uncovering some of the problems which would have to be solved (Greaves, 1965). During Phase II, data processing techniques were developed to cope with some of these problems, and recommendations and suggestions were made for gathering and processing large amounts of data from future satellite systems (Greaves, 1967).

2.1 Phase I

Using data from the TIROS VII satellite, the results of our initial studies confirmed that satellite infrared data could provide accurate measurements of sea surface temperature gradients. In the absence of surface ship conventional measurements to serve as ground truth data, good absolute temperature values were generally unattainable. This was due largely to uncertainties in atmospheric attenuation and in the calibration and degradation of the TIROS radiometers.

A critical problem which was uncovered is the detection and elimination of data points where clouds prevent an uncontaminated view of the sea surface. It was found that the usual sources of cloud cover information such as conventional meteorological observations and satellite TV data, were insufficient for determining all of the clear areas useful for satellite temperature measurements. Hand analysis indicated that by using the radiometric data themselves, particularly the Channel 5 sensor in the visible portion of the spectrum (0.55-0.75μm), clear areas could be detected in the daytime data on a point by point basis. Due to the relatively low resolution of the TIROS radiometer (approximately 30 n.mi. at the subpoint), regions of scattered cloud still presented difficulties, as the data represent averages over the entire scan spot.

For the nighttime data, it was determined that the TIROS radiometers were not sufficiently capable of accurately locating cloud-free areas. The primary cause of the failure in this case seems to have been the relatively high noise level in the basic data. Using daytime data, apparent cloud contaminated areas were determined using various nighttime cloud discrimination techniques. These areas were then compared with those indicated by the visible channel data. In general, little dependable correlation could be found.

At the close of Phase I, it seemed evident that for effective further use of the TIROS radiation data, modifications of the existing data reduction computer programs would be required. These modifications were subsequently carried out during the Phase II studies.

2.2 Phase II

During the Phase II studies two basic modifications were made to the existing TIROS VII data reduction programs. One change permitted the automatic listing (and ultimate mapping) of only the cloud free daytime data. The clear-cloudy decision for each data point was made on the basis of the corresponding visible channel data. Before thresholds could be established, it was first necessary to convert the visible channel data to the albedo format to eliminate the dependence on solar zenith angle. The second basic modification enabled the researcher to composite the clear sky data from more than one Final Meteorological Radiation Tape (FMRT) onto a single tape for subsequent mapping. The intended goal in this case was to experiment with the composite mapping program to seek optimal data averaging and processing techniques.

The first of the two programs outlined above was used successfully, although the time consuming task of analyzing the resultant temperature maps remained. In addition, the inability to distinguish cloud contamination in the TIROS nighttime data meant the effective loss of 50 percent of the recorded data. While the second program was successful operationally, there was little occasion to use it due to the poor orbital and scanning geometry characteristics of TIROS VII. Daytime passes over a given area on consecutive days where the scanning mode was usable, and the nadir angles sufficiently small, were extremely rare. Moreover, due to the variable nature of the sea surface temperature patterns, compositing data from passes which are widely separated in time can produce only gross scale average patterns.

Because of these limitations of the TIROS system, it was recommended at that time that future work be done using data from an earth oriented, sun synchronous satellite system such as Nimbus II. The remaining sections of this report describe at length the development of data processing techniques for the Nimbus II radiation data, and provide some examples of the use of these data.

3. THE BIBLIOGRAPHY

The Statement of Work of the current contract called for the development of a comprehensive bibliography on the general subject of remote sensing of oceanographic parameters, with particular emphasis on satellite measurements of sea surface temperatures. This bibliography entitled, Bibliography on the Use of Satellites for Oceanographic Observations was published in annotated form under separate cover in April 1968 (Widger, 1968).

The bibliography provides all identifiable, significant citations pertinent to the use of satellites specifically for oceanographic observations, with some emphasis on observations of sea surface temperature. Because many discussions of remote sensing of oceanographic parameters from other observing platforms, particularly aircraft, have direct pertinence to potential satellite observing techniques, many of the entries fall into this category. This is especially true in the case of infrared observations of sea surface temperature.

The bibliography does not, with certain limited exceptions, include entries on oceanography that are not directly pertinent to satellite observing techniques. Such more general oceanographic items can be located through the several general bibliographies on oceanography that already exist. Neither does it, in general, include entries solely pertinent to satellite observations of meteorological conditions over the oceans, since such material can be found in the several bibliographies on the "Use of Satellites in Meteorology" published by the American Meteorological Society in its Meteorological and Geoastrophysical Abstracts. These bibliographies are, however, specifically cited.

Abstracts are included for each entry for which they were available, either from the cited document itself or from its citation in other abstracting or bibliographic publications.

4. COMPUTER PROCESSING

As indicated in Section 2.2, the difficulties with the TIROS orbital and scanning geometries, together with the low resolution and generally high noise level of the TIROS data led to the recommendation of using a more advanced satellite configuration. The Nimbus II satellite, while it does not combine the desirable features of high resolution and cloud discrimination ability into a single sensor, it does possess these features in separate data gathering systems. This section describes the programs which have been derived for the optimal usage of the Nimbus II data. Complete listings of these programs have been provided in Appendix A.

Currently, Nimbus II HRIR and MRIR data may be ordered in a variety of formats from the National Space Science Data Center (NSSDC) at Goddard Space Flight Center (GSFC), Greenbelt, Maryland. The various formats available, and the ordering procedures are available in the Nimbus II User's Guide (ARACON Geophysics Company, 1966).

We feel that the modifications of these basic programs made in the course of this study are sufficiently general, and applicable to a variety of research efforts that they should be made readily available to other researchers. We strongly recommend, therefore, that the existence of these programs be made known to the potential users, and that their use be made a standard option which may be requested from NSSDC. As will be seen, the basic operating procedures do not differ from those currently used.

4.1 Original Programs

The Unified Nimbus HRIR and MRIR Mercator Map Programs were originally developed by NASA to map recorded experimental data for a selected area on the earth, and within a chosen time span. These data were first measured by the Nimbus radiometers and recorded on the Nimbus Meteorological Radiation Tapes (NMRT).

The experimental data are printed at grid points on a mercator projection of a specified geographical region. A grid point map indicating the number of measurements associated with each grid point is also produced. Any non-polar geographic region (up to approximately 70^{o} North or South latitude) can be displayed

at any scale factor by this grid point mapping program. The program can also output an optional listing of the latitude, longitude, nadir angle, and experimental value of the individual data measurements processed during the preparation of the grid point map.

Documentation publications and complete program listings, as well as operating instructions and procedures for the original programs, may be obtained from the Laboratory for Atmospheric and Biological Science, GSFC.

4.2 Modifications

4.2.1 HRIR Program Modifications

Modifications were made to the original Unified Nimbus HRIR Mercator Map Program to accomplish the following:

a. Extract and map HRIR data points where the recorded temperature is greater than or equal to some preset threshold value. If the threshold value is set high enough, one may be reasonably sure that the remaining data is cloud free. The penalty paid in such a case however, is that a large percentage of usable cloud free data may also be discarded along with the contaminated points.

b. Convert temperature values in degrees Kelvin to single digit alphanumeric codes for off-line printing or card punching. The punched card data obtained using this optional modification may then be processed through the Digital Color Printer developed by Allied Research in a separate in-house study. An example of the output of the color printer may be seen in Figure 6-1. A detailed discussion of the Digital Color Printer is given in Section 6.3.2.1.

c. Permit the composite mapping of multiple passes. This option may be used to construct time averages, or in situations of partial cloudiness when not enough clear-sky data is available on a single pass to permit meaningful analyses. Using a population map, data is averaged in those areas where there is clear-sky overlap from pass to pass.

4.2.2 MRIR Program Modifications

Modifications were made to the original Unified Nimbus MRIR Mercator Map Program to accomplish the following:

a. Extract and map MRIR data points from Channels 1, 2, 3, or 4 when the corresponding Channel 5 reflectance value (albedo format) is less than some pre-selected threshold. Analogous to the HRIR case above, too low a setting of the Channel 5 threshold guarantees cloud-free analyses, but loses much of the valid data. Of course, this option is applicable only to the daytime passes when Channel 5 albedo data is available.

b. Extract and map MRIR data points from any channel when the corresponding Channel 1, 2, 3 or 4 value is greater than some pre-selected threshold. This option was used primarily for nighttime cloud discrimination by mapping Channel 2 (temperature) data when the corresponding Channel 1 (water vapor) value exceeded some threshold. Details on this technique and selection of the threshold may be found in Section 5.2.2.

c. Convert temperature data to alphanumeric codes as in option (b) of the HRIR data above.

d. Permit the composite mapping of multiple passes as in option (c) of the HRIR data above.

4.3 Program Structure and Operation

4.3.1 HRIR Program

4.3.1.1 Structure

The program deck is available as a source deck consisting of a main program and 18 subroutines. The main program and five subroutines are written in FORTRAN II. The remaining subroutines are written in the FAP machine language. An object deck is also available. Execution is under the control of the IBM 7094 FORTRAN II monitor.

A general flow chart for the main program is given in Figure 4-1. This program is the control unit linking together the subroutines and input variables necessary to map the radiation data.

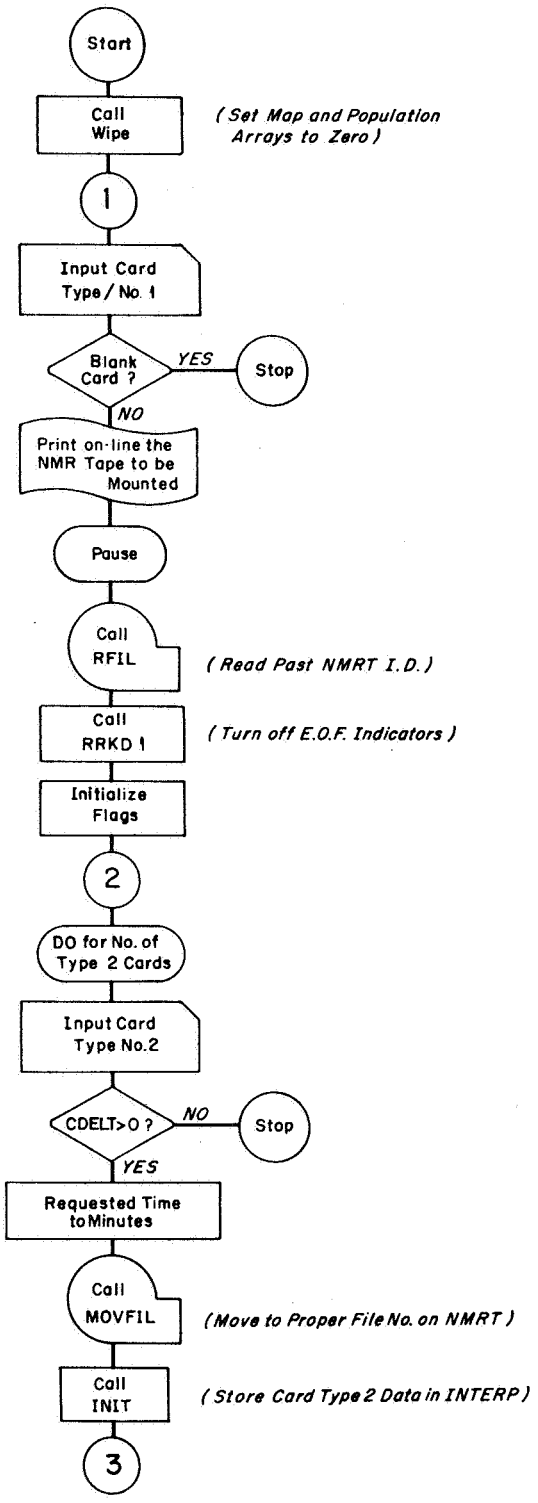

0941

Figure 4-1 Main Program Flow Chart

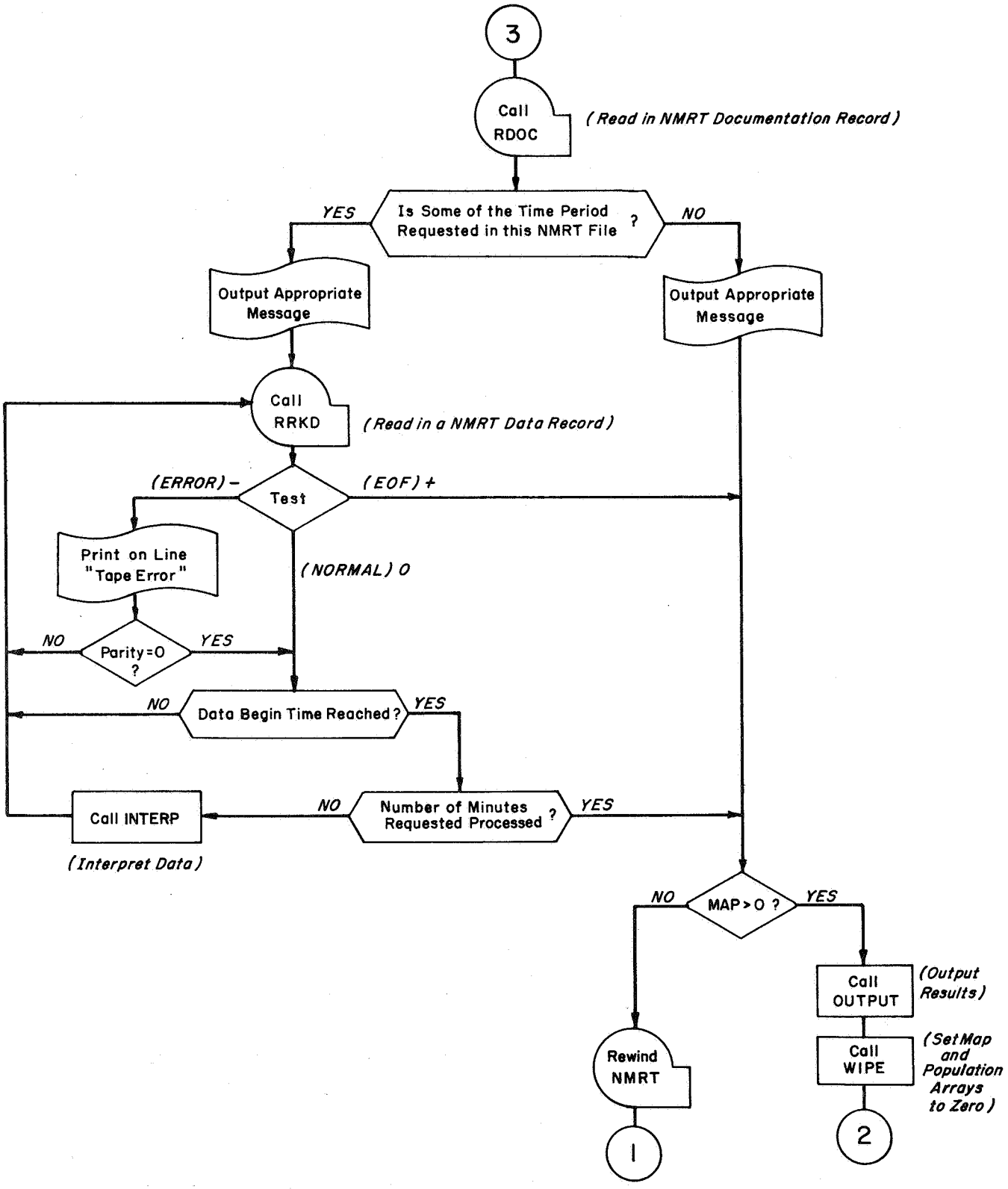

Figure 4-1 (Cont'd) Main Program Flow Chart

4.3.1.2 Magnetic Tape Mountings

The selected NMRT's are mounted on Tape Unit B-9 at 800 BPI. A blank tape is mounted on Tape Unit A-8 for card output. A scratch tape is mounted on Tape Unit A-3 for optional output information upon completion of main program.

4.3.1.3 Control Cards

There are two types of control cards used in this program. The Type 1 card contains the tape number of the NMRT and the number of Type 2 cards to follow. The format for the Type 1 card is given in Table 4-1. A Type 2 card is required for each map or each time segment within the request. A terminal blank card is placed at the end of the program deck, followed by an End of File (EOF) card. The format for the Type 2 card is given in Table 4-2.

Table 4-1
Type 1 Card Format (HRIR and MRIR)

Columns	Format	Symbol	Definition
1-5	15	JTAPE	Tape number of the NMRT to be mounted on B9.
6-7	12	JCARDS	Number of Type 2 cards to follow.

The card deck setup for mapping one pass or compositing more than one pass is shown in Figure 4-2.

4.3.1.4 Restrictions

a. The number of horizontal mesh intervals (DNBR) for any map should not exceed 77.

b. The number of rows created for any scaled mercator projection is a function of the Northern and Southernmost limits of a map, and this number must be less than 104. Special tables exist for checking the row count in advance.

c. When compositing orbits, input parameters CONI, CATN, CATS, SESH, DNBR, CUTOFW, CUTOFC on each Type 2 card should always be identical.

Table 4-2

Type 2 Card Format (HRIR)

Columns	Format	Symbol	Definition
1-3	F3.0	CDAY	Day of year of starting point of time interval to be mapped
4-5	F2.0	CHOUR	Hour of starting point of time interval to be mapped
6-7	F2.0	CMIN	Minute of starting point of time interval to be mapped
8-11	F4.0	CDELT	Time interval to be mapped in minutes
12-13	F2.0	CNADR	Value of nadir angle above which data is not considered
14-17	F4.0	CPASS	Pass number
18-20	F3.0	CONI	Easternmost longitude (measured from 0^{o} to 360^{o} westward)
21-23	F3.0	CATN	Northernmost latitude to be displayed in map; negative if in southern hemisphere.
24-26	F3.0	CATS	Southernmost latitude to be displayed in map; negative if in southern hemisphere
27-31	F5.3	SESH	Number of degrees of longitude per horizontal map interval. (Determines map scale)
32-34	F3.0	DNBR	Number of grid lines to form map
35			Blank
36	F1.0	PARITY	Non-zero value in this column causes a data record input with a parity error to be skipped in processing
37	F1.0	WRDAT	Non-zero value in this column causes information on each data point mapped to be written on A3 (optional listing)
38-39	I2	IFITGO	Number of data file of NMRT in which processing is to be done
40			Blank
41-42	I2	MAP	0-Composites maps; 1-Output maps in card form only; 2-Output maps in both card form and regular printed form
43-48			Blank
49-51	F3.0	CUTOFW	Used for card output. Any temperature greater than or equal to CUTOFW will be represented as a 9 punch on a card
52-54	F3.0	CUTOFC	Any temperature less than CUTOFC is rejected during map construction
55	A1	INK	Any printer character desired to represent no data on a card (usually left blank)

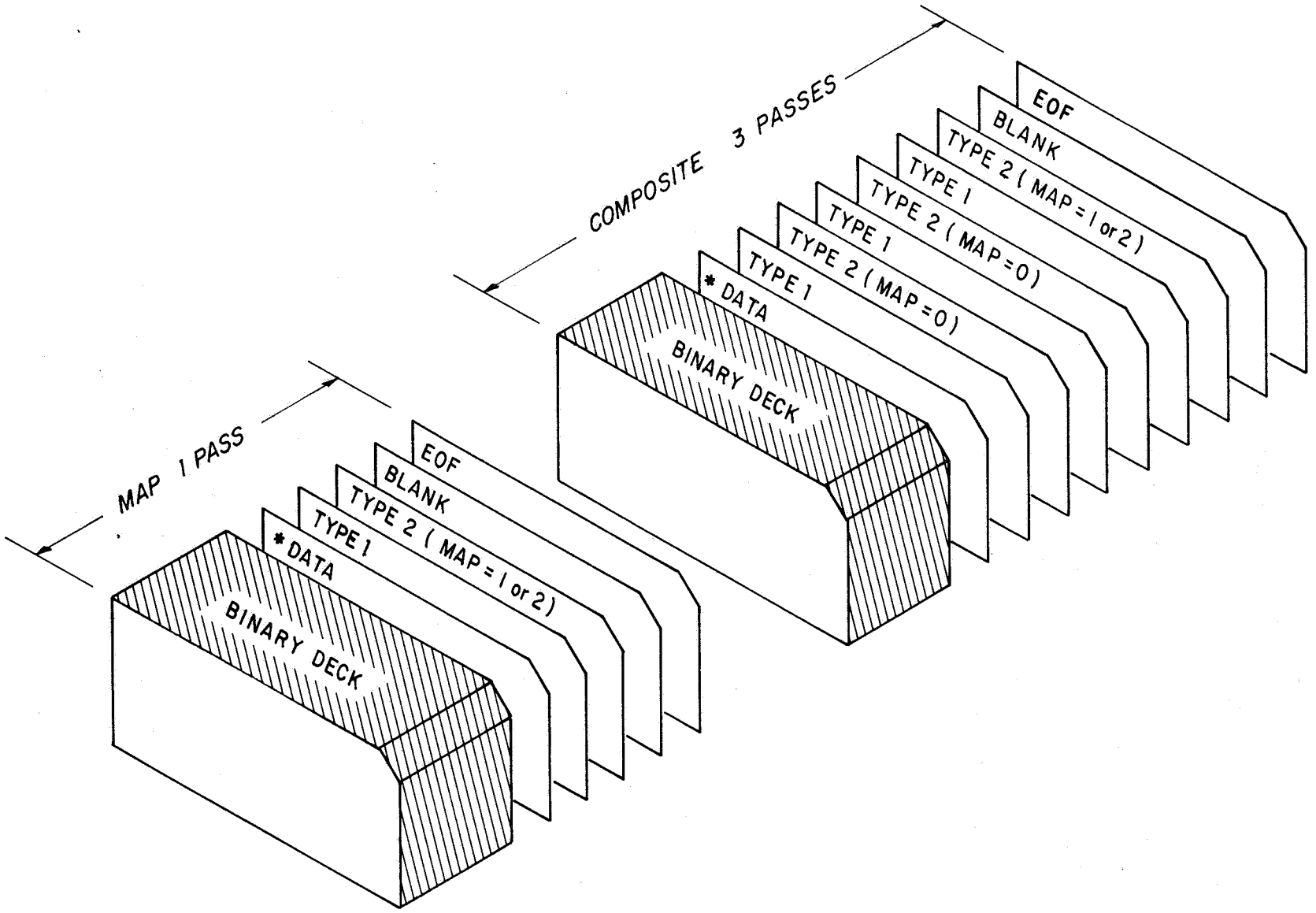

Figure 4-2 MRIR-HRIR Data Setup

4.3.2 MRIR Program

4.3.2.1 Structure

The program deck is available as a source deck consisting of a main program and 19 subroutines. The main program and six subroutines are written in FORTRAN II. The remaining subroutines are written in FAP. An object deck is also available. Execution is under the control of the IBM 7094 FORTRAN II monitor.

The general flow chart for the main program is identical to that presented for the HRIR program (Refer to Fig. 4-1).

4.3.2.2 Magnetic Tape Mountings

Identical with the HRIR case; refer to Section 4.3.1.2.

4.3.2.3 Control Cards

As before, there are two types of control cards used in this program. Card Type 1 remains unchanged. Refer to Table 4-1. Columns 1 through 39 of card Type 2 also remain unchanged. The format for the MRIR Type 2 cards is given in Table 4-3.

See Figure 4-2 for card deck setups.

4.3.2.4 Restrictions

a. Same as Section 4.3.1.4 (a) above.

b. Same as Section 4.3.1.4 (b) above.

c. When compositing orbits, input parameters CONI, CATN, CATS, SESH, DNBR, KCHAN, DISCRM, CUTOFW, CUTOFC, and IFV on each Type 2 card should always be identical.

Table 4-3

Type 2 Card Format (MRIR)

Columns	Format	Symbol	Definition
1-3	F3.0	CDAY	Day of year of starting point of time interval to be mapped
4-5	F2.0	CHOUR	Hour of starting point of time interval to be mapped
6-7	F2.0	CMIN	Minute of starting point of time interval to be mapped
8-11	F4.0	CDELT	Time interval to be mapped in minutes
12-13	F2.0	CNADR	Value of nadir angle above which data is not considered
14-17	F4.0	CPASS	Pass number
18-20	F3.0	CONI	Easternmost longitude (measured from 0^{o} to 360^{o} westward)
21-23	F3.0	CATN	Northernmost latitude to be displayed in map; negative if in southern hemisphere
24-26	F3.0	CATS	Southernmost latitude to be displayed in map; negative if in southern hemisphere
27-31	F5.3	SESH	Number of degrees of longitude per horizontal map interval (Determines map scale)
32-34	F3.0	DNBR	Number of grid lines to form map
35			Blank
36	F1.0	PARITY	Non-zero value in this column causes a data record input with a parity error to be skipped in processing
37	F1.0	WRDAT	Non-zero value in this column causes information on each data point mapped to be written on A3 (optional listing)
38-39	I2	IFITGO	Number of data file of NMRT in which processing is to be done
40	I1	KCHAN	MRIR channel number to be mapped
41-42	I2	MAP	0-Composites maps; 1-Output maps in card form only; 2-Output maps in both card form and regular printer form
43-48	F6.2	WSTAR	Channel 5 $\overline{W}$* reflectance value
49	I1	IFV	Number of discriminating channel
50-55	F6.3	DISCRM	Threshold value
56-57	I2	JSZAL	Solar zenith angle limitation for Channel 5 reflectance
58-60	F3.0	CUTOFW	Used for card output. Any temperature greater than or equal to CUTOFW will be represented as a 9 punch on a card
61-63	F3.0	CUTOFC	Used for card output. Any temperature equal to or less than CUTOFC will be represented as a 12 punch (+) on a card
64	A1	INK	Any printer character desired to represent no data on a card (usually left blank)

4.4 Subroutines

4.4.1 HRIR Subroutines

This section lists the HRIR subroutines and gives a brief summary of their purpose:

Subroutine	Purpose
WIPE	Called by main program to set NGATE flag to 1 for entry to SST for initialization of map arrays
MOVFIL	Called by main program to locate proper file on NMRT
RDOC	Called by main program to read NMRT documentation record
RFIL	Called by main program to read past NMRT I.D. file
INIT	Called by main program to store card Type 2 data for use by INTERP. Calculates upper and lower limits of map
INTERP	Called by main program to unpack data contained in an NMRT. Calls upon other subroutines to calculate nadir angle, latitude, longitude and map coordinates. Rejects data on basis of discriminant as they are called up
COMPA	Called by INTERP to calculate nadir angle of data point
TINI	Called by INTERP to calculate latitude and longitude of data point
MGRID	Called by INIT and INTERP to calculate number of map rows required and map coordinates
OUTPUT	Called by main program to set NGATE flag for requested options for entry to SST
SST	Called by INTERP, WIPE and OUTPUT to accomplish one of five tasks as a function of NGATE setting: (1) initialize map arrays (2) compile map data (3) calculate average (4) output maps in printed format (5) output maps in card format
IBLK	Called by SST to acquire no-data card code
HEAD	Called by INTERP to write heading line to identify data listed by WRITE
WRITE	Called by INTERP to write accepted data values

RRKD	Called by main program to input next data record
RRDK1	Called by main program to initialize redundancy and EOF indicators to off condition
FXFLO	Called by various subroutines. Fixed to floating point
FLOFX	Called by various subroutines. Floating to fixed point

4.4.2 MRIR Subroutines

MRIR subroutines MOVFIL, RFIL, TINI, MGRID, SST, RRKD, RRKD1, COMPA, FXFLO, and FLOFX are identical with the corresponding HRIR subroutines. The remaining eight HRIR subroutines have equivalent like-named counterparts in the MRIR programs, but with some changes due to basic data format differences (see Appendix A).

The MRIR program has one additional subroutine:

Subroutine	Purpose
N2C5R	Called by INTERP to calculate Channel 5 reflectance

5. CLOUD DISCRIMINATION

Since the early TIROS studies the presence of cloudiness has remained the primary deterrent to obtaining accurate SST maps of sufficiently wide coverage. While nothing can be done to remove the effects of cloudiness, considerable effort has been placed into the task of at least removing cloud contaminated data points from the temperature analyses.

5.1 Daytime Cloud Discrimination

5.1.1 HRIR Daytime Cloud Discrimination

The 3.5 to 4.1μm spectral region of the HRIR sensor extends far enough into the solar radiation spectrum so that daytime HRIR measurements are strongly influenced by reflected solar radiation. Clouds may appear either light or dark depending upon some combination of temperature and brightness, and are nearly impossible to accurately distinguish. As a result, daytime HRIR cases were not used in this study although evidence of the north wall of the Gulf Stream may be seen in some of the passes. The absolute temperature values recorded however, even in the clear areas, cannot be relied upon due to the solar reflectance problem.

5.1.2 MRIR Daytime Cloud Discrimination

Past studies have shown that, in the absence of sunglint, the reflectance, or albedo, of the sea surface is extremely low compared to cloud reflectance. By setting an appropriate albedo threshold value, cloud contaminated data points can be effectively eliminated (Conover, 1965). Analysis of the Nimbus II daytime MRIR data has resulted in the choice of a 15% albedo threshold value as the cut-off between clear and cloudy areas. This particular reflectance value corresponds most closely with abrupt changes in Channel 2 temperature as the sensor enters or leaves a cloudy area.

One difficulty, however, is that the presence of thin cirrus clouds is often not readily apparent in the reflectance channel data. Because of their cold black body equivalent temperatures though, these clouds do exert a marked influence on the Channel 1 data. Channel 1, which operates in the 6.4-6.9 μm water vapor absorption band, records the ambient temperature of the atmospheric moisture. As

a result, an investigation was conducted to determine the feasibility of jointly using the Channel 5 reflectance, and Channel 1 water vapor data (combine options (a) and (b) of Section 4.2.2 above) to delineate cloud contaminated areas.

The investigation was based on the joint analysis of daytime satellite data (MRIR) and ground based cloud observations extracted from WBAN 10 forms. Since cloud reports are readily available only over land areas, case studies were confined to the eastern coast of the U.S. The results of these studies showed that for the safest and most complete elimination of cloud contamination from the Nimbus day time data, it is necessary to use a combination of the 15 % albedo threshold and a 237°K water vapor threshold (clear, for Channel 1 temperature greater than 237°K). The ability to distinguish cloudiness using Channel 1 data has immediate application to the problem of nighttime cloud discrimination when albedo data is not available. Details of similar case studies run for the Gulf Stream region, and the choice of the 237°K Channel 1 threshold value, are provided below in the discussion of MRIR nighttime cloud discrimination.

5.2 Nighttime Cloud Discrimination

5.2.1 HRIR Nighttime Cloud Discrimination

The Nimbus II HRIR radiometer operated in a single spectral region so that the only readily available means for cloud discrimination were the temperature data themselves. The choice of a threshold value in this case is relatively arbitrary, although 280°K is one value commonly used. This value assures that most of the truly cloud-free data will be included, while the amount of cloud contamination is kept relatively small. Fog, low warm clouds, and high thin cirrus are cloud types most commonly missed by this technique.

The possibility of developing computer programs to eliminate cloud from the nighttime HRIR data using the MRIR water vapor data was considered. Because of the relatively short lifetime of the MRIR sensor (74 days, 15 May to 28 July 1966) relative to the HRIR (6 months) and the probable complexity of such a program, it was not felt that such an effort would be justified. To demonstrate that such an approach could be taken, however, a few cases were run where the melding of the MRIR and HRIR data was done by hand. An example of one such analysis may be seen in Figure 5-1

These are the nighttime HRIR data from Pass 380 of Nimbus II. Two types of cloud discrimination are used: HRIR temperature below 282°K, and MRIR Channel 1 data below 237°K. The area is off the southern coast of South Africa. In this region the warm Agulhas Stream flows south along the eastern coast of Africa to about 40°S. There, it encounters the cool Southern Hemisphere West Wind Drift at Cape Agulhas. Starting at Cape Agulhas, the cold Benguela Current moves northward along the western coast of Africa. In the cloud-free areas one may clearly see evidence of both the Agulhas and Benguela currents. The fine structure in the temperature patterns is typical of HRIR SST maps. There is at present considerable controversy as to the "reality" of these detailed patterns. Unless some direct connection to sensor noise is discovered, it is a question which may never be resolved. In fact there may be no solution. Due to the nature of remote IR measurements (i.e. sensing only the top few tenths of millimeters of the water surface), these patterns may be "real" only to IR instruments and would never be observed in the conventional ship data.

5.2.2 MRIR Nighttime Cloud Discrimination

In seeking a Channel 1, water vapor, threshold value for use in nighttime cloud discrimination, two types of analyses were performed. One was a simple matching of the Channel 1 patterns with the reflective patterns of Channel 5. The other was a statistical analysis of the significance of assumed Channel 1 clear area criteria.

5.2.2.1 Channel 1/Channel 5 Matching

Consecutive daytime MRIR passes for approximately one week were run for the Gulf Stream region. Cloud free areas, as indicated by using various Channel 1 thresholds, were compared with those obtained using the Channel 5,15% albedo cutoff. For each water vapor threshold, two numbers were calculated: the false alarm rate, i.e. the probability that a point indicated to be cloud was in fact clear, and the failure rate, i.e., the probability that a point indicated to be clear was in fact cloud. The results for a typical pass are shown in Figure 5-2. These data were derived from Pass 511 on 22 June 1966. It will be noted that for thresholds less than 239°K, the false alarm rate approaches 50%. As expected, the "false alarm" rate generally exceeds the failure rate. This is because the Channel 5 albedo

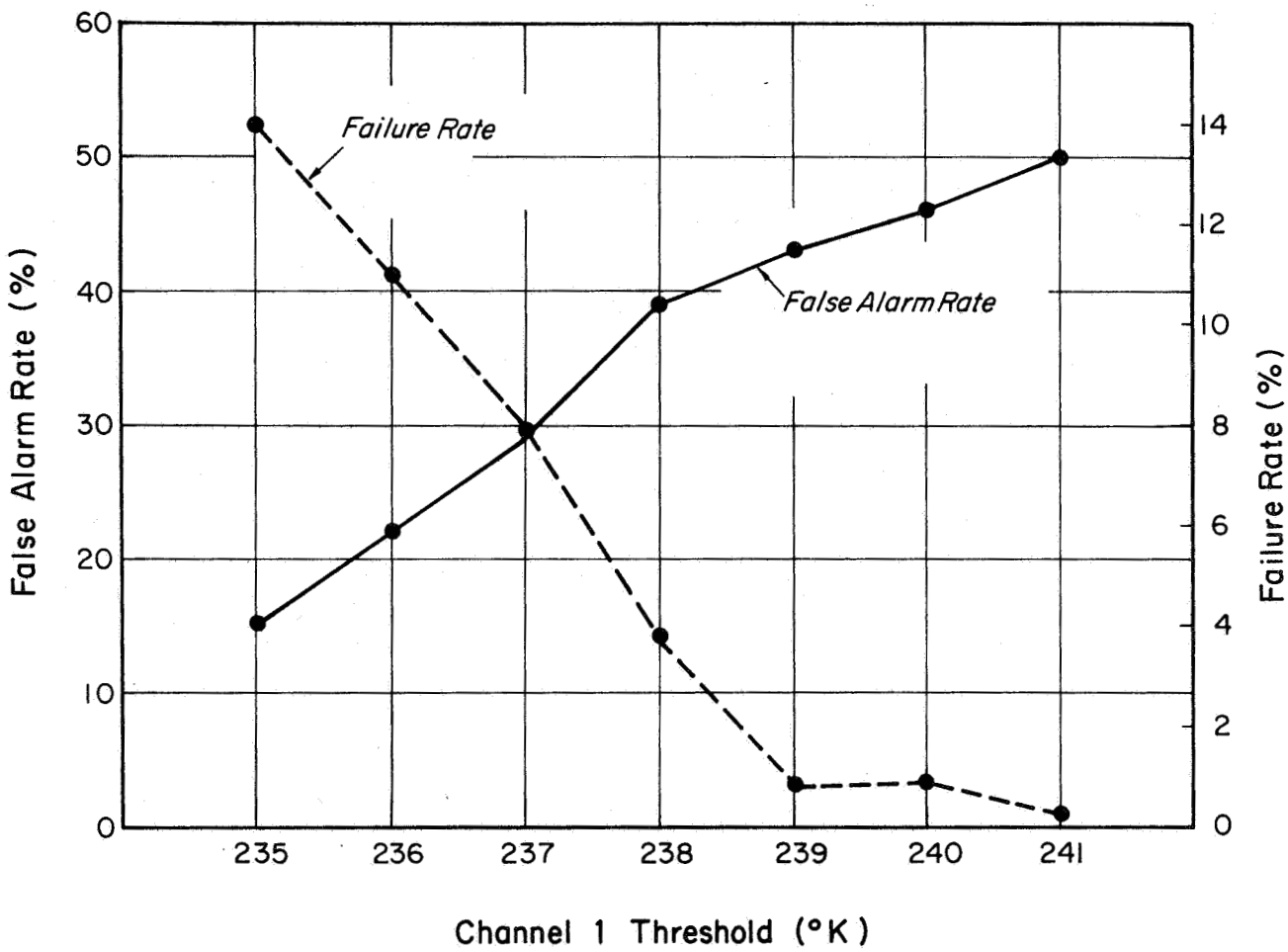

Figure 5-2 Channel 1 False Alarm - Failure Rate (Nimbus II, Pass 511)

6938

discrimination technique, as mentioned above, tends to miss certain cloud forms such as high thin cirrus. Analysis of several cases such as that shown in Figure 5-2 led to a choice of 237°K as the Channel 1 water vapor, clear-cloudy threshold. As usual, any such choice involves a trade-off between data quality and data quantity. In our studies quantity was often sacrificed to obtain higher quality, more cloud-free analyses.

Figure 5-3 shows the analyzed Channels 1, 2 and 5 data for orbit 470. Only the following isolines are shown:

Channel 1: 235°K
Channel 2: 280°K and 290°K
Channel 5: 20% albedo

From the figure, the following points may be made:

a. Areas having a Channel 1 temperature less than or equal to 235°K, correspond very well with areas having albedos less than or equal to 20%. An exception is the band of cool Channel 1 temperatures between 10° and 20° North.

b. Within this cool band, however, it is interesting to note that there are areas where the Channel 2 temperatures are less than 280°K (high thin cirrus?).

c. On the whole, Channel 2 temperatures less than 280°K fall within the areas where the Channel 1 temperature is less than 235°K, and the Channel 5 albedo exceeds 20%.

As would be expected, the downward revision of a Channel 5 threshold can be best matched by a corresponding increase in the Channel 1 threshold. Thus, the ultimate choice of a 237°K water vapor channel threshold is consistent with a slightly lower (15%) albedo threshold than the one used in this example.

5.2.2.2 Statistical Approach

A study was made of the statistical significance of several Channel 1 thresholds, T_t, used in conjunction with a Channel 5 albedo threshold, R_t, of 12%. The technique used was that of computing chi-square values based upon contingency tables. Each of the data points in a chosen area was counted as belonging to one of the four following categories:

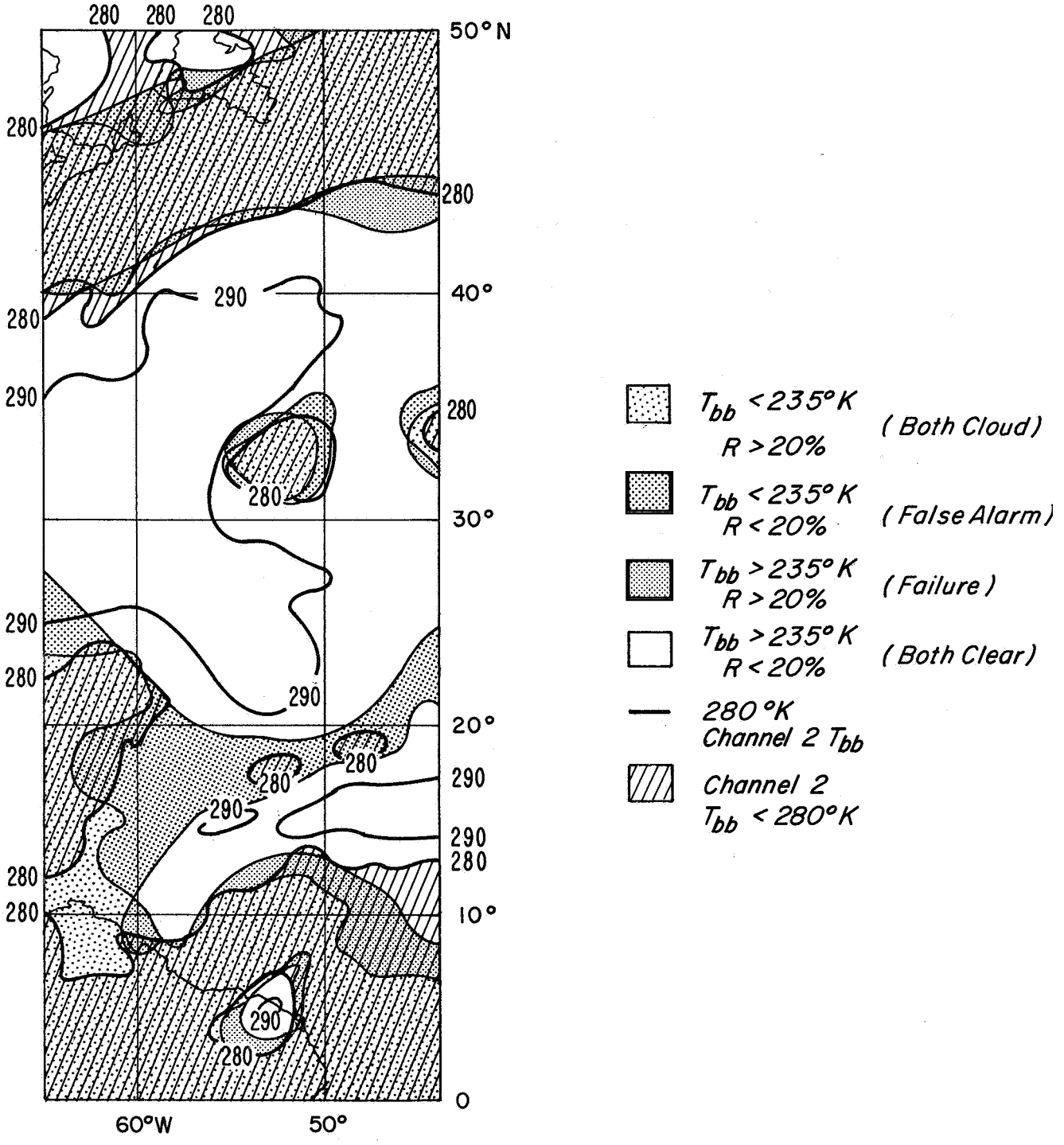

Figure 5-3 Analyzed Channels 1, 2 and 5 Data (Nimbus II, Pass 470)

6986

I : $R \leq 12\%$, $T \geq T_t$: both indicate clear

II : $R \leq 12\%$, $T < T_t$: false alarm

III : $R > 12\%$, $T \geq T_t$: failure

IV : $R > 12\%$, $T < T_t$: both indicate cloud

where R is the Channel 5 reflectance, and T is the Channel 1 temperature.

An example of these calculations for two widely separated Channel 1 thresholds is seen in Table 5-1 below.

Table 5-1

Cloud Discrimination Contingency Tables

T_t \ R_t	$\leq 12\%$	$> 12\%$
$\geq 235^{\circ}K$	1143	563
$< 235^{\circ}K$	227	315

$\chi^2 = 109.0$

T_t \ R_t	$\leq 12\%$	$> 12\%$
$\geq 241^{\circ}K$	386	128
$< 241^{\circ}K$	984	750

$\chi^2 = 56.1$

These data represent a composite of several MRIR passes over the same geographic area. As can be seen, at the lower Channel 1 threshold of $235^{\circ}K$, the failure rate exceeds the false alarm rate, while with the threshold at $241^{\circ}K$, the reverse is true. It should be noted that the calculated chi-squares are pessimistic insofar as the "false alarm" rate is artificially high due to the inability of the albedo channel to discern certain cloud forms.

A graph of the computed chi-square values for seven Channel 1 thresholds is presented in Figure 5-4. This parameter is seen to peak at a Channel 1 threshold of $237^{\circ}K$, although the curve is relatively flat from 235° to $237^{\circ}K$. In each case, the probability of a value of χ^2 being at least as great as those shown here is much less than 1%, so that the degree of association between the Channel 1 and Channel 5 thresholds is quite significant. As can be seen, the justification for rejection of the null hypothesis decreases sharply for Channel 1 temperatures greater than $239^{\circ}K$.

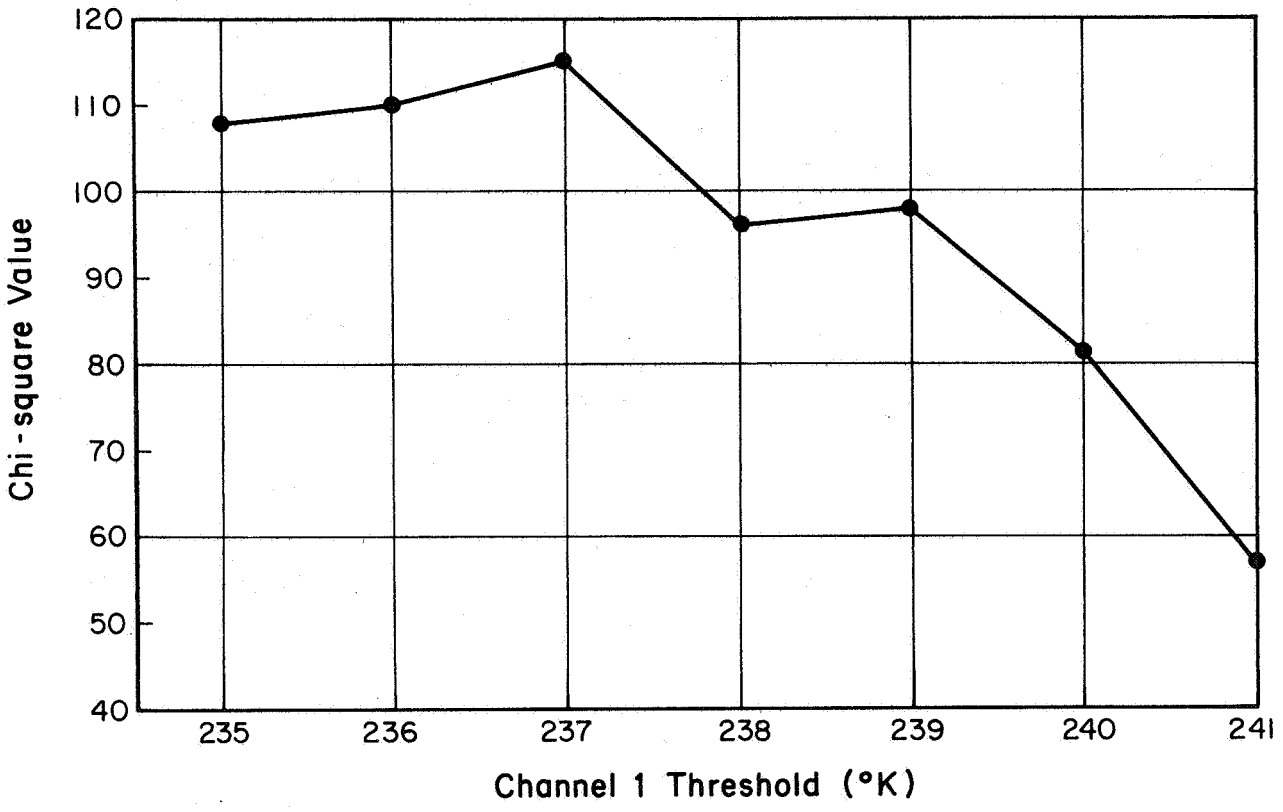

Figure 5-4 Computed Chi-Square Values

5.3 Summary

As has been shown, a combination of visible, IR window, and water vapor absorption data is best suited to the detection of cloud contaminated data points. In the nighttime cases only the temperature and water vapor data are available. Thin cirrus clouds may be missed by the visible channel, but are usually detected in the water vapor band. While tentative thresholds of 15% albedo, 280°K, and 237°K have been established for the visual, temperature, and water vapor channels respectively, no unique fail-safe set of thresholds are available. The use of manned spacecraft observations to further resolve clear-cloudy radiation differences, and to examine such problem areas as small (less than the sensor resolution) scattered cloudiness is discussed in Section 8.

6. RECOMMENDATIONS ON OPTIMUM DATA SOURCES, PROCESSING AND ANALYSIS

6.1 Data Sources

As outlined earlier in this report (Section 1.3), the most ideal satellite system for the operational measurement of cloud-free sea surface temperature data would be a near-polar orbiting sun synchronous vehicle with high resolution cross-track scanning in several spectral regions. The multiple spectral region feature if properly calibrated would permit real time flagging of cloud contaminated data, and hence the immediate mapping of clear sky temperature data. It should be noted that TIROS-M, scheduled to be launched during the second quarter of 1969, closely approximates such a system. It will be in a sun synchronous orbit and carry a two channel (.52 to .73μm, visible and 10.5 to 12.5μm, infrared), high resolution (4 n.mi. at subpoint), scanning radiometer. Real-time processing of the radiation data with a digital tape output is being planned by the National Environmental Satellite Center (NESC).

In the absence of real time measurements of visible radiation data to complement the infrared information, an alternate source of cloud data must be sought. Since October 1966, NESC has mapped satellite visible imagery on a daily global basis for a variety of users (Bristor, 1968). Earth locator information is used to determine the latitude and longitude of each digital brightness sample. These locations are replotted as a digital map in a standard polar stereographic or other type projection for easy comparison with other environmental data. A fine mesh (4096x4096) map array is reserved on computer disks for each polar hemisphere. Since January 1967, archival hemispheric tapes have been prepared with mesoscale (512x512) arrays. A point-to-point message format tape is available for relay and further treatment by computer.

The digitized cloud maps described above could serve as a substitute for other, more direct, cloud discrimination data if the latter are not available. These maps would, of course, be usable only for the daytime data. One problem which would be encountered is that the digitized cloud maps are not, in general, valid for the precise time of the infrared measurements. Possible solutions to this problem include the artificial enlargement of the indicated cloud areas as a function of the

magnitude of the time discrepancy, or even advecting the clear-cloudy information in time. Insofar as this latter approach requires a knowledge of the existing wind field, and neglects such phenomena as cloud dissipation and generation, its use is probably not feasible at the present time.

6.2 Data Processing

6.2.1 Use of Temperature Gradients

Within the present state-of-the-art, it is not possible to accurately account for the absolute effects of atmospheric attenuation on a real-time basis. (Present Nimbus data yields accuracies of $\pm$ 1 to 2°K only if corrections for atmospheric attenuation of $\pm$ 1 to 5°K are applied). To do so would require a detailed knowledge of the temperature and humidity structure of the intervening atmosphere. Ways to accomplish this are currently being investigated (Bandeen, 1968), but are not as yet available. Possible approaches include the use of a Temperature Humidity Infrared Radiometer (THIR) and a Filter Wedge Spectrometer (FWS), both of which are being developed to fly on Nimbus D in the first quarter of 1970.

Until it is possible to automatically include atmospheric attenuation effects, the operational use of satellite derived sea surface temperature information must be restricted to the use of temperature gradients only. These gradient data must then be combined with the absolute temperature values as recorded by conventional shipboard measurements.

In combining the satellite gradient data and ship data, FNWF currently produces a daily computer drawn SST map for the Northern Hemisphere utilizing a data base of 84 hours of conventional surface ship data. In view of the vast time and distance scale advantages of satellite radiation data, real-time melding of cloud-free, satellite derived, sea surface temperature gradient data with the conventional shipboard observations should be considered. Assuming the existence of a multispectral, high resolution radiometer, the cloud discrimination techniques discussed in Section 5 above would be immediately applicable to such a program. A flexible, three dimensional temperature surface, is, in effect, mathematically fit to the array of surface measurements which act as a forcing function on the satellite data. General mathematical techniques to meld gradient and absolute data are available and are adaptable to the CDC 6500 computers used by the Fleet Numerical Weather Facility (Danard, 1967). Of course, the use of gradient data does not affect the requirement for recognition of cloud contaminated data.

6.2.2 Atmospheric Attenuation

While it is not yet possible to remove entirely the effects of atmospheric attenuation, some corrections can be made for its variation, both with nadir angle and geographic location. Correcting for the variation with nadir angle would be a relatively simple task. The magnitude of this effect has already been evaluated in certain spectral regions for standard atmospheres (Wark, 1962). Current programs avoid the worst of the nadir angle problem by rejecting data acquired above some specified nadir threshold (see input CNADR on Card Type 2, Tables 4-2 and 4-3).

Correcting for the spatial variation of attenuation called for in large scale operational applications would be a considerably more difficult task. If this is not done, however, the varying attenuation patterns caused by changes in air mass will introduce false temperature gradients into the analyses. Possible sources of humidity data might include FNWF's 12 hourly analysis of the atmospheric mass structure, or some variation of the Nimbus II Channel 1 water vapor data. The possibility of using data from a water vapor absorption band has already been investigated (Fritz, 1967 and Bandeen, 1968).

6.2.3 Data Compositing

Insofar as the ship data used by FNWF in their daily SST maps must be accumulated over 3-1/2 days (to insure enough data for meaningful analyses,), it may be desirable to increase the effective coverage of the satellite data by compositing it over a number of passes. Again, the techniques for doing so have been developed. Just how much coverage can eventually be obtained as a function of the compositing interval is highly dependent upon the particular geographic region in question. Additionally, the variation in time of the desired surface temperature patterns places limits upon the duration of compositing time which can be tolerated. Compositing over too long a period may average out or obscure the patterns intended for study. Considerations such as these are particularly useful in planning research programs, or in evaluating the potential usefulness of satellite data for particular applications. A more detailed discussion of such considerations with particular emphasis on the Gulf Stream region will be presented in Section 7.1.

6.3 Data Analysis

6.3.1 Operational Use

The approach to the problem of data analysis depends to a great extent upon the use to which the data will eventually be put. Certainly for operational applications, computer drawn analyses represent the only feasible solution. In case of the FNWF daily SST maps of the Northern Hemisphere, the requirement for rapid dissemination and transmission of these data necessitates a simple format consisting of computer drawn isolines of uniform temperature. Computer generated color presentations are currently possible, but require elaborate and expensive techniques and equipment, and cannot be easily transmitted to other locations.

6.3.2 Research Use

6.3.2.1 Digital Color Printer

For research applications, the tedious and time-consuming hand analysis of the resultant temperature maps continues to be the most prevalent approach. Even the interpretation of computer-drawn analyses can be extremely difficult, often requiring hand coloring of the temperature patterns. In an attempt to by-pass this problem, particularly in the development of the Gulf Stream time history to be discussed in Section 7.2 a simple photographic device developed under a separate in-house study by Allied Research was employed.

The Digital Color Printer may be used to produce color coded analyses of any digital array. The number of possible color selections is limited chiefly by the ability of the human eye to distinguish between them. In its present format, 12 colors are available (one for each row of a standard punched computer card), although by going to a system of mixing colors in a three primary color arrangement, 125 separate hues may be obtained. In the present system the numerical values of any digital array must first be converted to a single digit, alphanumeric code for output in a punched card format. (As seen in Section 4, this option is now included in both the modified MRIR, and HRIR programs.) The punched cards are

then placed on a color filter platen and their image is effectively swept past a slit aperture producing a row of color coded spots corresponding to a row of numbers of the original digital array. The color strips of the filter platen may be easily interchanged or replaced so that particular features of the analysis may be emphasized without re-running the program.

An example of the output of the Digital Color Printer may be seen in Figure 6-1. These HRIR data are recorded over the Gulf Stream area at local midnight on 28 August 1966 during pass 1396 of Nimbus II. The scale of the original digitized data was 1:1 million, so that the width of each of the colored squares seen in the Figure is about 7.5 miles. Each of the nine colors represents a 2 degree Kelvin temperature increment ranging from 300°K at the red end to 283°K and cooler in the blue. On the left side of the map, the relatively cool land areas of the east coast, including Cape Hatteras and the DelMarVa Peninsula stand out against the warmer waters of the Atlantic Ocean and the Chesapeake Bay and the Delaware Bay. The north wall of the Gulf Stream is clearly seen in the central portion of the picture, outlining a major meander. The cooler temperatures seen in the southeast portion of the analysis are due to partial cloudiness.

Figure 6-2 shows a hand drawn analysis of the same data. While the location of the Gulf Stream can be inferred, its position is not nearly as obvious as it was in Figure 6-1. It is clear that the use of the Digital Color Printer, or similar devices can save a considerable amount of time and effort which would otherwise have been spent in analyzing and interpreting the traditional grid-print maps.

6.3.2.2 Single-Digit Analyses

In working with the Digital Color Printer it was found that a simple printout of the punched card data resulted in a temperature array which was much easier to analyze than the standard grid-print map. The improvement of course, is due to the ability of the human eye to discern patterns in a field of single-digit alphanumeric symbols. Objections have been raised that the extra step required in such a format, to mentally convert from symbols to temperature values, negates the analysis advantages. We feel, however, that if a sufficiently familiar set of ordered symbols, such as the english alphabet, is used, the advantages of a shorter analysis time will far exceed the disadvantage of converting from symbols to temperatures.

One possible application would be the "full resolution" mapping of the HRIR data where every digitized point in a swath is output in alphanumeric form. A special symbol could be reserved for output at even 5^{o} latitude-longitude intervals. Connecting these special symbols by straight lines would result in a gridded, full resolution HRIR map on a single piece of paper of manageable size. The initial work has already begun at Allied to develop such a full resolution program.

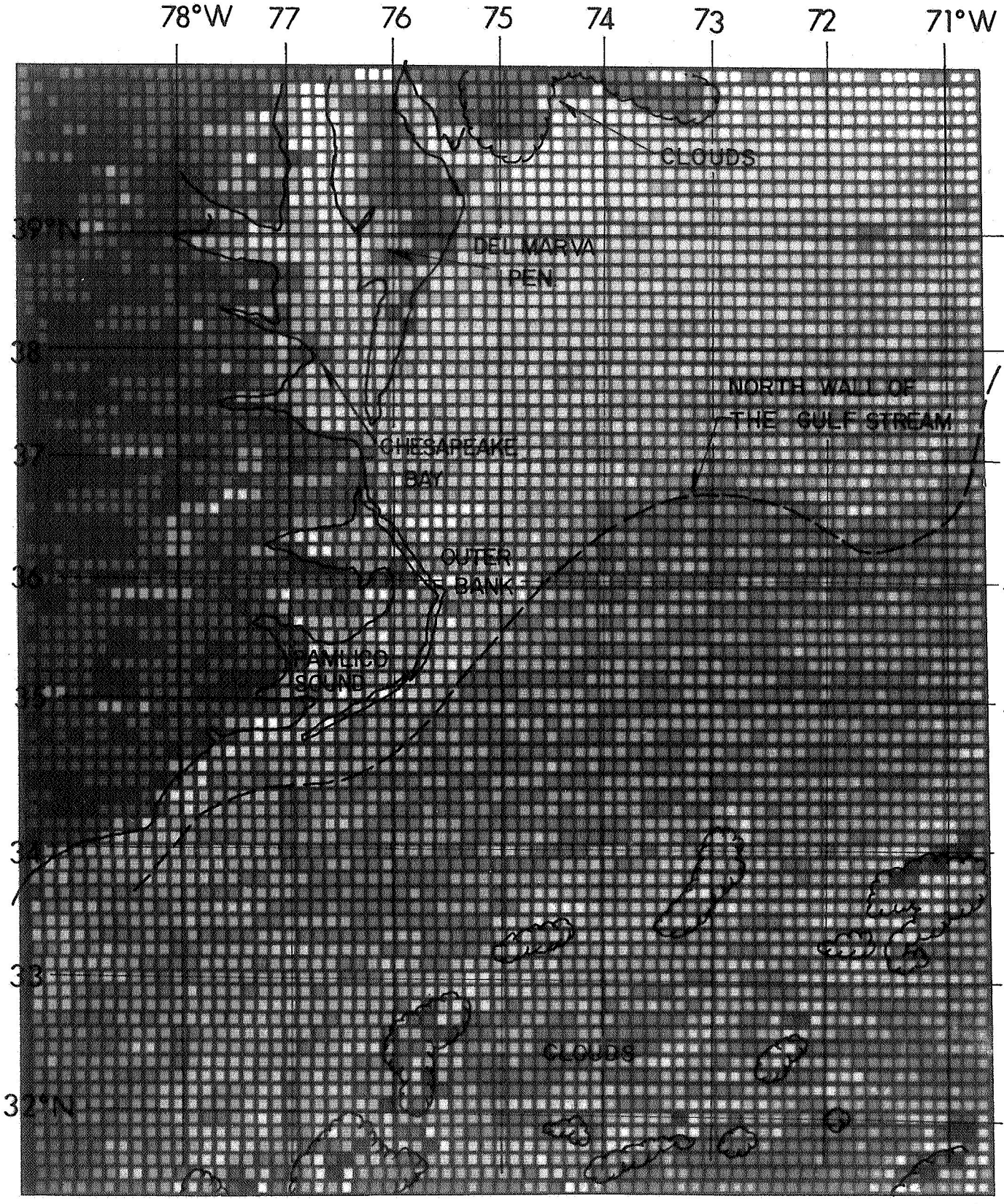

Figure 6-1 Digital Color Printer Output (Nimbus II, Pass 1396)

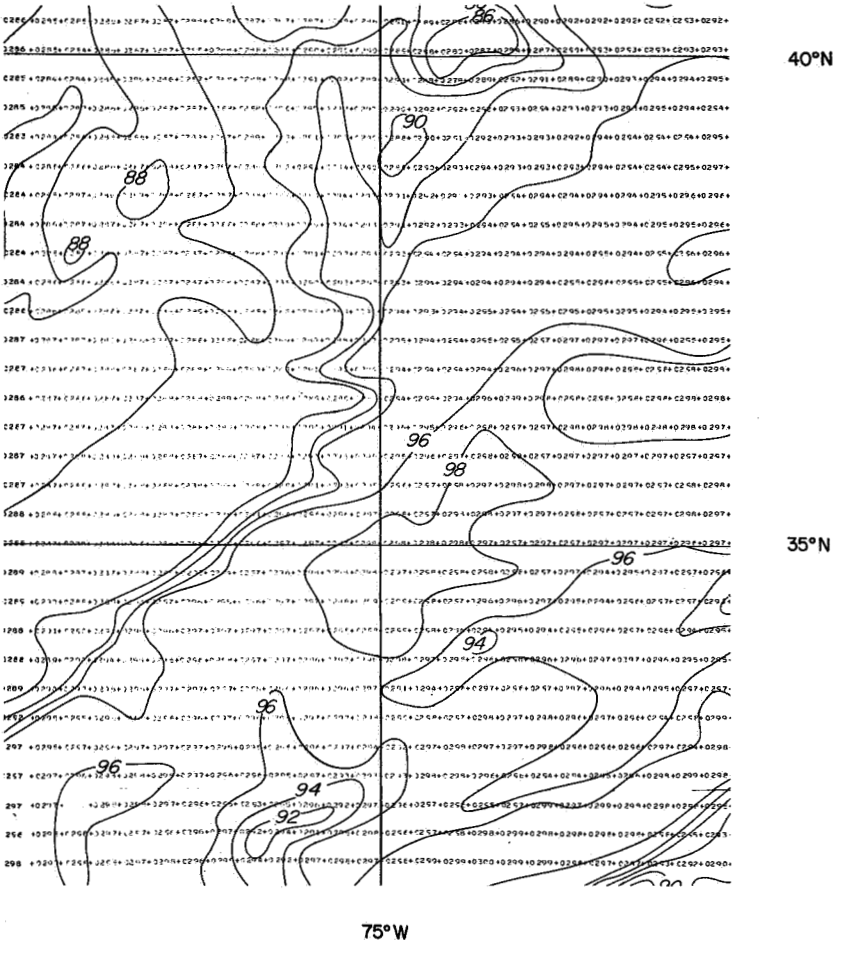

Figure 6-2 Hand-Drawn Analysis (Nimbus II, Pass 1396)

7. MEASUREMENT OF SEA SURFACE TEMPERATURE PATTERNS AND THEIR SYNOPTIC CHANGES

7.1 Remote Measurement of a Time-Varying Phenomenon

A brief glance at any full-disk earth picture reveals that the primary problem in developing a time history of some changing surface feature is the cloud cover. There is a tendency for those oceanographic areas which exhibit the greatest synoptic change, such as the Gulf Stream or any major current, to have frequent and persistent fronts and cloud cover. It is extremely rare that such a large scale feature can be viewed under completely cloud free conditions. These considerations led to a number of questions. How often is it really necessary to view a given area under cloud-free conditions? Would it be sufficient to view it every other day, or every third day, or once a week? If an area is partly cloudy on consecutive days, is it possible to generate meaningful temperature pattern analyses by making composite maps? For a region with varying surface features, what is the probability of obtaining a workable amount of coverage before the patterns change? Is it even possible, except under unusual meteorological circumstances?

The answers to these questions depend to a great extent upon both the nature of the body of water being studied, and upon the climatological characteristics of the intervening atmosphere. As an example of the remote measurement of changing sea surface temperature patterns, the behavior and structure of the Gulf Stream will be considered in Section 7.2. The following paragraphs present a statistical approach to the cloud cover problem. In presenting examples of the generation and application of the cloud statistics, the Gulf Stream region is emphasized.

7.1.1 World-Wide Cloud Data Bank

In a separate study, Allied Research has prepared probability distributions of world-wide cloud cover for use in the simulation of earth-oriented observations from space (Sherr, 1968). The practical use of cloud statistics in computer simulation routines dictates the subdivision of the earth into nominally homogeneous cloud climatic regions. The number of such regions is arbitrarily set by consideration of the data volume that must be handled by the computer and by the amount of suitable

data available. Figure 7-1 presents the selection of 29 cloud regimes derived from standard climatology, general cloud summaries, conventional and satellite observations, and cloud data from selected stations. Note that the Gulf Stream area is included primarily in Regions 13 and 20.

For each of the 29 regions, both unconditional and temporal and spatial conditional cloud cover statistics were derived. The unconditional statistics were derived for eight times of day and for each month of the year. Because of insufficient data, the conditional statistics received only a seasonal stratification. Five cloud-amount categories were defined:

Category 1	Clear skies
Category 2	1, 2 and 3-tenths cloud cover
Category 3	4 and 5-tenths cloud cover
Category 4	6, 7, 8 and 9-tenths cloud cover
Category 5	Overcast.

Unconditional cloud cover statistics are frequency distributions of fractions of sky covered, expressed in percent frequency. The temporal conditional tables present the probability of cloud amount X occurring at some given point 24 hours after the occurrence of cloud amount Y at the same point. The spatial conditional tables present the probability of cloud amount X occurring at some given time 200 miles distant from the occurrence of cloud amount Y at that same time. Data for these tabulations were derived from 10 to 15 years of weather records from approximately 100 observing stations distributed throughout the world. The three to five years of satellite data were used particularly in the preparation of the spatial conditional tables.

Mathematical procedures are provided to adjust the conditional distributions to other time and distance separations. In the case of the temporal conditionals, special procedures are available to account for diurnal effects as 12 or 36 hour intervals are approached. Techniques are also presented to allow the basic statistics (representing approximately a 30 n.mi. circular area) to be scaled into distributions representing enlarged area sizes. These techniques are required due to the marked change in cloud cover distribution as a function of sampled area size. (The cloud cover over a true point can have but two values - clear and overcast. The cloud cover over the entire earth seems to stay reasonably constant at about 40%. Intermediate sized areas have cloud distributions which pass from the U-shape of small areas to more bell-shaped distributions at rates which depend upon the prevalence of large-scale cloud systems.)

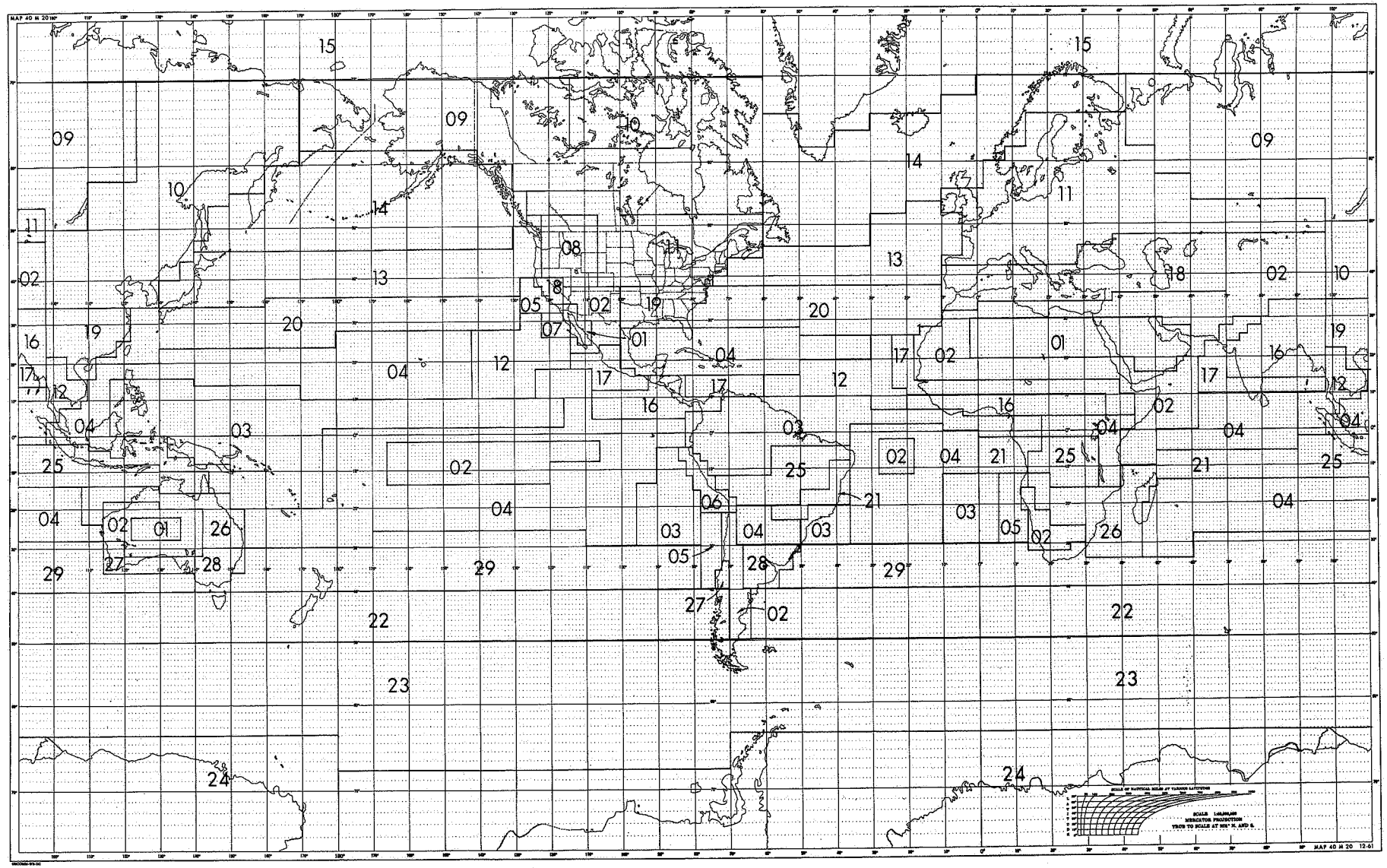

Figure 7-1 Region Location Map for Cloud Cover Data

Tables 7-1 and 7-2 present the conditional and unconditional cloud statistics for Regions 13 and 20 for the months of June and October respectively. Note that from the unconditional tables, cloud categories 4 and 5 are the most probable for both regions for both June and October. As an example of the interpretation of these tables, consider the early evening (1900 local time) data for Region 13 for the month of October. Typically, cloud categories 4 and 5 are most probable, while there is only a 1% probability of clear skies. Looking at the conditional tables, one sees that, given initially overcast skies, the probability that the skies will still be overcast 24 hours later is 39%, and that the probability of overcast conditions 200 miles away is 57%. As might be expected, both of these values exceed the unconditional overcast probability of 36% . Given initially clear skies, the probability of continued clear skies 200 miles away is 61%. Note, however, that the most probable cloud coverage 24 hours later is overcast skies. This sort of anti-persistence is typical of areas with high frontal activity.

7.1.2 Use of Cloud Data Bank

7.1.2.1 Procedures

Simulation of cloud influence on specified sensor systems and mission objectives can be readily performed with considerable sophistication. For purposes of illustration, the overall logic employed for a Monte Carlo simulation of an infrared mission to provide SST maps within a specified cloud region will be described. All distribution tables are first organized as cumulative probabilities in ascending order of cloud cover.

Figure 7-2 is a block diagram of the program. Mission iteration number, NOQ, and pass number, n, are initialized. The first draw is made from the unconditional table for the appropriate region by finding which cloud group probability interval contains the random number, RAN. If the cloud group selected, C(1), is number 1 (clear), a suitable tabulation is made to indicate that complete coverage occurred with one pass, and another mission is initiated. If the cloud group is other than number 1, a photo coverage percentage, B, is assigned and the pass number is incremented by 1. A new cloud cover is drawn from the temporal conditional cloud table, using the row designated by the cloud cover drawn on the previous pass (given), and the column designated by a newly selected RAN. The new cloud cover is then used to calculate the incremented clear sky coverage ΔB.

Table 7-1

Cloud Statistics, Gulf Stream Region, June

CLIMATOLOGICAL REGION NUMBER 13 STATISTICS FOR MONTH 6

	UNCONDITIONAL PROBABILITIES TIME (LST)									CONDITIONAL PROBABILITIES 24 HOUR TEMPORAL						CONDITIONAL PROBABILITIES 200 NM SPATIAL				
	01	04	07	10	13	16	19	22		1	2	3	4	5		1	2	3	4	5
1	.01	.04	.02	.01	.01	.01	.02	.01		1	.0	.27	.06	.40	.27	1	.10	.10	.25	.35	.20
2	.14	.17	.15	.08	.10	.11	.12	.10	GIVEN	2	.0	.20	.11	.23	.46	GIVEN 2	.14	.20	.40	.16	.10
3	.07	.09	.08	.08	.07	.08	.05	.06		3	.01	.15	.06	.32	.46	3	.17	.10	.17	.40	.16
4	.33	.23	.23	.33	.32	.33	.34	.38		4	.01	.14	.07	.35	.43	4	.02	.02	.12	.34	.50
5	.45	.47	.52	.50	.50	.47	.47	.45		5	.02	.09	.07	.30	.52	5	.01	.05	.06	.07	.81

CLIMATOLOGICAL REGION NUMBER 20 STATISTICS FOR MONTH 6

	UNCONDITIONAL PROBABILITIES TIME (LST)									CONDITIONAL PROBABILITIES 24 HOUR TEMPORAL						CONDITIONAL PROBABILITIES 200 NM SPATIAL				
	01	04	07	10	13	16	19	22		1	2	3	4	5		1	2	3	4	5
1	.0	.01	.01	.0	.02	.01	.0	.0		1	.01	.14	.0	.14	.71	1	.48	.37	.04	.07	.04
2	.08	.07	.08	.06	.10	.12	.05	.05	GIVEN	2	.01	.15	.09	.40	.35	GIVEN 2	.31	.48	.14	.05	.02
3	.04	.04	.05	.04	.06	.02	.04	.04		3	.02	.21	.09	.37	.31	3	.0	.33	.34	.33	.0
4	.34	.35	.32	.30	.24	.27	.33	.35		4	.01	.07	.03	.34	.55	4	.0	.15	.25	.50	.10
5	.54	.53	.54	.60	.58	.58	.58	.56		5	.0	.07	.04	.28	.51	5	.0	.10	.15	.25	.50

Table 7-2

Cloud Statistics, Gulf Stream Region, October

CLIMATOLOGICAL REGION NUMBER 13 STATISTICS FOR MONTH 10

	UNCONDITIONAL PROBABILITIES TIME (LST)									CONDITIONAL PROBABILITIES 24 HOUR TEMPORAL						CONDITIONAL PROBABILITIES 200 NM SPATIAL				
	01	04	07	10	13	16	19	22		1	2	3	4	5		1	2	3	4	5
1	.03	.07	.04	.0	.0	.01	.01	.0		1	.18	.27	.0	.18	.37	1	.61	.04	.13	.13	.09
2	.17	.15	.13	.07	.07	.07	.09	.09	GIVEN	2	.07	.17	.09	.26	.41	GIVEN 2	.50	.40	.05	.05	.0
3	.09	.08	.11	.06	.10	.09	.10	.08		3	.03	.12	.10	.32	.43	3	.05	.15	.55	.20	.05
4	.29	.27	.26	.44	.47	.47	.44	.43		4	.01	.10	.10	.40	.39	4	.04	.0	.16	.60	.20
5	.42	.43	.46	.43	.36	.36	.36	.40		5	.0	.11	.11	.39	.39	5	.05	.03	.05	.30	.57

CLIMATOLOGICAL REGION NUMBER 20 STATISTICS FOR MONTH 10

	UNCONDITIONAL PROBABILITIES TIME (LST)									CONDITIONAL PROBABILITIES 24 HOUR TEMPORAL						CONDITIONAL PROBABILITIES 200 NM SPATIAL				
	01	04	07	10	13	16	19	22		1	2	3	4	5		1	2	3	4	5
1	.01	.01	.0	.03	.02	.04	.05	.01		1	.22	.33	.07	.19	.19	1	.76	.05	.05	.05	.09
2	.18	.16	.13	.28	.31	.30	.32	.16	GIVEN	2	.04	.39	.14	.25	.18	GIVEN 2	.17	.17	.08	.08	.50
3	.14	.12	.14	.12	.14	.10	.13	.14		3	.01	.22	.18	.33	.26	3	.13	.12	.15	.30	.30
4	.45	.45	.45	.29	.24	.25	.23	.45		4	.01	.18	.14	.41	.26	4	.14	.09	.14	.45	.18
5	.22	.26	.28	.28	.29	.31	.27	.24		5	.02	.14	.12	.36	.36	5	.13	.06	.12	.16	.53

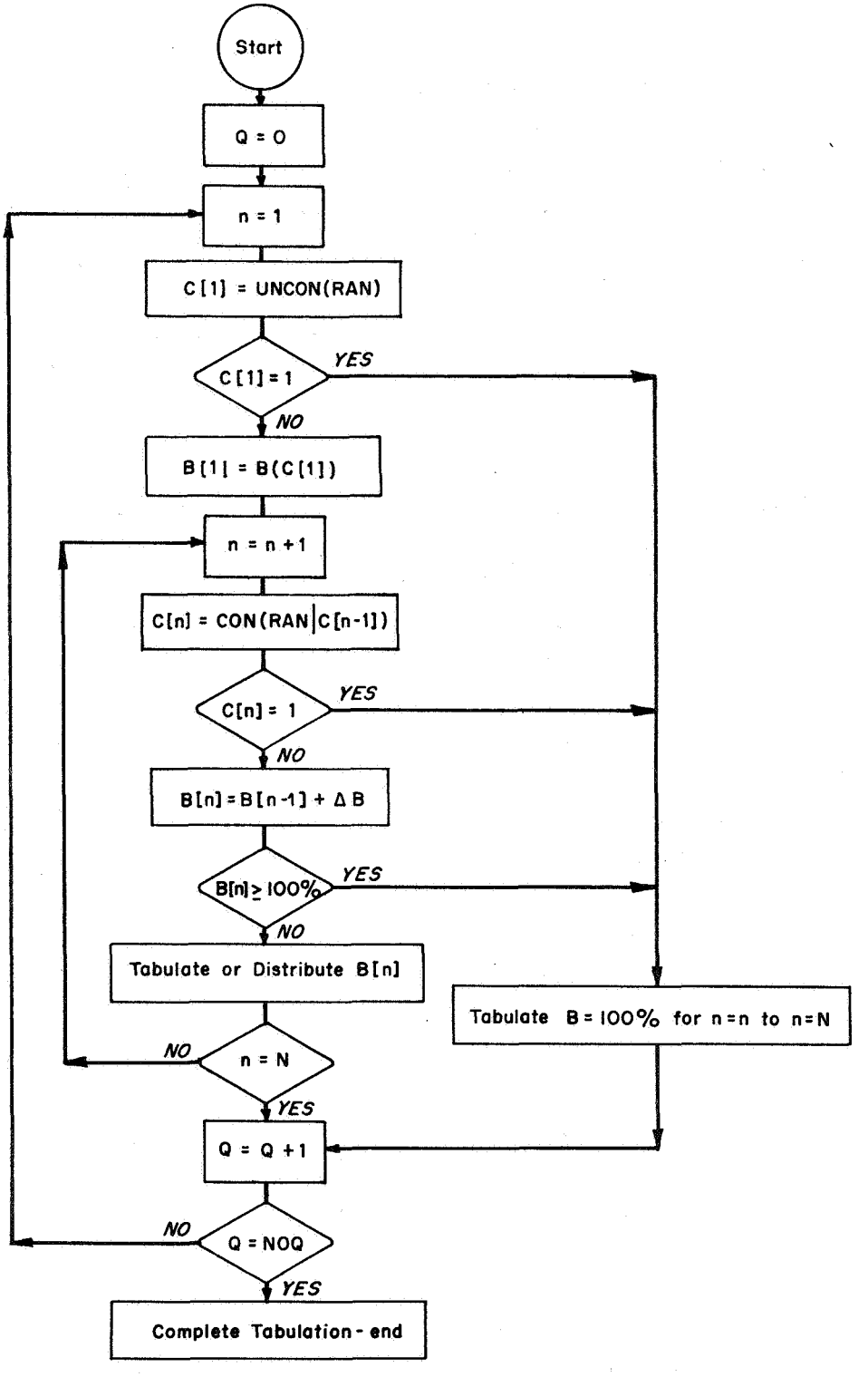

Figure 7-2 Monte Carlo Program to Generate Probability Distribution of Infrared Coverage

The incremental photo coverage is a stochastic function of the existing photo coverage and the new cloud group. The form of the function depends upon the dissection of the cloud, which can be estimated from the original cloud cover distribution. If we assume that the clouds are always randomly scattered over the whole area, the incremental photographic coverage of pass n is given by:

$$\Delta B(n) = [1 - B(n-1)]\,[1 - A(n)]$$

where $\Delta B(n)$ is the incremental photo coverage added on the nth pass,
$B(n-1)$ is the photo coverage after n-1 passes, and
$A(n)$ is the cloud amount of the nth pass.

The incremental coverage may add no new information at all, or it may result in total coverage. If it does, the 100% coverage branch is followed. If not, the coverage achieved is recorded as a function of the number of passes. This process is repeated for the N passes allowed in the total mission. The simulation is iterated NOQ times. This simulation approach can provide a quantitative measure of the influence of cloud on specified mission objectives on a regional basis.

7.1.2.2 Application to Gulf Stream

Using the cloud statistics from Tables 7-1 and 7-2, the Monte Carlo Program described above was applied to the Gulf Stream region for the months of June and October. The results are presented in Figures 7-3 and 7-4. Figure 7-3 shows the anticipated cloud coverage for the month of June assuming daily noontime MRIR observations. A simulation of the daily HRIR nighttime observations for the month of October is presented in Figure 7-4. In both cases, a scaled-up area of 300 by 300 n.mi. was employed. Both were computer generated using 300 consecutive mission iterations. The separate curves are labeled by pass number.

The shapes of the curves in Figures 7-3 and 7-4 are generally typical of those developed for other geographic areas. From Figure 7-3, for example, we see that if we are restricted to three-day composites due to changing temperature patterns, we have only a 10% chance of seeing 75% of the area. If a 90% coverage is demanded, there is only a 60% probability of achieving that much coverage, even after eight days. The sharp drop-off of the curves in both figures shows that it may be unrealistic to hold out for very high cloud-free coverage.

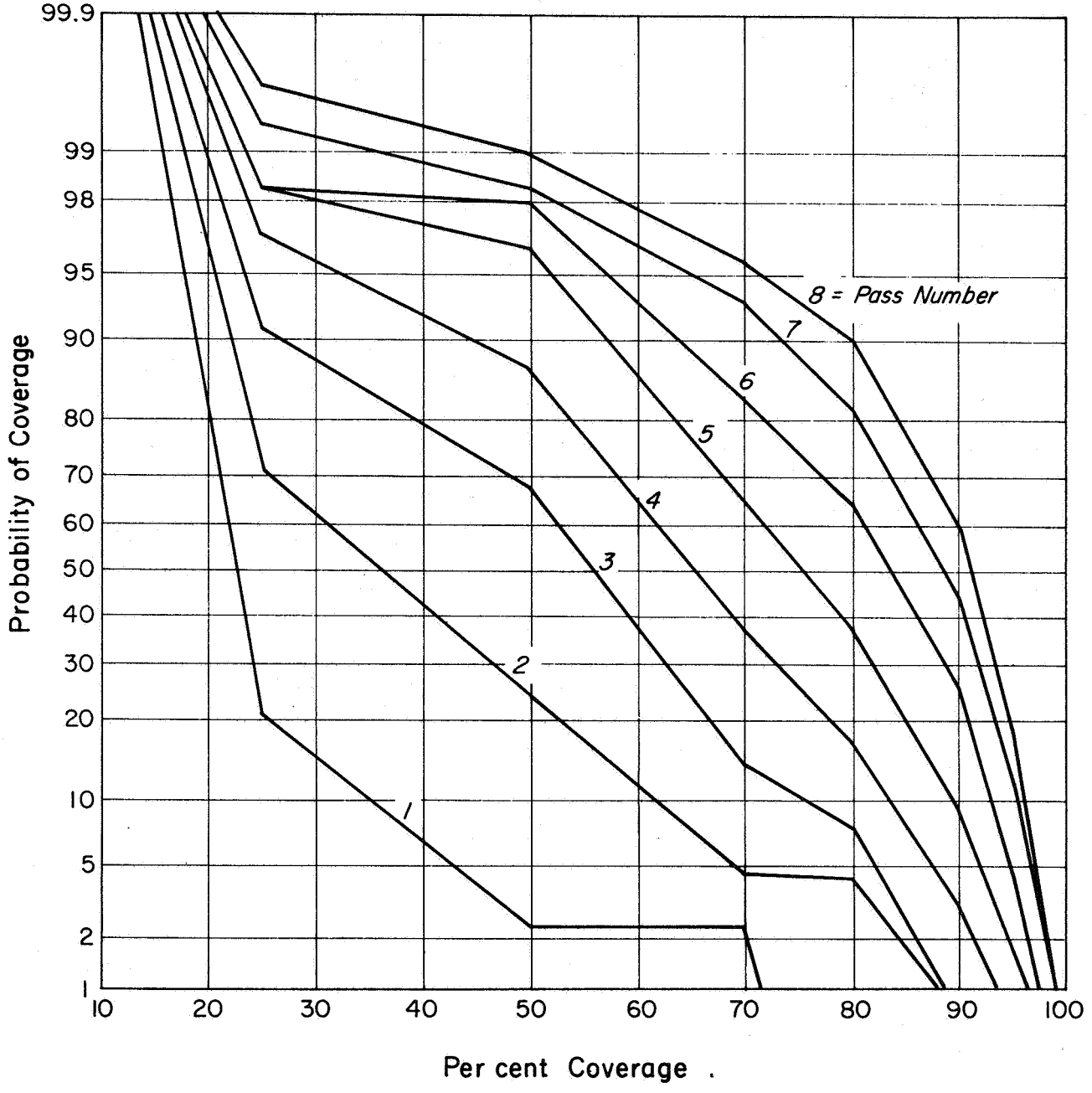

Figure 7-3 Statistics for Gulf Stream Region, Noon to Noon Passes, June

6931

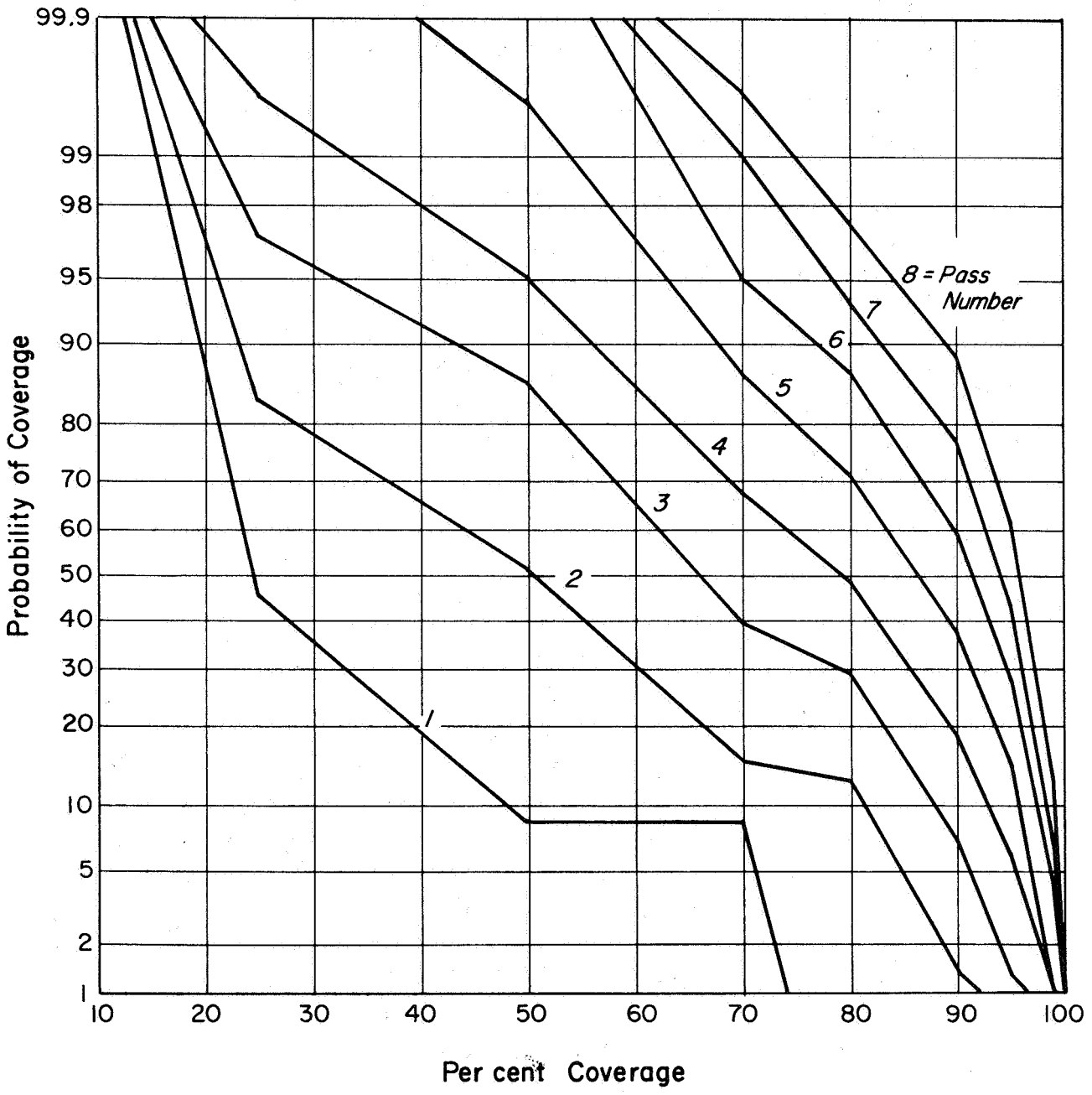

Figure 7-4 Statistics for Gulf Stream Region, Midnight to Midnight Passes, October

The increased coverage available in the October nighttime passes (Fig. 7-4) reflects both seasonal and diurnal effects. Now there is a 35% probability of seeing 75% of the area in three passes, and an almost 90% probability after 8 passes of seeing 90% of the area. Thus, it is quite possible that the development of a nighttime cloud discrimination ability will more than double the usable data. Even using the nighttime data, however, it can be seen that certain experiments dealing with short-term, transient oceanographic features will have a very low probability of success. As will be seen in the following section, these statistical results are verified by the MRIR analyses.

7.1.3 MRIR Verification of Cloud Statistics

Twenty consecutive daytime MRIR passes over the Gulf Stream region from 10 to 30 June 1966 were run using the modified programs with a 15% albedo clear-cloudy cut off. The boundaries of the area considered were 34° to 44° North and 58° to 78° West. This region was subdivided into seven smaller areas 5° on a side to approximate the 300 × 300 n.mi. area for which the computer statistics were generated. The 1:5 million Mercator map scale was used. Only ocean areas were included in the analyses. (The relatively higher reflectance of land areas is often mis-interpreted as cloud.)

The procedure was to form frequency distributions of area coverage using all 20 passes. The passes were considered singly and in groups of five consecutive passes, thereby simulating the unconditional statistics for a single pass, and five-pass coverage respectively. Data for 15 overlapping sets of five consecutive passes each, were generated for each of the seven sub-areas. Figure 7-5 presents a comparison of the unconditional statistics for a 300 × 300 n.mi. area as generated from the cloud data bank, and as measured in the 20 individual passes. The shift toward lesser cloud amounts reflects clearer than average sky conditions prevailing over the Gulf Stream area for the month of June 1966. This effect is also seen in the measured five-pass coverage shown in Figure 7-6. The measured data present a much more optimistic picture of clear sky probabilities. It should be recalled, however, that the measured June data are representative of only a single year, while those derived from the cloud data bank are based on 10 to 15 years of observations. Considering the differences in the data base, and in the number of independent iterations, it is felt that the MRIR results support the basic statistical procedures.

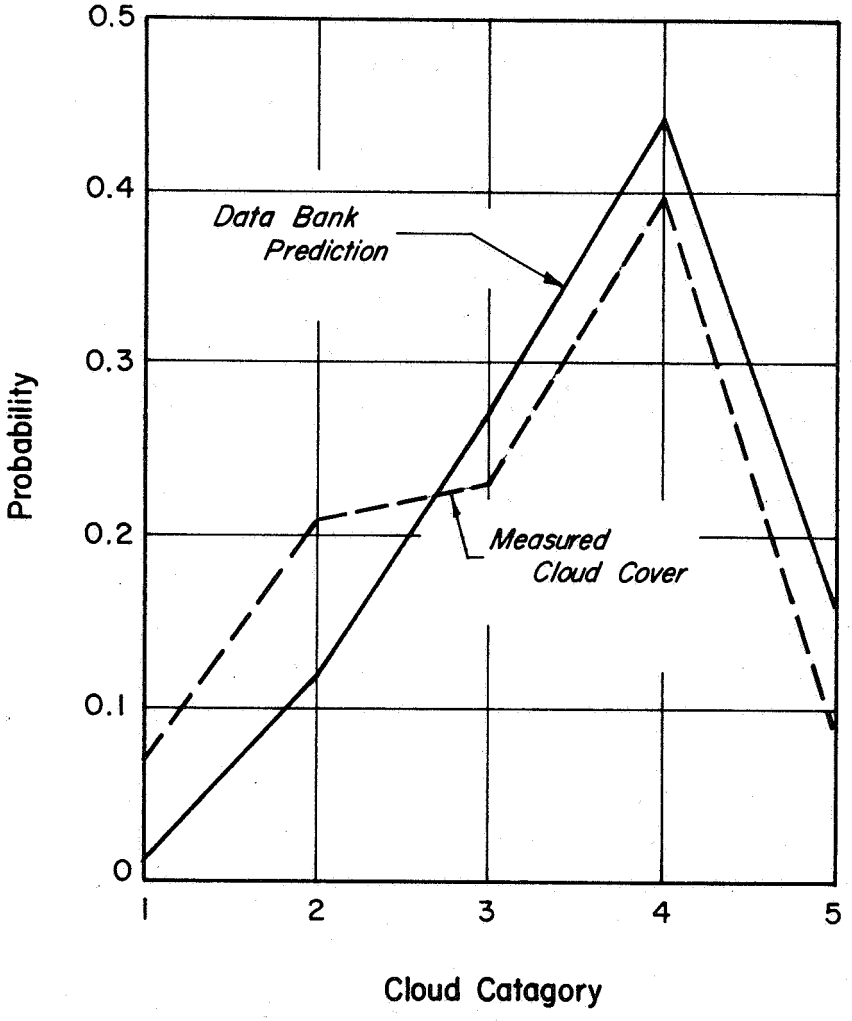

Figure 7-5 Comparison of Computed and Measured Unconditional Statistics

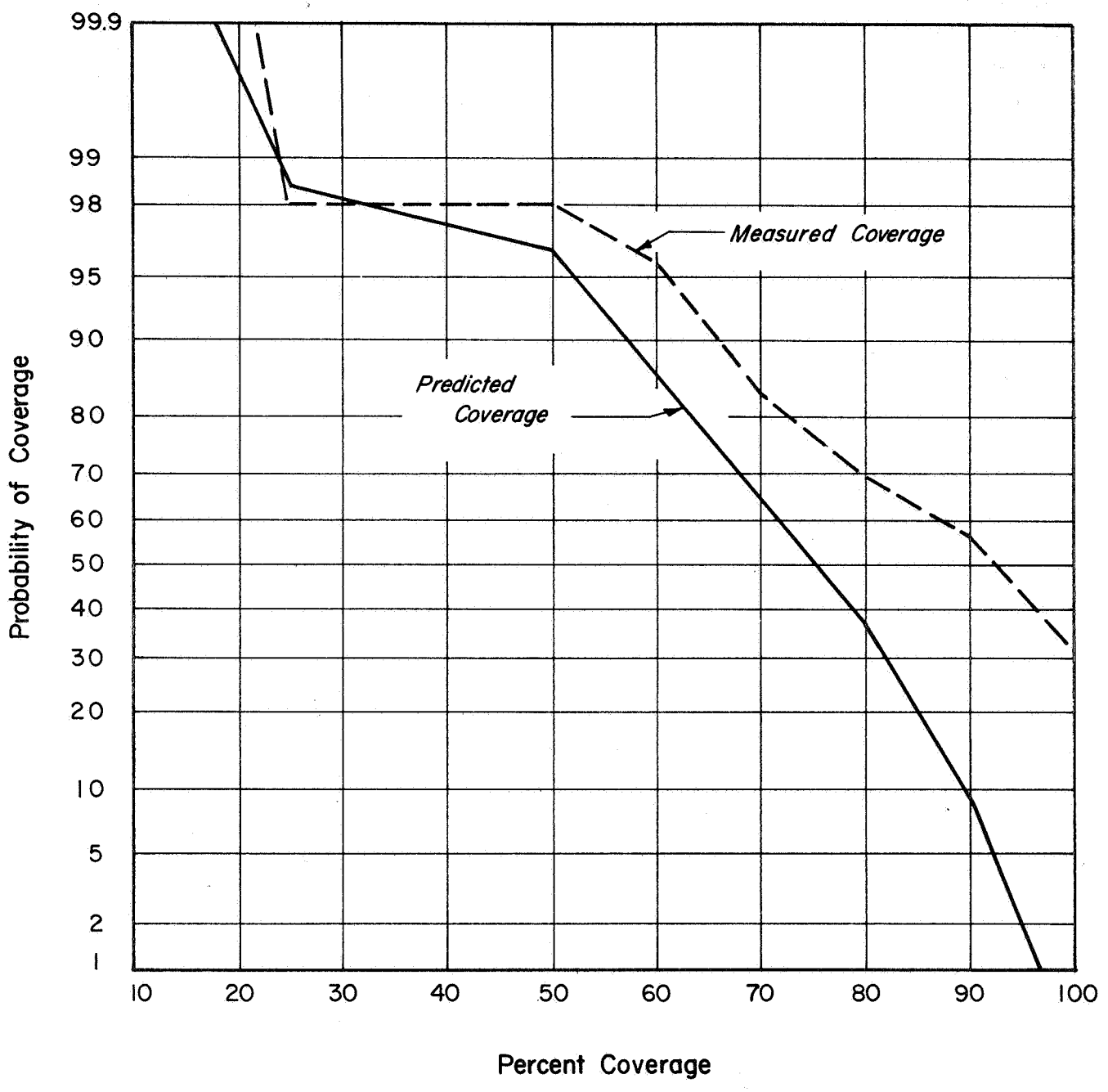

Figure 7-6 Comparison of Computed and Measured Five-Pass Coverage

6988

The shape of the two curves in Figure 7-6 are quite similar, while the upward displacement of the "measured" curve can be at least partially accounted for by the unusually cloud-free conditions evident in Figure 7-5. It is nevertheless possible, however, that a more extensive measurement program could reveal a pessimistic tendency in the currently used cloud model. For example, in the equation presented for the incremental coverage occurring on the nth pass, $\Delta B(n)$, in Section 7.1.2.1, unless the cloud amount on the nth pass, A(n), is zero, complete coverage will never be achieved. For this reason, it is now felt that straight line extrapolation of the predicted curves beyond 90% coverage may be more realistic. It is nevertheless felt that the current techniques can provide valid information as to the feasibility of a variety of potential remote sensing projects.

7.2 The Gulf Stream Region

7.2.1 Description

Any description of the Gulf Stream region presented here must necessarily be confined to a brief general discussion of its physical characteristics. An excellent review of the whole Gulf Stream problem may be found in the introductory textbook by Von Arx (1962).

The surface water of the Gulf Stream is mainly derived from the southern part of the North Equatorial Current. Water driven by the trades moves slowly across the equatorial North Atlantic, through the Antilles into the Caribbean Sea, and through the Yucatan Channel into the southeastern portion of the Gulf of Mexico before entering the Straits of Florida and the Gulf Stream system.

From Cape Hatteras it extends toward the northeast at a mean bearing of about 070 degrees. To the southeast of this meandering current are the relatively uniform waters of the Sargasso Sea, while to the northwest are the slope waters off the eastern continental shelf. The main current has an effective width of from 25 to 40 n.mi., and a velocity ranging from 45 to 140 n.mi. per day. The meander patterns tend to migrate and amplify downstream, becoming increasingly complex, often breaking off to form warm or cold water eddies. The average wavelength of these meanders is about 200 n.mi., while the mean peak-to-peak height is 70 n.mi. Propagating speed of the meanders themselves seems to range from 4 to 10 n.mi. per day (Naval Oceanographic Office, 1967), although recent evidence suggests that they may at times become quasi-stationary (Wilkerson, 1967). Temperature

gradients of 5 to 10°K per 10 n.mi. exist across the northeastern boundary (north wall) of the stream. The temperature gradients tend to be smaller in the summer and fall when they are masked by intense surface heating of the cold Labrador water.

7.2.2 HRIR Observations

In the 174 day history of HRIR observations, the Gulf Stream was detected on approximately 75 separate occasions. For possible use by other investigators, Table 7-3 presents a listing of these sightings giving the pass number, the date, and a four-level subjective rating as to the usefulness of the data ranging from poor to excellent. Almost 28% of the nighttime sightings occurred during the month of October 1966. Because of this unusually high rate of observation, the October data were chosen for the development of a time history of the Gulf Stream meander movement. Data from 12 passes (11 separate days) with a rating of fair or better were run and analyzed for the period 1 through 31 October. (Passes 1848 and 2128 could not be processed due to problems in the digital NMRT's.)

Figures 7-7 through 7-14 indicate the determined position of the north wall of the Gulf Stream for those days where a sufficient portion of it could be positively identified. A solid line is used to indicate the stream boundary when its location is reasonably certain. Dashed lines are used to bridge areas of cloud contamination. These interpolations were made on the basis of maintaining internal pattern consistency, and occasionally maintaining pattern consistency from pass to pass. When the cloud cover becomes sufficiently wide-spread so that extrapolation of the stream boundary is more or less arbitrary, no boundaries are shown. In all cases, geographic referencing was achieved by alligning the temperature patterns at the left of the analyses with the eastern coastline of the United States.

The first analysis (Fig. 7-7) is that of HRIR pass 1889 on 4 October 1966. Three meanders are apparent beginning off the coast of Cape Hatteras. (There is some evidence that the first two meanders may actually comprise only one meander with some cloud contamination occurring at its northern-most peak.) The third of the meanders is represented in dashed lines, since its exact position could not be determined from this analysis. The location indicated is based upon the position of a large meander observed in the following analysis.

Table 7-3

Nighttime HRIR Gulf Stream Observations

Pass	Date (1966)	Rating	Pass	Date (1966)	Rating
64	20 May	Poor	1583	11 September	Poor
144	26 May	Poor	1596	12 September	Good
197	30 May	Fair	1609	13 September	Fair
223	1 June	Poor	1622	14 September	Poor
238	2 June	Excellent	1675	18 September	Good
251	3 June	Excellent	1676	18 September	Good
275	4 June	Fair	1742	23 September	Poor
291	6 June	Good	1756	24 September	Fair
305	7 June	Fair	1795	27 September	Fair
411	15 June	Good	1836	30 September	Poor
450	18 June	Poor	1848	1 October	Excellent
463	19 June	Fair	1849	1 October	Poor
504	22 June	Excellent	1889	4 October	Fair
584	28 June	Excellent	1929	7 October	Good
624	1 July	Excellent	1942	8 October	Excellent
664	4 July	Fair	1955	9 October	Good
744	10 July	Poor	1995	12 October	Excellent
837	17 July	Fair	2008	13 October	Good
890	21 July	Poor	2009	13 October	Good
904	22 July	Good	2021	14 October	Poor
917	23 July	Fair	2022	14 October	Excellent
1037	1 August	Good	2035	15 October	Good
1051	2 August	Good	2048	16 October	Poor
1263	18 August	Fair	2062	17 October	Poor
1276	19 August	Good	2115	21 October	Good
1396	28 August	Fair	2128	22 October	Good
1410	29 August	Poor	2208	28 October	Excellent
1423	30 August	Good	2222	29 October	Good
1476	3 September	Fair	2235	30 October	Poor
1489	4 September	Fair	2248	31 October	Poor
1529	7 September	Good	2315	5 November	Fair
1543	8 September	Poor	2355	8 November	Poor
1569	10 September	Poor	2381	10 November	Poor
1582	11 September	Poor	2448	15 November	Good

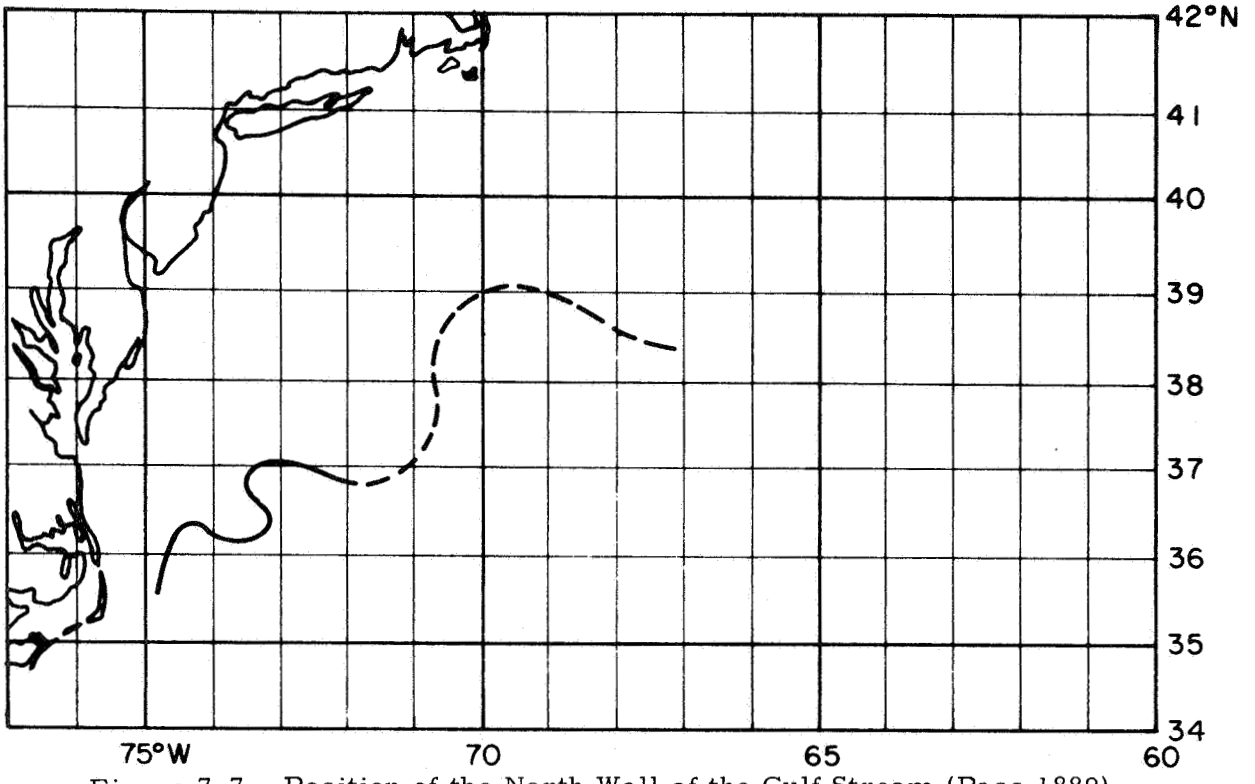

Figure 7-7 Position of the North Wall of the Gulf Stream (Pass 1889)

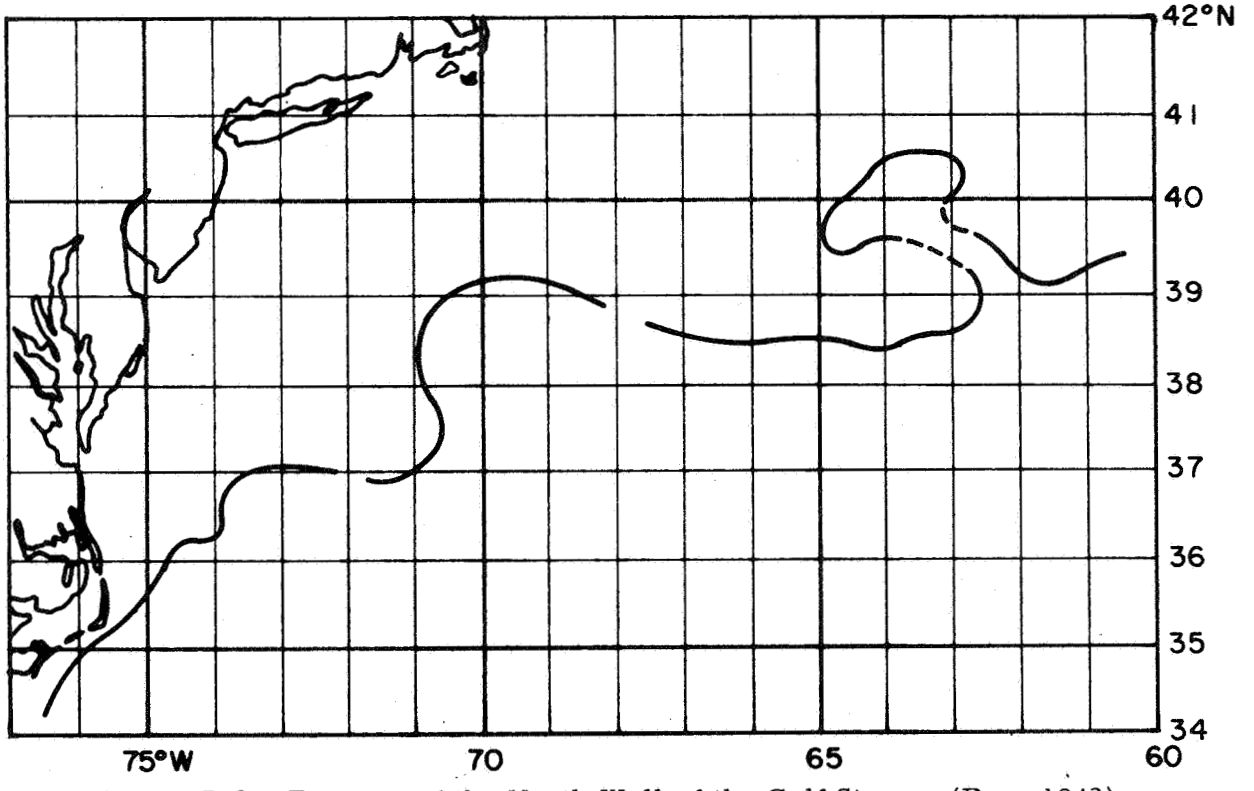

Figure 7-8 Position of the North Wall of the Gulf Stream (Pass 1942)

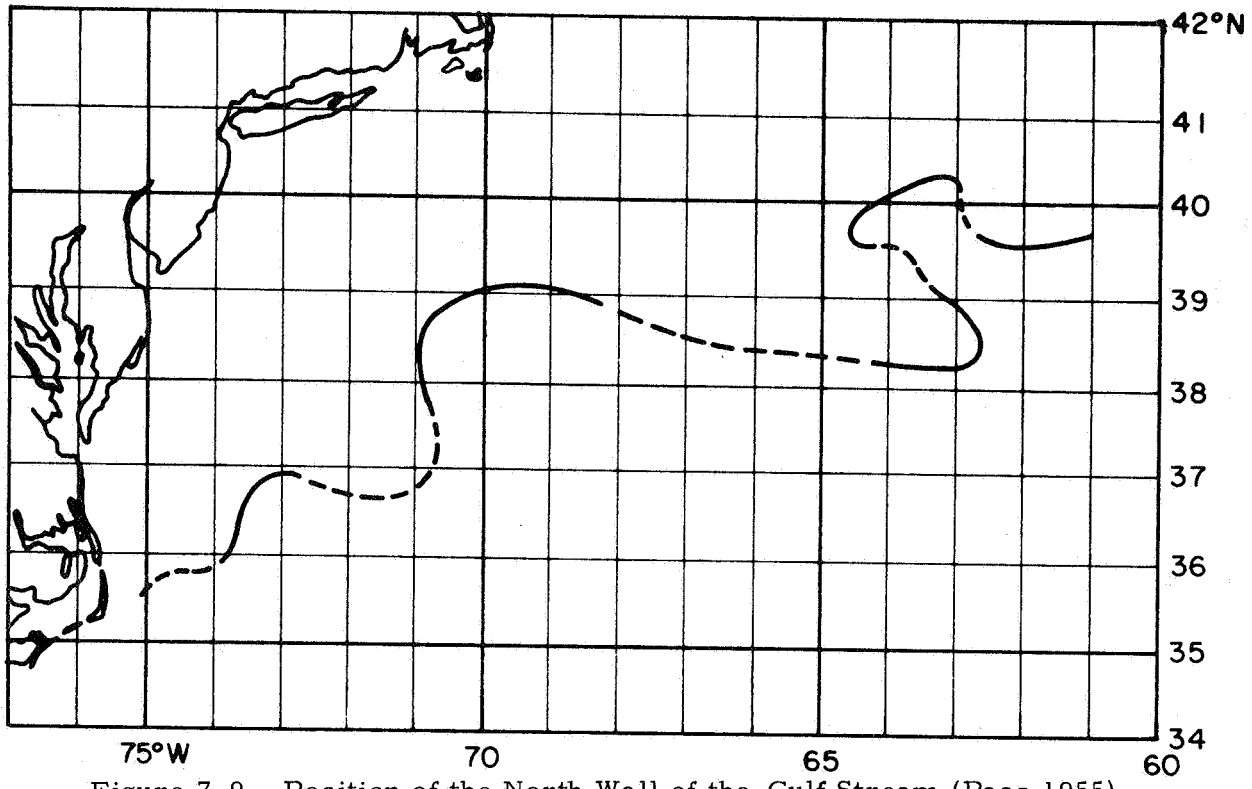

Figure 7-9 Position of the North Wall of the Gulf Stream (Pass 1955)

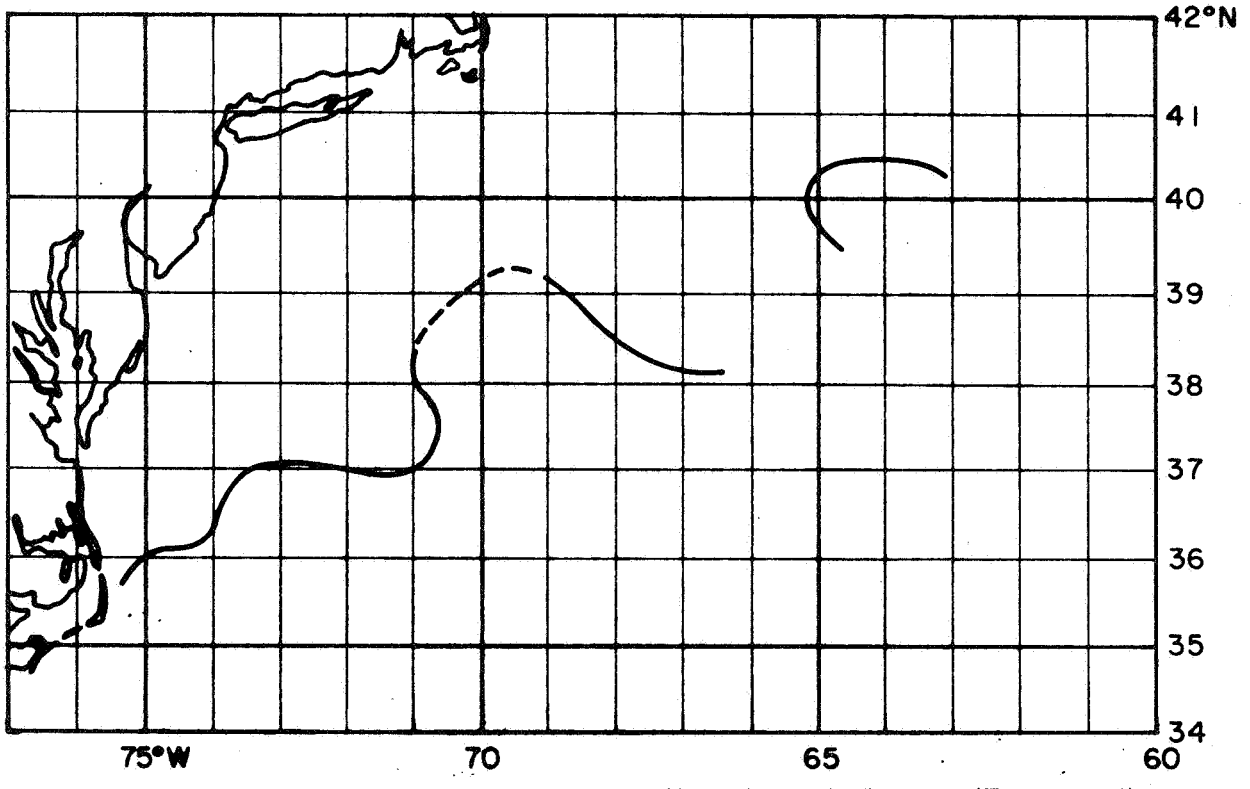

Figure 7-10 Position of the North Wall of the Gulf Stream (Pass 1995)

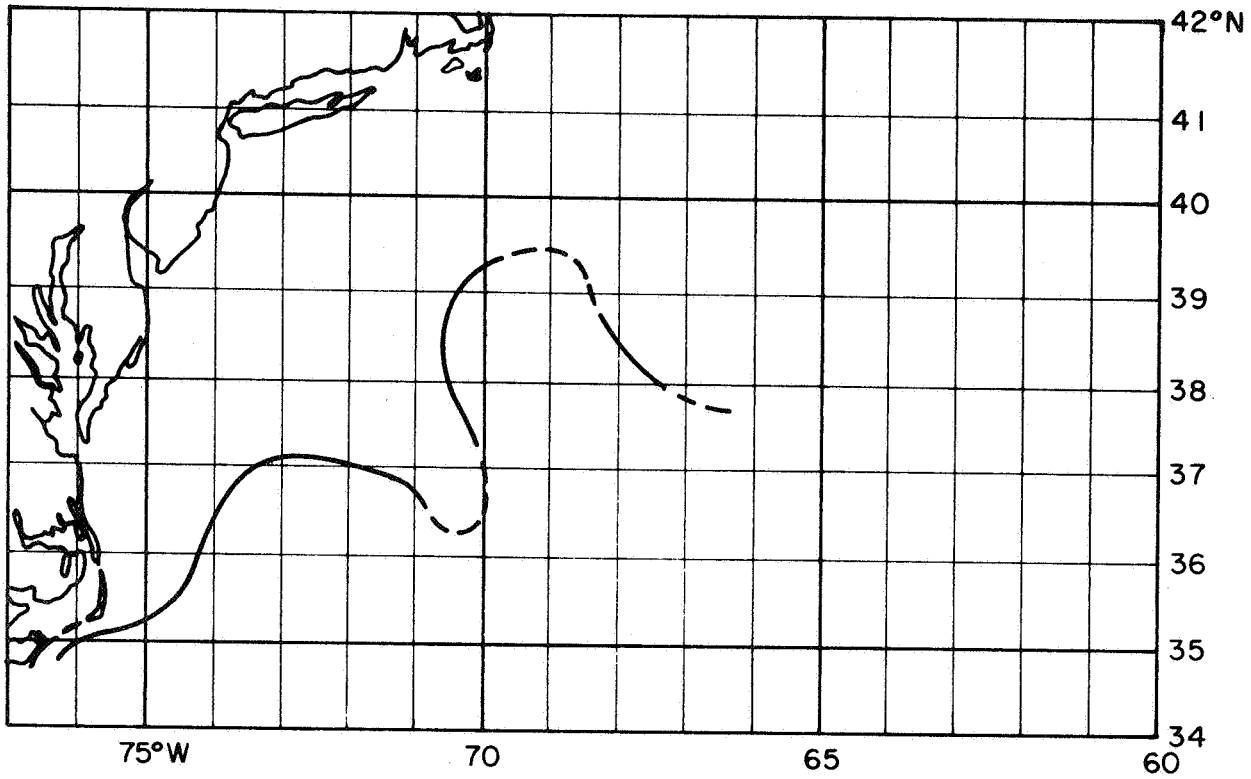

Figure 7-11 Position of the North Wall of the Gulf Stream (Pass 2022)

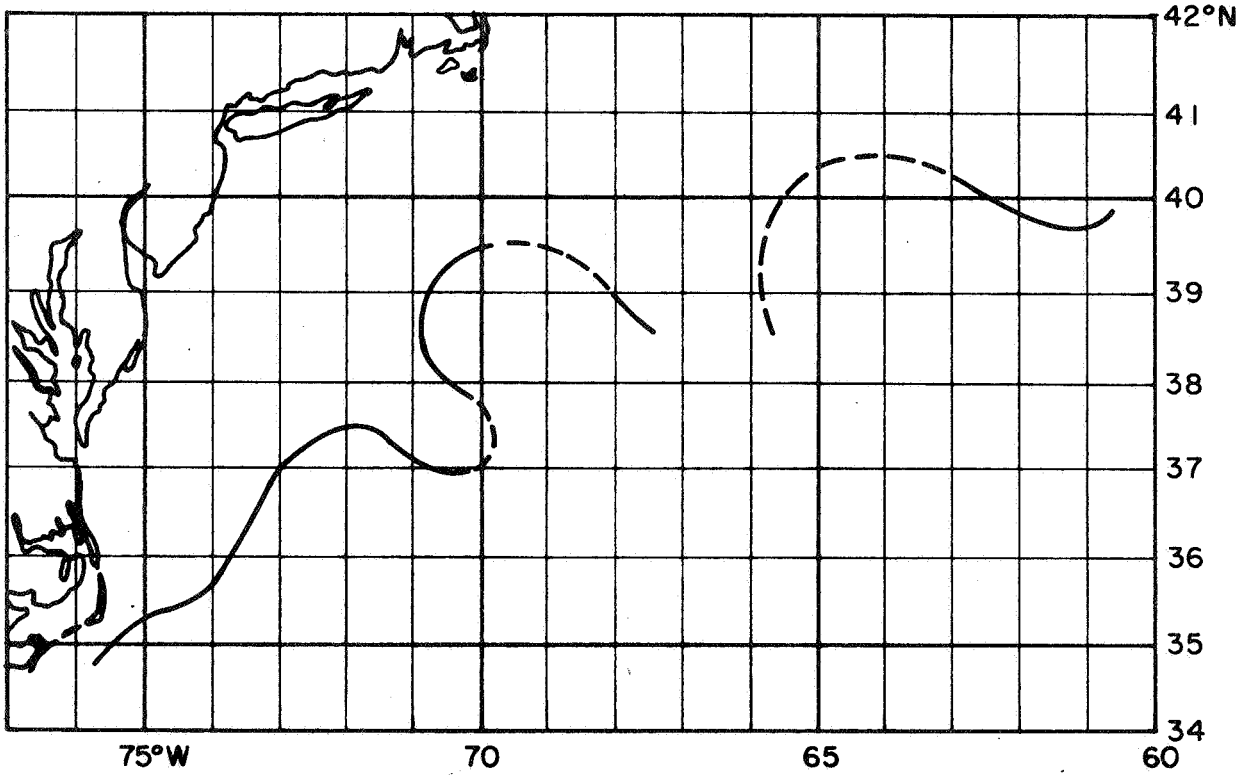

Figure 7-12 Position of the North Wall of the Gulf Stream (Pass 2035)

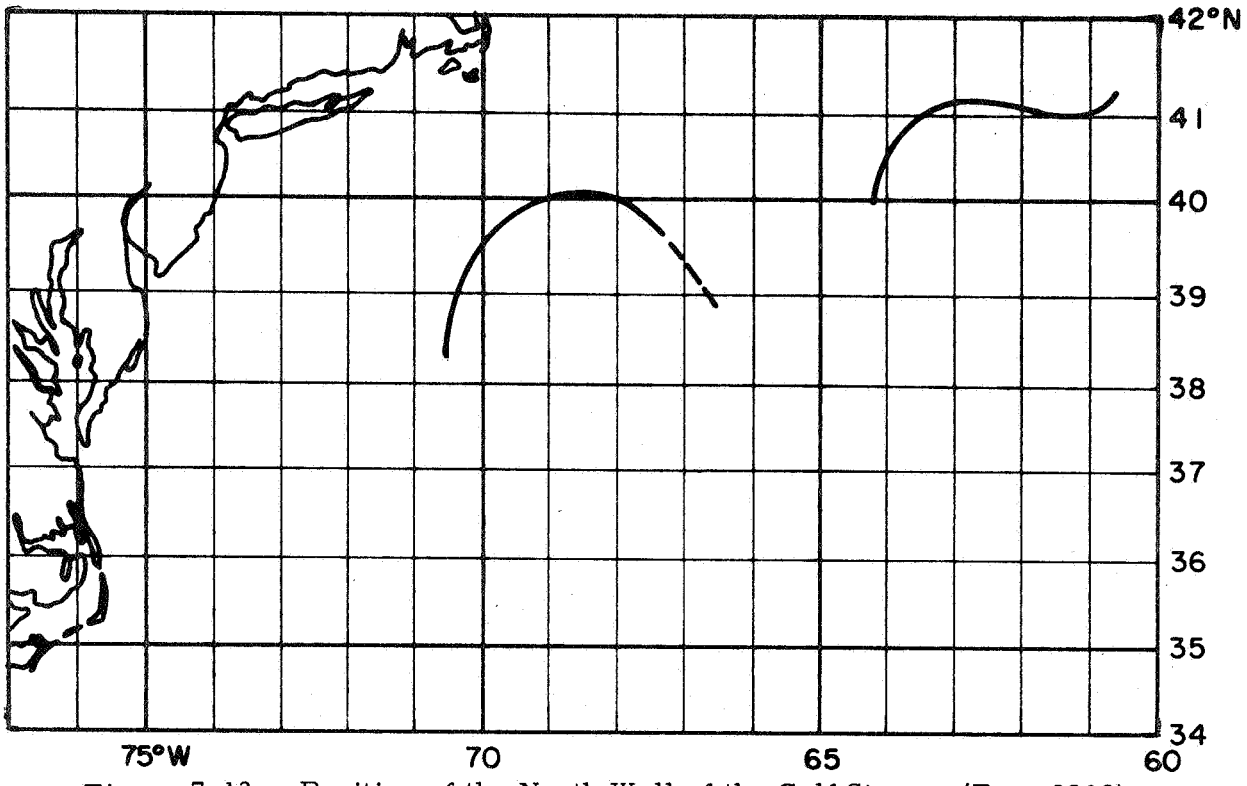

Figure 7-13 Position of the North Wall of the Gulf Stream (Pass 2208)

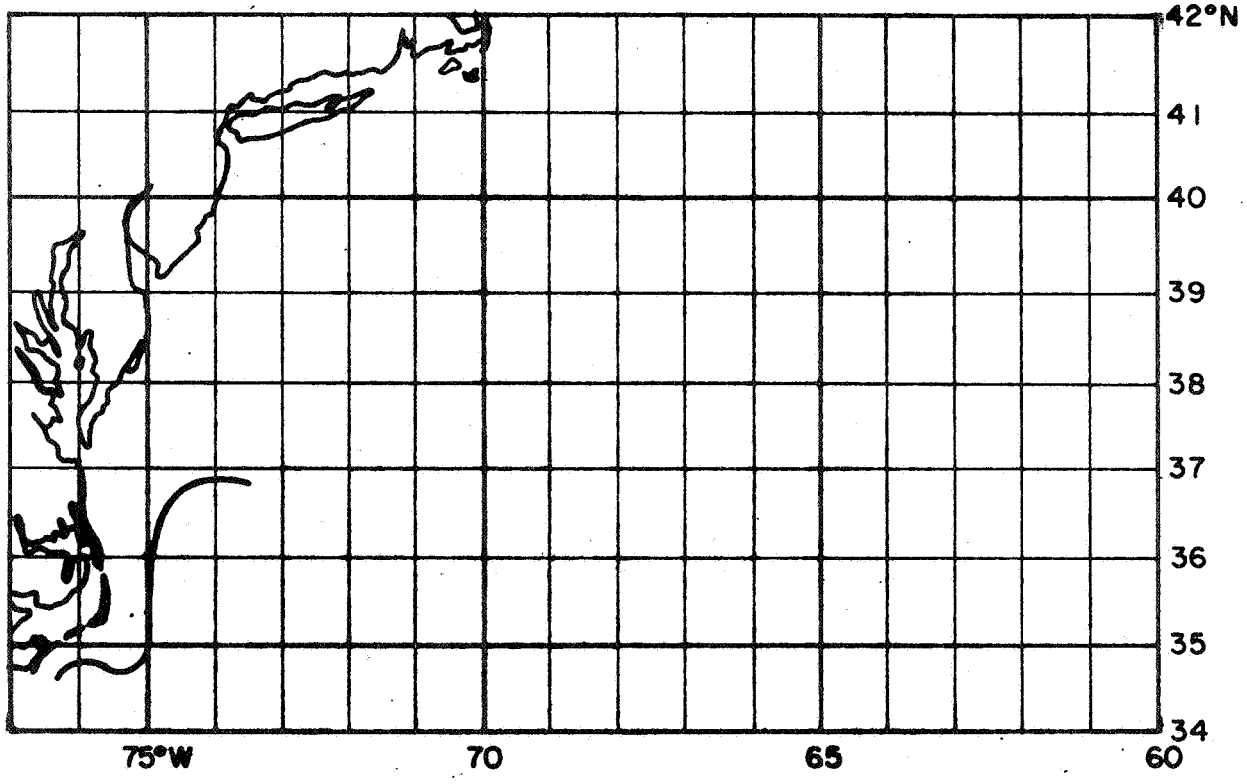

Figure 7-14 Position of the North Wall of the Gulf Stream (Pass 2222)

Pass 1942, occurring four days later on 8 October is shown next (Fig. 7-8). This time evidence of three major meanders can be clearly seen. The first of these seems to be comprised of two smaller meanders, although cloud contamination may again be at fault. The third meander extends far to the north and may represent the formation of a warm water eddy. From the leading edges of the first major meander in the last two analyses, a barely discernible meander movement of 4 n. mi. per day was inferred. The Digital Color Printer analysis of pass 1942 may be seen in Figure 7-15. The overlay shows the eastern coastline, as well as the stream boundary, and the location of cloud contamination. The individual colors represent 2°K temperature intervals beginning with 297 to 298°K (and higher) at the warm (red) end.

In the analysis of pass 1955 (Fig. 7-9) on the following day, four separate meanders are visible. Again, the last of these may actually represent the formation of a warm water eddy.

The linkage between the fourth apparent meander in the next analysis (Fig. 7-10) three days later and the rest of the stream boundary is unclear due to the presence of cloud contamination. Meander movement between the 8th and the 12th of October was too small to measure accurately. A Digital Color Printer analysis of this pass (1995) is presented in Figure 7-16. The color coding and overlay formats remain the same.

In pass 2022 on 14 October (Fig. 7-11) only the first three meanders are visible. Their position is relatively unchanged from the previous analysis.

On the following day in pass 2035 (Fig. 7-12) there is again evidence of a well developed fourth meander. Comparison of this pass with that of 8 October revealed a difference in speed between individual meanders with higher speed tending to occur near the coast. The meander located at 73°W and 37°N in Figure 7-8 moved with an apparent speed of almost 8 n. mi. per day during the seven intervening days, while the next meander toward the northeast moved at about half that rate. In view of the downstream size amplification of the meanders, this result seems quite reasonable.

The next usable pass occurred 13 days later (pass 2208). Figure 7-13 shows this analysis where only the last two meanders are detectable. Comparison with Figure 7-12 indicates a 4 to 5 n. mi. per day movement of both these meanders.

The final analysis (Fig. 7-14) reveals only a short portion of the Gulf Stream boundary as recorded on pass 2222 on 29 October. No direct correlation could be found between these individual meanders and those evident in the western portion of the 15 October analysis.

The wavelength of the faster moving near-shore meanders ranged from 60 to 100 n. mi., and averaged about 85 n. mi.. Assuming a propagation velocity of 8 n. mi. per day, it is clear that in order to maintain the integrity of the individual meanders when compositing multiple passes, no more than 4 or 5 days of data should be simultaneously processed. Referring back to Figure 7-4, it can be seen that if a 75% area coverage is desired, there is only a little better than 50% chance that this coverage can be obtained in four passes. Relaxing the time or coverage restrictions would of course, significantly improve the chances of success.

In summary, it has been demonstrated that time histories of synoptic scale sea surface temperature pattern changes can be developed from high resolution spacecraft data. The task could be made far simpler if an automated cloud distinguishing technique were available using a multi-spectral high resolution sensor. Gulf Stream meander movements of 4 to 8 n. mi. per day have been observed, with higher speeds occurring near the shore. Due to the higher speed and shorter wavelength of these near-shore meanders, shorter averaging periods must be employed in the data compositing programs.

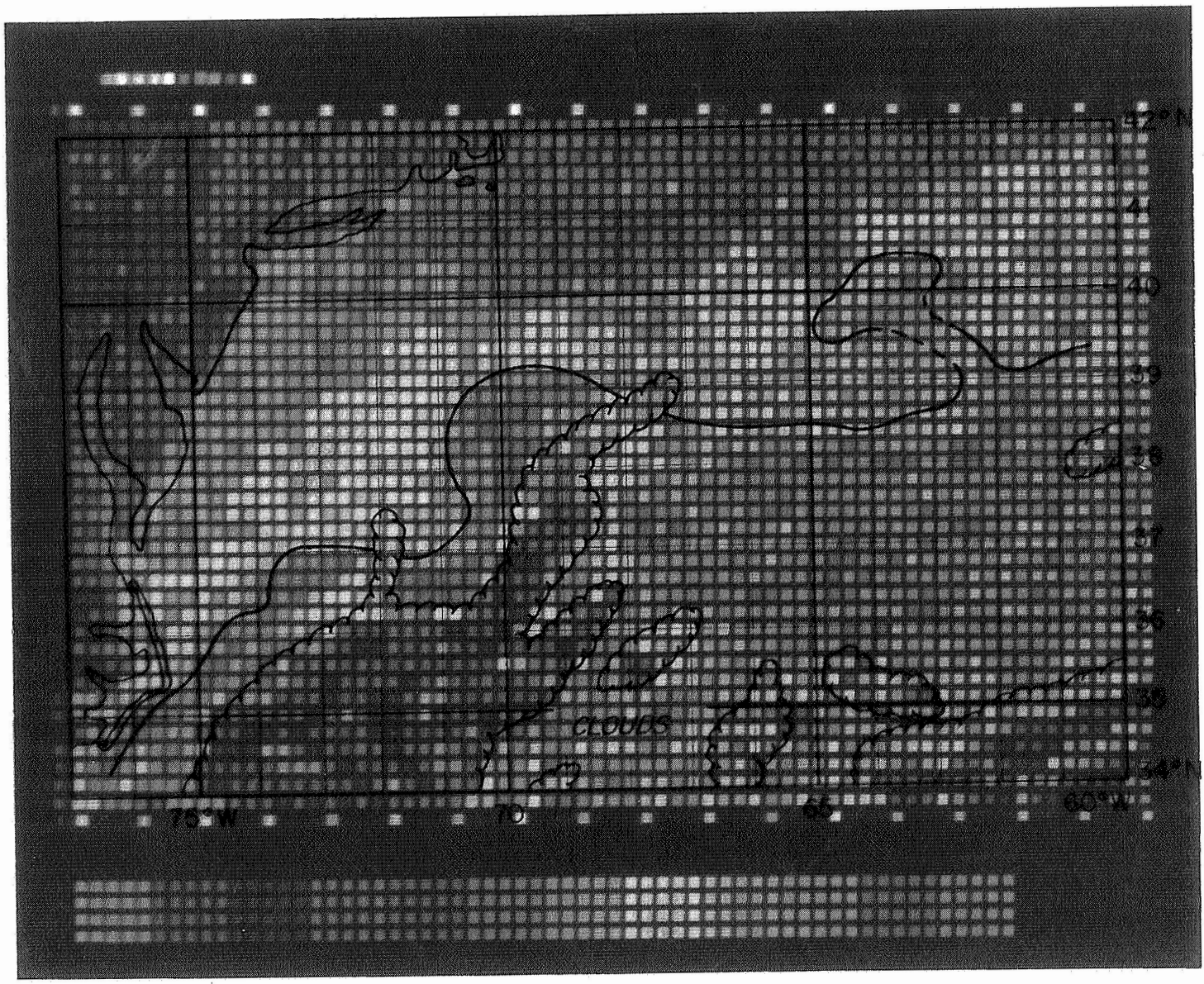

Figure 7-15 Digital Color Printer Output (Nimbus II, Pass 1942)

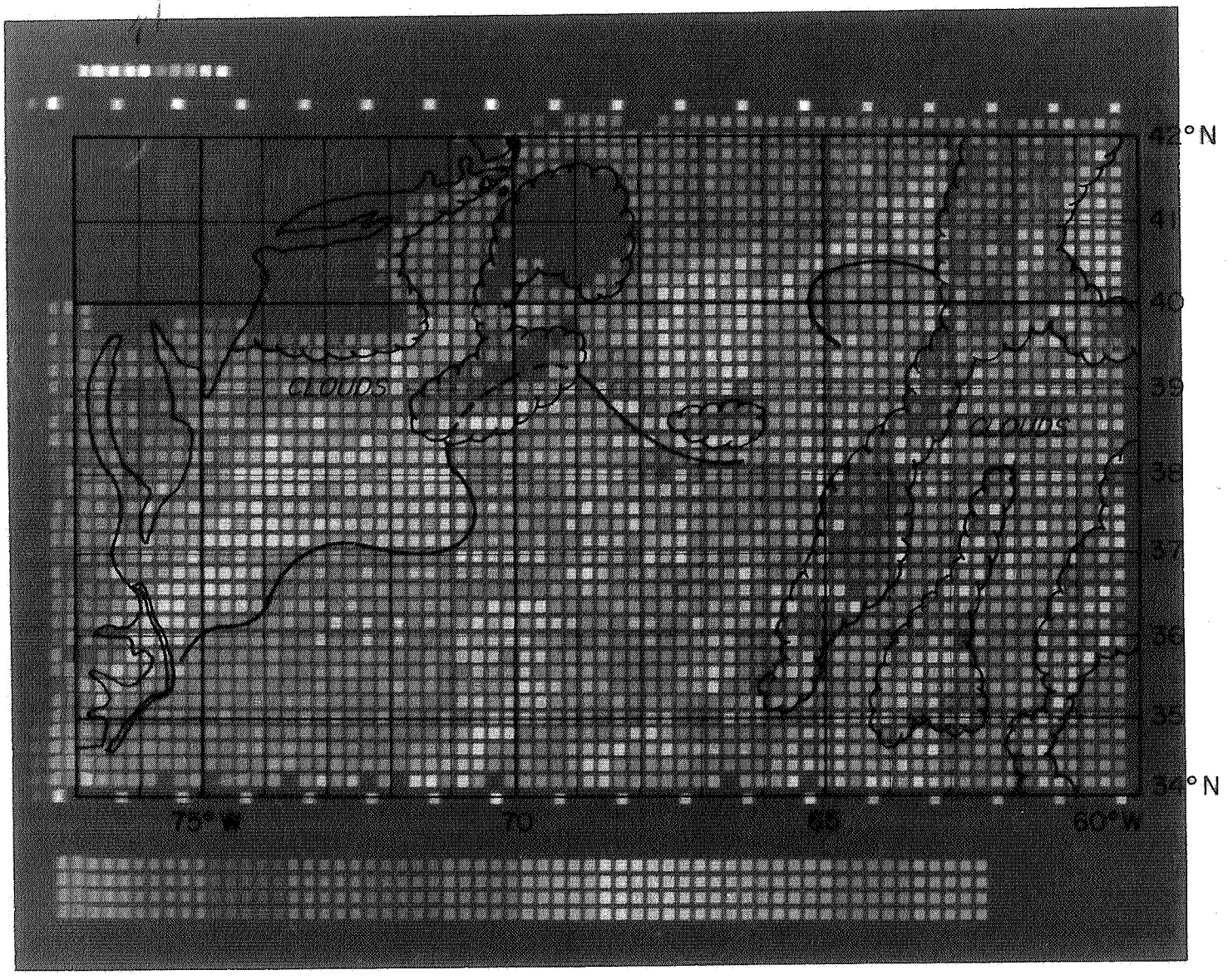

Figure 7-16 Digital Color Printer Output (Nimbus II, Pass 1995)

8. USE OF MANNED OBSERVATIONS IN SEA SURFACE TEMPERATURE DETERMINATION

8.1 Objectives

As has been shown, a desirable feature in the mapping of IR sea surface temperatures is computer recognition and elimination of cloud contaminated data points. Present knowledge of radiometric differences between clear and cloudy regions is as yet insufficient to properly define cloud contamination in all situations. The radiance contrast, in the visible and the IR, between an extensive thick cloud deck and a large clear region is readily discernible in present satellite data. However, this radiance contrast can provide no clear indication of the effects of thin cirroform clouds, or particularly of situations involving scattered cumulus in which the sensor resolution element is only partially filled by clouds. With the data presently available, the identification of these situations is not always possible.

The techniques of using simultaneous measurements in the visible and other spectral regions to establish threshold values for cloud contamination can be optimized only if the characteristics of the transition between clear and cloudy areas are better understood. A clear cut distinction in radiance between cloudy and clear atmosphere does not exist in any wavelength region. However, the trade-off between useful sea surface coverage and the false alarm rate can be optimized if the radiance characteristics of clouds can be determined.

In order to improve current knowledge of these radiance characteristics, interest must be selectively focused on special cloud cover situations. As indicated previously, these include thin cirroform clouds and scattered cumulus. Since these phenomena are essentially targets of opportunity, it would be desirable that measurements and observations be performed by means of a manned satellite. The advantages of manned observation in the conduct of these measurements lies not only in his ability to select the proper targets for observation, but also in his ability to document the situation being observed. With the proper training, his description of the response of the sensors in relation to changing cloud cover situations would be invaluable in subsequent data reduction.

While the primary objective of the proposed measurements is to obtain data to establish better cloud discrimination techniques, a second objective may be achieved through coordination between surface ship stations and the manned satellite.

This is the establishment of calibration functions between satellite values and the conventionally measured sea surface temperatures. The role of the astronaut in this phase of the measurement program is probably not as significant, although his description of the concurrent cloud cover over the ship station would still be useful.

8.2 Measurement and Instrumentation Requirements

The achievement of the experimental objectives as outlined above requires coordinated efforts by the manned spacecraft and by oceanographic ship stations providing the "ground truth" data to aid the interpretation of the satellite observations. Specifically, the following types of measurements and observations are considered to be essential.

Spacecraft Measurements:

a. Radiometric measurements in a visual wavelength region and in a clear atmospheric "window";

b. Color movies of the scene viewed by the radiometer;

c. Voice record of the astronaut's description of the visual appearance of the clouds within the field of view of the sensors.

Oceanographic Ship Station Measurements:

a. Radiometric sea surface temperature in the same wavelength interval as the satellite "window" measurements;

b. "Bucket" sea surface temperature as normally measured;

c. Color photographic record of cloud cover by means of an all-sky camera.

The instrumentation required to achieve these measurements certainly requires no new breakthroughs either in technology or design. With respect to the satellite measurements, the most significant aspect of the equipment design is in the optical coupling of the field of view of the radiometers with that of the camera and the sight through which the astronaut makes his observations at the times of data acquisition. Mechanically, the various sensors should be so linked as to be scanned by a simple manipulative action initiated by the astronaut. A highly desirable feature in the data recording system is the ability to generate event markers at the initiation of the astronaut. This feature would provide time references relating the voice record of the astronaut's description to the changing field of view of the sensors. Furthermore, past experiences with analyses of satellite measurements

indicate that a highly desirable feature in the radiometric design is a means by which the calibration of the sensor can be checked prior to, and subsequent to data acquisition. Systems for on-board calibration built into the sensors or external to the sensors should not be too difficult to design in view of the presence of the astronaut to perform the necessary manipulative actions.

The specification of color photography was dictated by experience in analysis of both color and black and white photographs obtained from space. Color photographs not only make use of brightness contrasts but also of spectral contrasts so that depiction of different features in the field of view is enhanced. This enhancement in the photographs obtained by the astronauts in Gemini and Mercury photography experiments is quite evident.

Shipboard equipment necessary to achieve ground truth observation are available as "off-the-shelf" items, and need not be elaborated.

8.3 Visible Radiometer System

In the design of the various satellite sensors to be used in the proposed experiments, considerable attention must be given to the response of the visible radiometer system. It is this sensor which will ultimately provide the information regarding threshold discrimination. With this in mind, the following simplified analysis is included as an illustration of the expected signal levels.

The actual (isotropic) energy flux density in the interval 0.5 - 0.75μm reflected from clouds and clear areas may be derived from the measured effective radiant emittance values of Channel 5 of TIROS VII by the following equation (Fritz, 1954).

$$W = \left(\frac{\overline{W}}{\overline{\phi}} \right) D \text{ Watts - Meter}^{-2}$$

where

W = reflected flux density (assuming isotropic reflectance) watts - meter^{-2}

$\overline{W}$ = Channel V measured effective radiant emittance, watts - meter^{-2}

D = Correction factor for the instrument

$\overline{\phi}$ = Mean instrument response function weighted by the spectral flux of the sun, i.e.

$$\bar{\phi} \equiv \frac{\int W_\lambda \phi_\lambda d_\lambda}{\int W_\lambda \, d_\lambda}$$

where

W_λ = spectral solar flux density.

To get some idea of the difference between the reflected flux density from cloudy and clear areas, the measured effective radiant emittance may be converted to albedos, again based on the assumption of isotropic reflectance, since (Wexler, 1964)

$$A = \frac{W}{\bar{W}^* \cos \theta}$$

where

A = albedo, $(1 \leq A \leq 0)$

$\bar{W}^*$ = energy (watts - meter^{-2}) received by Channel 5 reflected by a perfect diffused reflector illuminated by the sun at normal incidence.

θ = solar zenith angle.

Therefore, in terms of the albedo, the expected reflected solar flux density would be

$$W = \frac{A \, D \, \bar{W}^* \cos \theta}{\bar{\phi}} \text{ watts - meter}^{-2}$$

The total power measured by a satellite photometer may then be computed (again assuming diffuse reflection) by the following equation:

$$P = \left[\frac{A \, D \, W^* \cos \theta}{\pi \, \bar{\phi}} \times \frac{\pi \, \xi^2 \, R^2}{4} \times \frac{\pi \, d^2}{4R^2} \right] \text{ watts}$$

where

ξ = plane angle of view of photometer in radians

R = distance from detector to reflecting surface

d = radius of detector surface.

The first term is the reflected intensity in watts - meter^{-2} - steradian^{-1}. The second term is the area of the reflecting surface intercepted by the photometer beam. The third term is the solid angle subtended by the detector surface. Rewriting this equation as:

$$\frac{P}{d^2 \xi^2} = \frac{(A\ D\ \bar{W}^*\ \cos\theta)\ \pi}{16\ \bar{\phi}} \quad \text{watts-radian}^{-2}\text{ - meter}^{-2},$$

we can derive a set of parametric curves for the design of a photometer system. Figure 8-1 is such a set of parametric curves where $P/d^2\xi^2$ is plotted against A using θ as the parameter. (The products $d^2\xi^2$ (meter^2 - radian^2) are the geometric characteristics of the photometer.) These curves are derived based on the values of $\bar{\phi}$ and D for Channel 5 of TIROS VII. Vertical dashed lines have been drawn in the figure to represent possible threshold values for these measurements.

8.4 Astronaut Training

Since the role of the astronaut is primarily that of a qualified observer, his training should be an integral part of the experimental planning. The objective of the training should be directed towards sharpening his observation and reporting capabilities. To this end, the use of visual simulation techniques is advised. Color photography of different types of cloud cover situations from the Mercury, Gemini and manned Apollo programs exists in sufficient quantity for such a purpose and should be employed.

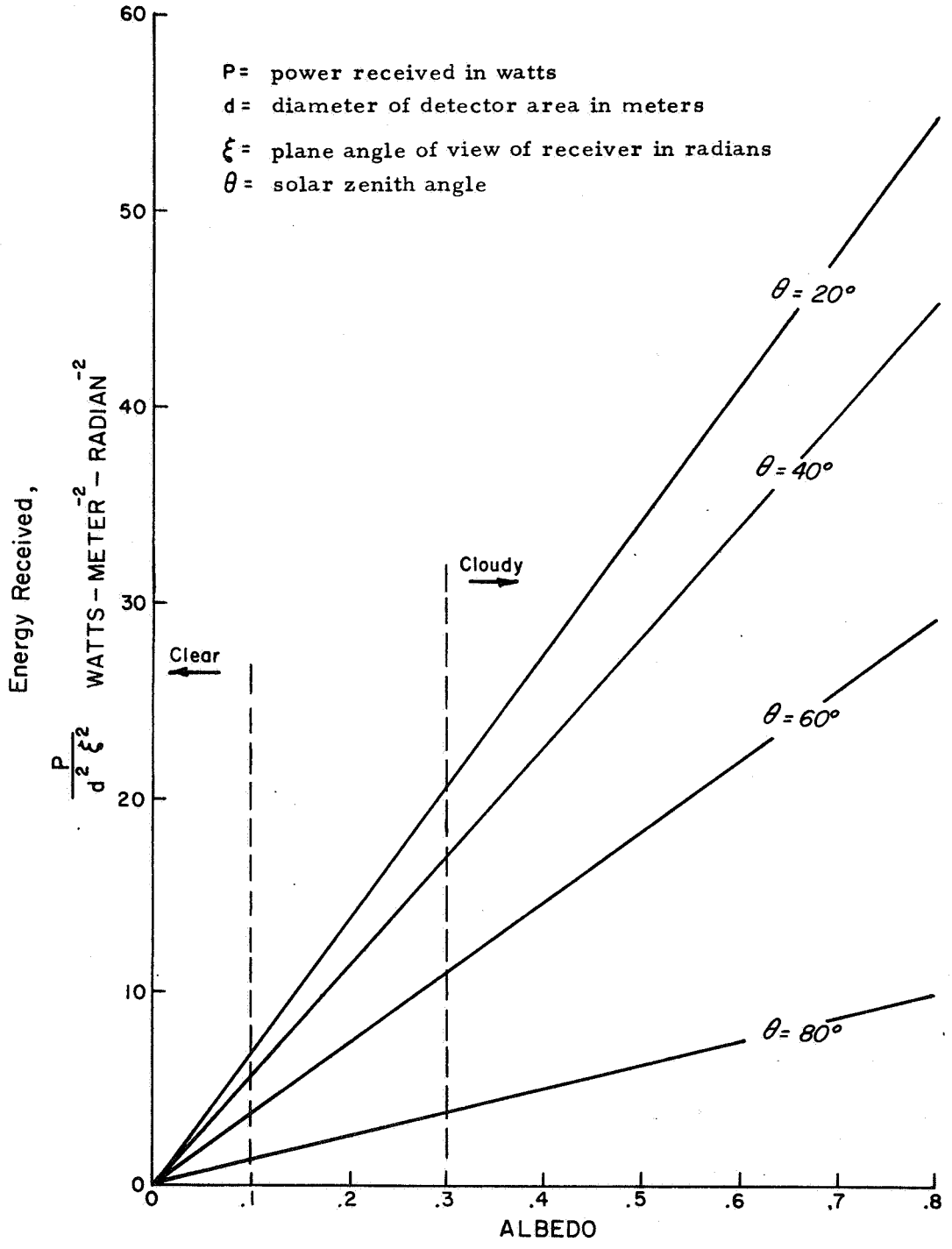

Figure 8-1 Expected Signal Levels Reflected from Diffused Clouds

9. SUMMARY AND CONCLUSIONS

A detailed knowledge of the sea surface temperature patterns and their variation in time would be of significant benefit to the commercial fisheries, to the military for use in Anti-Submarine Warfare, and to meteorologists for use in long-range weather prediction. To obtain the required density of observations (both in space and time) by shipboard measurements alone would be a practical impossibility. Before optimal use can be made of satellite data, however, techniques must be developed for the automatic elimination of cloud contamination, and for rapid processing of the temperature pattern information.

Using Nimbus II data, a two phase study was conducted. The low resolution, multi-spectral MRIR data were used in the development of data processing techniques, while the high resolution, single spectral region HRIR data were used in the actual measurement of sea surface temperature patterns and their synoptic changes.

Modifications were made to the original Nimbus Mercator Map Programs to accomplish the following:

a) Extract and map HRIR data points where the recorded temperature is greater than or equal to some preset threshold value. Because the HRIR sensor was a single channel radiometer, this is the only means of internally eliminating cloud contaminated data.

b) Extract and map MRIR temperature data using the Channel 5 albedo values as clear-cloudy discriminators. This cloud discrimination technique is applicable only to daytime passes.

c) Extract and map MRIR temperature data using the Channel 1 water vapor absorption temperatures as clear-cloudy discriminators. This technique is primarily used for nighttime cases, but may also be used in conjunction with the daytime albedo discriminator.

d) Convert temperature values in ^{o}K to single digit alphanumeric codes for off-line printing and card punching. The punched cards may subsequently be used to produce color coded analyses using Allied's Digital Color Printer.

e) Permit the composite mapping of multiple passes for time averaging, or for cases of recurrent partial cloudiness.

It was found that for the optimal detection of cloud contaminated data in daytime passes, a combination of a visible and a water vapor channel threshold should be used. While there are no unique threshold values in any spectral region, a 15% albedo, and a 237^{o}K water vapor temperature cut-off were established through the

application of failure rate versus false-alarm rate considerations. The 237°K Channel 1 temperature cut-off is also applicable to the problem of nighttime cloud discrimination. With the HRIR data, only the temperature values themselves are available to automatically discriminate cloudiness. A 280°K temperature threshold is suggested, although the failure rate may be uncomfortably high due to the inability to detect certain cloud forms such as high thin cirrus or low warm fog and stratus.

In the planning of remote measurement experiments in oceanography, as well as in other fields, some consideration must be given to the problem of intervening cloud cover. Depending upon climatological conditions and upon the time variation of the phenomena to be observed, certain proposed experiments may have a very low probability of success, or even be totally infeasible. As an example of the application of these considerations, Monte Carlo pass simulation programs were run for the Gulf Stream region, drawing upon information from a world-wide cloud data bank. Graphs of area coverage versus the probability of that coverage were generated as a function of the number of passes at established time intervals. Among other things, these graphs reveal that it may be unrealistic to hold out for very high cloud-free coverage. An analysis of the data from a sequence of MRIR passes essentially verified the computer derived statistical predictions.

A time history of the Gulf Stream meander movement for the month of October 1966 was developed using the nighttime HRIR data. On the whole, the determined meander speeds were in agreement with those values found in earlier conventional surface ship observations. Near-shore meanders were found to propagate downstream at a rate of about 8 n. mi per day. The larger meanders toward the northeast propagated more slowly at rates of 4 to 5 n. mi per day.

Present knowledge of radiometric differences between clear and cloudy regions is as yet insufficient to properly define all cloud contamination situations. Areas of small scattered cloudiness or cirrus clouds may still present considerable difficulty. In order to improve current knowledge of these radiance characteristics, interest must be selectively focused on special cloud cover situations. The advantages of manned observations lie in man's ability to select the proper target for observation, and to document the situation being observed. The types of measurements needed were outlined, and possible equipment configurations were discussed.

Until it is possible to accurately account for the effects of atmospheric attenuation in the satellite data it will be necessary to utilize the temperature gradient information only. It is recommended that ways be sought to meld cloud-free satellite derived temperature gradients with conventional surface ship reports to

produce daily SST maps. Such an operational procedure should probably be conducted by the Fleet Numerical Weather Facility in California. Ways must also be sought to account for the spatial variation of atmospheric attenuation before meaningful analyses can be developed. Possible data sources include FNWF's 12 hourly analysis of the atmospheric mass structure, or some on-board radiometer designed to infer the vertical humidity structure.

It is now felt that the operational use of satellite measured sea surface temperature data is within reach. Most of the problems associated with the detection of cloud contamination in day and nighttime data have been investigated and resolved. Techniques for melding gradient data with absolute values already exist. The effects of atmospheric attenuation on the temperature measurements are understood. A reliable humidity data source is still lacking, but new sensors and techniques are currently being developed. The ability to measure sea surface temperature patterns and to trace their development has been demonstrated. Future efforts should be directed toward the realization of an operational satellite/ship sea surface temperature measurement system.

REFERENCES

ARACON Geophysics Co., 1966: Nimbus II Users' Guide, Prepared by ARACON Geophysics Co. for the Nimbus Project, Goddard Space Flight Center, Greenbelt, Md.

Bandeen, W., 1968: Experimental Approaches to Remote Atmospheric Probing in Infrared from Satellites, NASA Technical Note, TM X-63188, Goddard Space Flight Center, Greenbelt, Md.

Bristor, C.L., 1968: Computer Processing of Satellite Pictures, Technical Memorandum NESCTM-3, National Environmental Satellite Center, Washington, D.C.

Conover, J.H., 1965: "Cloud and Terrestrial Albedo Determination from TIROS Satellite Pictures," J. of Applied Meteorology, 4 (3), pp 378-386.

Danard, M.B., M.M. Holl, and J.R. Clark, 1967: Fields by Correlation Assembly - Special Adaptations of the Basic FCA Program, Technical Memorandum No. 5 under Contract N0022866C1325, Meteorology International, Inc., Monterey, Calif.

Fisher, E.L., 1958: "Hurricanes and the Sea Surface Temperature Field," J. of Meteorology, 15 (3), pp 328-333.

Fritz, S., 1954: "Scattering of Solar Energy by Clouds of Large Drops," J. of Meteorology, 11, p. 291.

Fritz, S., and P.K. Rao, 1967: "On the Infrared Transmission Through Cirrus Clouds and the Estimation of Relative Humidity from Satellites," J. of Applied Meteorology, 6, pp. 108-1096.

General Electric Co., 1967: The Potential of Observation of the Oceans from Spacecraft, Prepared for Nat. Council on Marine Resources and Engineering Development, Doc. No. PB 177 726, Philadelphia, Pa.

Greaves, J.R., R. Wexler, and C.J. Bowley, 1965: The Feasibility of Sea Surface Temperature Determination Using Satellite Infrared Data, Interim Report under Contract NASW-1157, Allied Research Associates, Inc., Concord, Mass., republished as NASA CR-474.

Greaves, J.R., and J.H. Willand, 1967: Processing of Satellite Infrared Data for Sea Surface Temperature Determination, Final Report under Contract NASW-1157, Allied Research Associates, Inc., Concord, Mass.

Hela, I., and T. Laevastu, 1962: Fisheries Hydrography, Fishing News Ltd., London.

Namias, J., 1963: "Large-Scale Air-Sea Interactions Over the North Pacific for Summer, 1962, Through the Subsequent Winter," J. of Geophysical Res., 68 (22), pp 6171-6186.

National Academy of Sciences, National Research Council, 1965: Economic Benefits from Oceanographic Research, Publication 1228, Washington, D.C.

U.S. Naval Oceanographic Office, 1967: The Gulf Stream, 2 (1)

Newell, H.E., 1968: "Current Program and Considerations of the Future for Earth Resources Survey," Presented at Fifth Symposium on Remote Sensing, U. of Mich., Ann Arbor, Mich.

Panel on Oceanography, President's Science Advisory Committee, 1966: Effective Use of the Sea, The White House, Washington, D.C.

Sherr, P.E., A.H. Glaser, J.C. Barnes, and J.H. Willand, 1968: World-Wide Cloud Cover Distributions for Use in Computer Simulation, Final Report under Contract NAS 8-21040, Allied Research Associates, Inc., Concord, Mass.

Von Arx, W.S., 1962: Introduction to Physical Oceanography, Addison-Wesley Pub. Co., L. of C. No. 61-5026, 422 pp.

Wark, D.Q., G. Yamamoto, J.H. Lienesch, 1962: "Methods of Estimating Infrared Flux and Surface Temperatures from Meteorological Satellites," J. of the Atmospheric Sciences, 19, pp. 369-384.

Wexler, R., 1964: "Infrared and Visual Radiation Measurements from TIROS III," J. of Applied Optics, 3 (2), pp. 215-220.

Widger, W.K., Jr., and J.R. Greaves, 1968: Bibliography on the Use of Satellites for Oceanographic Observations, Interim Report under Contract NASW-1651, Allied Research Associates, Inc., Concord, Mass.

Wilkerson, J.C. 1967: "Nimbus II Satellite Observations of the Gulf Stream ," Presented at 48th Annual Meeting of American Geophysical Union, Washington, D.C.

Wolff, P.M., L.P. Carstensen, and T. Laevastu, 1965: Analyses and Forecasting of Sea-Surface Temperature, Tech. Note No. 8, FNWF, Monterey, Calif.

Wolff, P.M., 1965a: "Operational Analyses and Forecasting of Ocean Temperature Structure," Oceanography from Space, W.H.O.I., Woods Hole, Mass., pp. 125-148.

APPENDIX A

A.1 HRIR Main Program and Subroutines

```
      L00169  --  UNIFIED NIMBUS HRIR MERCATOR MAP PROGRAM  --

      COMMON LOCPT                                                          00090
      DIMENSION LOCPT(210)                                                  00100
49    CONTINUE
      CALL WIPE                                                             00170
45    READ INPUT TAPE 2,275,JTAPE,JCARDS
275   FORMAT(I5,I2)
      IF(JTAPE) 1020,251,1021
1021  PRINT 673,JTAPE
673   FORMAT(1H1,12HLOAD AM TAPE,I5,22H ON FS AND PRESS START////////)
      PAUSE
      CALL RFIL                                                             00110
      CALL RRKD1                                                            00120
      TEST=0.                                                               00130
      IFIPR=1                                                               00140
      DO 630 KK = 1,JCARDS
      CTREC = 0
      RTINTS=0.                                                             00160
      READ INPUT TAPE 2,202 ,CDAY,CHOUR,CMIN,CDELT,CNADR,CPASS,CCN1,CATN
     1,CATS,SESH,DNBR,PARITY,WRDAT,IFITGO,MAP,CUTOFW,CUTOFC,INK
  202 FORMAT(F3.0,2F2.0,F4.0,F2.0,F4.0,3F3.0,F5.3,F3.0,1X,2F1.0,I2,1X,I2
     1,6X,2F3.0,1A1)
      IF(CDELT)251,251,253                                                  00210
  253 CDEL2=CDELT                                                           00220
      CBEG=24.0*CDAY*60.0+CHOUR*60.0+CMIN                                   00230
      CEND=CBEG+CDELT                                                       00240
      IVCT=IFITGO-IFIPR                                                     00250
      IFIPR=IFITGO                                                          00260
      CALL MOVFIL(TEST,IVCT)                                                00270
      CALL INIT(CNADR,CCN1,CATN,CATS,SESH,DNBR,CUTOFC,CUTOFW,MAP,INK)
      CALL RDOC(TDAYA,THRA,TMINA,TDAYB,THRB,TMINB,XMBR,FREQ,BLOCK,SWREC,    00290
     1ANPT)                                                                 00300
      TBEG=24.0*TDAYA*60.0+THRA*60.0+TMINA                                  00310
      TEND=24.0*TDAYB*60.0+THRB*60.0+TMINB                                  00320
      KDAYA = TDAYA                                                         00330
      KHRA = THRA                                                           00340
      KMINA = TMINA                                                         00350
      KDAYB = TDAYB                                                         00360
      KHRB=THRB                                                             00370
      KMINB = TMINB                                                         00380
      KCDAY = CDAY                                                          00390
      KCHOUR = CHOUR                                                        00400
      KCMIN = CMIN                                                          00410
      KCDEL=CDELT                                                           00420
      IF(CBEG-TEND)10,12,12                                                 00430
   10 IF(CBEG-TBEG)14,13,13                                                 00440
   13 IF(CEND-TEND)201,201,15                                               00450
   14 IF(CEND-TEND)18,18,17                                                 00460
   18 IF(CEND-TBEG)19,19,20                                                 00470
   12 WRITE OUTPUT TAPE 3,203
  203 FORMAT(78H0    MAP TIME INTERVAL REQUESTED BEGINS LATER THAN FINAL    00490
     1TIME OF THIS FMRT-MRIR/ 19H     NO MAP PRODUCED)                      00500
      NN=5                                                                  00510
      GO TO 199                                                             00520
   15 WRITE OUTPUT TAPE 3,204
  204 FORMAT( 80H0    MAP TIME INTERVAL REQUESTED TERMINATES BEFORE INITI   00570
```

```
      LC0169  --  UNIFIED NIMBUS HRIR MERCATOR MAP PROGRAM  --

     1AL TIME OF THIS FMRT-MRIR/ 19H     NO MAP PRODUCED)                    00580
      NN=1                                                                   00590
      GO TO 199                                                              00600
   15 WRITE OUTPUT TAPE 3,6
    6 FORMAT( 77H0   MAP TIME INTERVAL REQUESTED TERMINATES AFTER FINAL     00650
     1TIME OF THIS FMRT-MRIR/ 58H    MAP FOR THE PART OF TIME INTERVAL C    00660
     2OVERED WAS PRODUCED)                                                  00670
      NN=4                                                                   00680
      GO TO 199                                                              00690
   17 WRITE OUTPUT TAPE 3,7
    7 FORMAT( 90H0   MAP TIME INTERVAL REQUESTED BEGINS BEFORE AND ENDS     00730
     1AFTER TIME PERIOD OF THIS FMRT-MRIR/ 54H    MAP FOR PART OF TIME I    00740
     2NTERVAL COVERED WAS PRODUCED)                                         00750
      NN=3                                                                   00760
      GO TO 199                                                              00770
   20 WRITE OUTPUT TAPE 3,8
    8 FORMAT( 82H0   MAP TIME INTERVAL REQUESTED BEGINS EARLIER THAN INI    00810
     1TIAL TIME OF THIS FMRT-MRIR/ 54H    MAP FOR PART OF TIME INTERVAL     00820
     2COVERED WAS PRODUCED)                                                 00830
      NN= 2                                                                  00840
      GO TO 199                                                              00850
  201 NN=6                                                                   00880
  199 WRITE OUTPUT TAPE 3,9,KDAYA,KHRA,KMINA,KDAYB,KHRB,KMINB,KCDAY,
     1KCHOUR,KCMIN,KCDEL,CPASS
    9 FORMAT( 32H0    TIME INTERVAL OF FMRT-MRIR I4,5HDAYS I2,4HHRS I2,1    00900
     13HMIN    TO    I4,5HDAYS I2,4HHRS I2,3HMIN/ 32H0   TIME INTERVAL R    00910
     2EQUESTED     I4,5HDAYS I2,4HHRS I2,15HMIN    PLUS    I4,3HMIN,8H
     3  PASS,F5.0)
      GO TO (620,200,200,200,620,200),NN
  200 CALL RRKD(TEST,RDAY,RHR,RMIN)                                          00940
C                                                                            00950
C                  TEST=0 IS NORMAL RETURN AFTER SUCCESSFULLY READING A      00960
C                  DATA RECORD FROM FMRT-MRIR                                00970
C                  TEST IS NEGATIVE WHEN TAPE ERROR DETECTED                 00980
C                  TEST IS POSITIVE WHEN EOF DETECTED                        00990
      IF(TEST) 225,250,620
  225 PRINT 205                                                              01010
  205 FORMAT(13H   TAPE ERROR)                                               01020
      IF(PARITY) 200,250,200                                                 01030
  250 RTIME=24.0*RDAY*60.0+RHR*60.0+RMIN                                     01040
      IF(CBEG-RTIME) 300,300,200                                             01050
  300 IF(CTREC   )301,301,302                                                01060
  301 RTIMES=RTIME                                                           01070
  302 RTINT=RTIME-RTIMES                                                     01080
      CDELT=CDELT-RTINT                                                      01090
      RTINTS=RTINTS+RTINT                                                    01100
      IF(CDELT) 620,303,303
  303 CALL INTERP(XMRR,FREQ,BLOCK,SWREC,ANPT,LOCPT,WRDAT)
      RTIMES=RTIME                                                           01130
      CTREC=CTREC+1.                                                         01140
      GO TO 200                                                              01150
  620 CONTINUE
      IF(MAP)630,630,1030
 1030 WRITE OUTPUT TAPE 8,444,CPASS
      WRITE OUTPUT TAPE 3,444,CPASS
  444 FORMAT(7H  BEGIN,F5.0)
```

```
      L00169  --  UNIFIED NIMBUS HRIR MERCATOR MAP PROGRAM  --

      CALL OUTPUT
      WRITE OUTPUT TAPE 8,445,CPASS
      WRITE OUTPUT TAPE 3,445,CPASS
  445 FORMAT(5H  END,F5.0)
      CALL WIPE
630   CONTINUE
      REWIND 19
      GO TO 45
1020  CONTINUE
 1000 CALL OUTPUT
      GO TO 49
  251 PAUSE 77777                                                        01200
      CALL EXIT                                                          01210
      END(0,1,0,1,0,0,1,1,0,1,0,0,0,0,0)




      SUBROUTINE HEAD
      WRITE OUTPUT TAPE 3,10
   10 FORMAT(1H1,58X40HLATITUDE OF     LONGITUDE OF         HRIR/27X75HSP
     1OT NUMBER     NADIR ANGLE     VIEWED POINT    VIEWED POINT      DAT
     2A VALUE)
      RETURN
      END(0,1,0,1,0,0,1,1,0,1,0,0,0,0,0)




      SUBROUTINE WRITE(SPOTK,XNADA,XLATX,XLONX,DATA)
      ISPTK=SPOTK
      WRITE OUTPUT TAPE 3,1,ISPTK,XNADA,XLATX,XLONX,DATA
    1 FORMAT(31X13,11XF7.3,9XF7.3,9XF7.3,9XF7.3)
      RETURN
      END(0,1,0,1,0,0,1,1,0,1,0,0,0,0,0)
```

```
         ENTRY RDCC
         ENTRY SKIP
         ENTRY SVSKP
         ENTRY RFIL
         ENTRY FREQ

FXFLO
FLCFX

 RDCC    TRA      *+5
         AXT      0,4
         AXT      0,2
         AXT      0,1
         TRA      12,4
         SXA      *-4,4
         SXA      *-4,2
         SXA      *-4,1
         AXT      10,2
 RDCC1   RTBB     9
         RCHB     GETDC
         CLA      1,4
         STA      TDAYA
         CLA      2,4
         STA      THRA
         CLA      3,4
         STA      TMINA
         CLA      4,4
         STA      TDAYB
         CLA      5,4
         STA      THRB
         CLA      6,4
         STA      TMINB
         CLA      7,4
         STA      MRR
         CLA      8,4
         STA      FREQ
         CLA      9,4
         STA      BLOCK
         CLA      10,4
         STA      SWREC
         CLA      11,4
         STA      ANRT
         TCOB     *
         TEFB     DONE
         TRCB     TRY
         CLA      TDOC+2
         CALL     FXFLC
         PZE      35
         HTR      *
         STO*     TDAYA
         CLA      TDOC+3
         CALL     FXFLC
         PZE      35
         STO*     THRA
         CLA      TDCC+4
```

```
        CALL    FXFLC
        PZE     38
        HTR     *
        STO*    TMINA
        CLA     TDCC+6
        CALL    FXFLO
        PZE     35
        HTR     *
        STO*    TDAYB
        CLA     TDCC+7
        CALL    FXFLO
        PZE     35
        HTR     *
        STO*    THRB
        CLA     TDCC+8
        CALL    FXFLO
        PZE     35
        HTR     *
        STO*    TMINB
        CLA     TDCC+10
        CALL    FXFLO
        PZE     26
        HTR     *
        STO*    MRR
        CLA     TDCC+11
        CALL    FXFLO
        PZE     35
        HTR     *
        STO*    FREQ
        CLA     TDCC+14
        STO*    BLOCK
        CLA     TDCC+15
        STC*    SWREC
        CLA     TDCC+16
        STC*    ANPT
        TRA     RCCC+1
FIX1    DEC     1835
TDAYA   PZE
THRA    PZE
TMINA   PZE
TDAYB   PZE
THRB    PZE
TMINB   PZE
MRR     PZE     0
FREQ    PZE     0
BLOCK   PZE     0
SWREC   PZE     0
ANPT    PZE     0
LCCPT   PZE     0
TRY     BSRB    9
        TIX     RCOC1,2,1
        HTR     *
GETDC   ICRP    TDCC,0,-1
        IOCP    0,0,0
DONE    HTR     *
SKIP    SXA     SVSKP,4
```

```
        CLA*    1,4
        CALL    FLCFX
        PZE     35
        HTR     *
        PAX     0,2
        TRA     *+4
        RTEB    9
        RCHB    SKIPR
        TCCB    *
        TIX     *-3,2,1
SVSKP   AXT     0,4
        TRA     2,4
SKIPR   IORTN   TDCC,0,-1
FFIL    SXA     *+6,4
        RTEB    9
        RCHB    COMB
        TCCB    *
        TEFB    *+2
        TRA     FFIL+1
        AXT     0,4
        TRA     1,4
COMB    IORTN   TDCC,0,-1
TDCC    BSS     50
        END
```

```
        ENTRY WIPE
        ENTRY INIT
        ENTRY INTERP
        ENTRY OUTPUT
        ENTRY IBLK

MGRID
SST
LIRPN
EXFLC
HEAD
COMPA
TIN1
WRITE

 INIT   TRA     *+5             PLACE READ-IN DATA IN LOCS FOR THIS SUB
        AXT     0,4
        AXT     0,2
        AXT     0,1
        TRA     11,4
        SXA     *-4,4
        SXA     *-4,2
        SXA     *-4,1
        CLA*    1,4
        STO     NADR
        CLA*    2,4
        STO     CON1
        STO     CON
        CLA*    3,4
        STO     CATN
        STC     CATNN
        CLA*    4,4
        STO     CATS
        STC     CAT
        CLA*    5,4
        STO     D
        STC     DD
        CLA*    6,4
        FSB     =1.
        STO     E
        CLA*    7,4
        STC     CLTCFC
        CLA*    8,4
        STC     CLTOFW
        CLA*    9,4
        STO     MAP
        CLA*    10,4
        STO     INK
        CALL    MGRID,CON1,CON,CATN,CATS,CAT,D,E,XI,YJ,ZERO
        CLA     YJ
        FAD     =.5
        STO     GRIDI
        TRA     INIT+1
 WIFE   TRA     *+5
        AXT     0,4
        AXT     0,2
```

```
        AXT     0,1
        TRA     1,4
        SXA     *-4,4
        SXA     *-4,2
        SXA     *-4,1
        CLA     =1B17
        STC     NGATE
        CALL    SST,XI,YJ,E,DATA,GRIDI,NGATE
        TRA     WIPE+1
*       SUBROUTINE TO INTERPRET DATA  CALLS FOR MERCATOR I,J POINTS
INTERP  TRA     *+5
        AXT     0,4
        AXT     0,2
        AXT     0,1
        TRA     8,4
        SXA     *-4,4
        SXA     *-4,2
        SXA     *-4,1
        CLA     =2B17
        STC     NGATE
        CLA*    $LIBPN          PICK-UP LOC WHERE 1ST WORD OF REC IS STORED
        STA     LOC
        STA     LOC1
        ADD     =7
        STA     RDATA           PUT LOC OF 1ST WORD,1ST SWATH IN LOC RDATA
        CLA*    1,4               WHICH IS TAGGED WITH XR1
        STO     MRATE           PUT INPUTS TO SUB IN PROPER LOCS
        CLA*    2,4
        STO     FREQ
        CLA*    3,4
        STC     BLOCK
        CLA*    4,4
        STC     SWREC
        CLA*    5,4
        STO     ANPT
        ALS     18
        STD     IN2             STORE NO. OF ANCH POINTS IN CALL SEQS BELOW
        STD     IN4
        STD     IN6
        STD     IN8
        CLA     6,4             DET. 1ST LOC OF ANCHOR LONG. TABLE AND
        SUB     =100E35            STORE IN CALL SEQS BELOW
        STA     IN3
        STA     IN7
        STA     LONATB          SET LOC OF 1ST ANCHOR NADIR ANGLE IN LONG.
*                                     TABLE
        STA     LONTBL
        ADD     =2E35
        STA     LONTBX
        SUB     =1B35            2-27-67 RAS
        STA     LONTAB
        STA     LONTST          SAVE 1ST ANCHOR LONG. LOC
        CLA     6,4             DET. 1ST LOC OF ANCHOR LAT. TABLE AND
        SUB     =200B35           STORE IN CALL SEQS BELOW
        STA     IN1
        STA     IN5
        STA     LATATB          SET LOC OF 1ST ANCHOR NADIR ANGLE IN LAT.
*                                   TABLE
        ADD     =1B35
        STA     LATTAB
```

```
        STA     LATST           SAVE 1ST ANCHOR LAT. LOC
        CLA*    7,4
        STO     WRDAT
        AXT     0,1             ZERO XR1
        CLA     ANPT            PUT NO. OF ANCHOR POINTS IN XR2
        PAX     0,2
RDOC2   CLA*    RDATA           BEGIN LOOP TO PUT ANCHOR NADIR ANGLES IN
        CALL    FXFLO           ANCHOR LAT AND LONG TABLES USING XR2
        PZE     29
        HTR     *
        STO*    LONATB
        STO*    LATATB
        CLA     LONATB
        ADD     =2E35
        STO     LONATB
        CLA     LATATB
        ADD     =2E35
        STO     LATATB
        TXI     *+1,1,-1
        TIX     RDOC2,2,1       LOOP BACK UNTIL ALL NADIR ANGLES ARE USED
        CLA     RDATA
        ADD     ANPT
        STO     RDATA
        AXT     0,1
BEGIN   CLA     WRDAT
        TZE     NHDR
        CALL    HEAD
NHDR    CLA     ANPT            BEGIN LOOP TO UNPACK NEXT SWATH
        PAX     0,2             PUT NO. OF ANCHOR POINTS IN XR2
        CLA*    RDATA
        ANA     MASKB
        TZE     INTERP+1        RETURN TO MAIN PROG IF LAST FILLED SWATH OF
        STO     POP               LAST REC IS REACHED
        CALL    FXFLO
        PZE     35
        HTR     *
        FAD     =1.0
        STO     SN1
        TXI     *+1,1,-3        SKIP TWO SWATH WORDS
MKTAB   CLA*    RDATA           BEGIN LOOP TO FORM ANCH LAT AND LONG TABLE
        ANA     MASKA
        CALL    FXFLO
        PZE     11
        HTR     *
        STO*    LATTAB
        CLA     LATTAB
        ADD     =2B35
        STO     LATTAB
        CLA*    RDATA
        ANA     MASKB
        CALL    FXFLO
        PZE     29
        HTR     *
        STO*    LONTAB
        CLA     LONTAB
        ADD     =2E35
        STO     LONTAB
        TXI     *+1,1,-1
        TIX     MKTAB,2,1       LOOP BACK UNTIL ANCH LAT AND LONG TAB. DONE
        SXA     SAVE,1
```

```
        OCT     076000000016    2-13-67 RAS
        AXT     1,1             2-13-67 RAS
        CLA     ANPT            2-13-67 RAS
        STA     GCAT            2-13-67 RAS
CCAT    AXT     **,7            2-13-67 RAS
GOPHER  TNX     MK7,7,1         2-13-67 RAS
        TXI     *+1,1,-2        2-13-67 RAS
GNU     CLA*    LCNTBL          2-13-67 RAS
        FSB*    LCNTBX          2-13-67 RAS
        LAS     =180.           2-13-67 RAS
        TRA     HCUND           2-13-67 RAS
        TRA     HOUND           2-13-67 RAS
        TRA     GOPHER          2-13-67 RAS
HOUND   TMI     HORSE           2-13-67 RAS
        CLA*    LCNTBX          2-13-67 RAS
        FAD     =360.           2-13-67 RAS
        STO*    LCNTBX          2-13-67 RAS
        TRA     GNU             2-13-67 RAS
HORSE   SCD     *+2,7           2-13-67 RAS
        LXA     GCAT,5          2-13-67 RAS
        TXI     *+1,5,**        2-13-67 RAS
        SXA     IMPALA,1        2-13-67 RAS
AFE     CLA*    LCNTBL          2-13-67 RAS
        FAD     =360.           2-13-67 RAS
        STO*    LCNTBL          2-13-67 RAS
        TXI     *+1,1,2         2-13-67 RAS
        TIX     AFE,5,1         2-13-67 RAS
IMPALA  AXT     **,1            2-13-67 RAS
        TRA     GNU             2-13-67 RAS
MK7     OCT     -076000000016   2-13-67 RAS
        LXA     SAVE,1          2-13-67 RAS
        STZ     SPOTK           INITIALIZE SWATH POINT
        CLA     POP             PUT DATA POPULATION FOR SWATH IN XR2
        PAX     0,2
 INTR   CLA     SPOTK           BEGIN LOOP TO ACCUM. PHYS DATA ACC. SWATH
        FAD     =1.0              POINT GEOG. LOCATION
        STO     SPOTK           SELECT NEXT SWATH POINT
        CALL    COMPA,MRATE,FREQ,SPOTK,SN1,NADA   CALC SWATH POINT NADIR
        CLA     NADA
        SSP
        CAS     NADR
        TRA     JUMA
        TRA     INC1
        TRA     INC1
 INC1   CLA*    PDATA
        ANA     =0777777000000  11-16-67 R.A.S.
        TMI     JUMA
        CALL    FXFLO
        PZE     14
        PXD     ,0
        TZE     JUMA
        CAS     CUTOFF
        TRA     *+3               11-16-67 R.A.S.
        TRA     *+2               11-16-67 R.A.S.
        TRA     JUMA
        STO     DATA
        CLA     NADA
```

```
        CALL    TIN1            CALC. LAT. OF SWATH POINT
IN1     PZE     **
IN2     PZE     3,0,**
        FSB     =90.0           SUBTRACT 90 DEG FROM LAT.
        STO     LATX
        CLA     NADA
        CALL    TIN1            CALC. LONG. OF SWATH POINT
IN3     PZE     **
IN4     PZE     1,0,**
        CAS     =360.0          CORRECT LONG. IF OVER 360 DEG
        TRA     IN4A
        TRA     IN4B
        TRA     IN4B
IN4A    FSB     =360.0
        TRA     IN4+1
IN4B    STO     LONX
        TPL     *+3
        FAD     K360
        STO     LONX
        CLA     WRDAT
        TZE     JUM1
        CALL    WRITE,SPOTK,NADA,LATX,LONX,DATA
JUM1    CLA     CATNN
        STO     CATN
        CLA     DD
        STO     D
        CALL    MGRID,CON1,LONX,CATN,CATS,LATX,D,E,XI,YJ,ZERO
        CLA     ZERO
        TNZ     JUMA
        CALL    SST,XI,YJ,E,DATA,GRIDI,NGATE
JUMA    TIX     *+2,2,1
        TRA     IN9             TRANSFER OUT OF LOOP IF ALL SWATH PTS. DONE
        CLA     SPOTK           SELECT NEXT SWATH POINT AND ACCUM. AS ABOVE
        FAD     =1.
        STO     SPOTK
        CALL    COMPA,MRATE,FREQ,SPOTK,SN1,NADA
        CLA     NADA
        SSP
        CAS     NADR
        TRA     JUMB
        TRA     IN02
        TRA     IN02
IN02    CLA*    RDATA
        ALS     18              11-16-67 R.A.S.
        TMI     JUMB
        CALL    FXFLO
        PZE     14              11-16-67 R.A.S.
        PXD     ,0
        TZE     JUMB
        CAS     CLTOFC
        TRA     *+3             11-16-67 R.A.S.
        TRA     *+2             11-16-67 R.A.S.
        TRA     JUMB
        STO     DATA
        CLA     NADA
        CALL    TIN1
IN5     PZE     **
IN6     PZE     3,0,**
```

```
        FSB     =90.0
        STO     LATX
        CLA     NADA
        CALL    TIN1
IN7     PZE     **
IN8     PZE     1,0,**
        CAS     =360.0
        TRA     IN8A
        TRA     IN8B
        TRA     IN8B
IN8A    FSB     =360.0
        TRA     IN8+1
IN8B    STO     LONX
        TPL     *+3
        FAD     K360
        STO     LONX
        CLA     WRCAT
        TZE     JUM2
        CALL    WRITE,SPCTK,NADA,LATX,LONX,DATA
JUM2    CLA     CATNN
        STO     CATN
        CLA     DD
        STO     D
        CALL    MGRID,CON1,LONX,CATN,CATS,LATX,0,E,XI,YJ,ZERO
        CLA     ZERO
        TNZ     JUMB
        CALL    SST,XI,YJ,E,DATA,GRIDI,NGATE
JUMB    TXI     *+1,1,-1
        TIX     INTR,2,1        LOOP BACK UNTIL ALL SWATH PTS ARE PROCESSED
IN9     CLA     SWREC           COUNT ONE SWATH COMPLETED AT LOOP FINISH
        SUB     =1835
        STO     SWREC
        TZE     INTERP+1        RETURN TO MAIN PR. IF ALL SWATHS DONE
        CLA     RDATA           PUT LOC OF 1ST WORD OF NEXT SWATH IN LOC
        ADD     BLOCK             RDATA WHICH IS TAGGED WITH XR1
        STA     RDATA
        AXT     0,1             ZERO XR1
        CLA     LATST           RE-SET LOCS FOR INITIAL ENTRYS IN ANCH LAT
        STA     LATTAB            AND LONG TABLE
        CLA     LONTST
        STA     LONTAB
        TRA     BEGIN           LOOP BACK UNTIL ALL SWATHS OF REC ARE PROC.
LONATB  PZE     0
LATATB  PZE     0
 WRCAT  PZE     0
 LATST  PZE     0
LONTST  PZE     0
 MRATE  PZE     0
 FREQ   PZE     0
 BLOCK  PZE     0
 SWREC  PZE     0
 ANPT   PZE     0
LONTAB  PZE     0
LATTAB  PZE     0
 RDATA  PZE     0,1
 MASKB  OCT     000000077777
 SN1    PZE     0
 MASKA  OCT     077777000000
 POP    PZE     0
```

```
 SPCTK  PZE     0
 CATA   PZE     0
 LATX   PZE     0
 LCNX   PZE     0
 NACA   PZE     0
 NACR   BSS     1
 TWC    DEC     2
 IMASK  OCT     777777
 ONEB8  DEC     1E8
 LCC    PZE     C,1
 LOC1   PZE     C,1
 ONEF   DEC     1.C
 TWCE   DEC     2B8
 TEMP1  BSS     1
 TEMP2  BSS     1
LCNTEL  PZE     0,1
LCNTBX  PZE     C,1
 SAVE   PZE     0
 CON1   PZE     0
 CON    PZE     C
 CATN   PZE     0
 CATNN  PZE     0
 CATS   PZE     0
 CAT    PZE     0
 C      PZE     0
 DD     PZE     C
 E      PZE     0
 XI     PZE     C
 YJ     PZE     C
 ZERC   PZE     0
 K360   DEC     360.
CLTOFW  PZE     C
CLTOFC  PZE     0
 MAF    PZE     0
 GRIDI  PZE     0
 NGATE  PZE     0
 INK    BSS     1
CLTPUT  TRA     *+5
        AXT     C,4
        AXT     0,2
        AXT     0,1
        TRA     1,4
        SXA     *-4,4
        SXA     *-4,2
        SXA     *-4,1
        CLA     =3B17
        STO     NGATE
        CALL    SST,XI,YJ,E,CATA,GRIDI,NGATE
        CLA     MAF
        CAS     =2B17
        TRA     *+3
        TRA     *+2
        TRA     JHW
        CLA     =4E17
        STO     NGATE
        CALL    SST,XI,YJ,E,DATA,GRIDI,NGATE
 JHW    CLA     =5B17
        STO     NGATE
        CLA     CLTOFW
```

```
        STO     XI
        CLA     CLTOFC
        STC     YJ
        CALL    SST,XI,YJ,E,DATA,GRIDI,NGATE
        TRA     OUTPUT+1
IBLK    TRA     *+5
        AXT     0,4
        AXT     0,2
        AXT     0,1
        TRA     2,4
        SXA     *-4,4
        SXA     *-4,2
        SXA     *-4,1
        XEC     IBLK+1
        CLA     INK
        STO*    1,4
        TRA     IBLK+1
        END
```

A.2 MRIR Main Program and Subroutines

```
      LC0165  --  UNIFIED NIMBUS      MRIR MERCATOR MAP PROGRAM  --

      COMMON LOCPT                                                          00090
      DIMENSION LOCPT(210)                                                  00100
49    CONTINUE
      CALL WIPE                                                             00170
45    READ INPUT TAPE 2,275,JTAPE,JCARDS
275   FORMAT(I5,I2)
      IF(JTAPE) 1020,251,1021
1021  PRINT 673,JTAPE
673   FORMAT(1H1,12HLOAD AM TAPE,I5,22H CN BG AND PRESS START////////)
      PAUSE
      CALL RFIL                                                             00110
      CALL RRKD1                                                            00120
      TEST=0.                                                               00130
      IFIPR=1                                                               00140
      DO 630 KK = 1,JCARDS
      CTREC = 0
      RTINTS=0.                                                             00160
C          COL 41,42 0 COMPOSITES,1 OUTPUT CARDS,2 OUTPUT PAPER-CARDS
C          COL 49 IS COMPARE CHANNEL
C     COLUMNS 43-48  WSTAR FOR CHANNEL 5 REFLECTANCE.  F6.2
C          COL 50-55 COMPARE CHANNEL CUTOF VALUE (F6.3)
C     COLUMNS 56-57 SCLAR ZENITH ANGLE LIMITATION FOR CH. 5 REFL.
      READ INPUT TAPE 2,202 ,CDAY,CHOUR,CMIN,CDELT,CNADR,CPASS,CON1,CATN    00180
     1,CATS,SESH,DNBR,PARITY,WRDAT,IFITGO,KCHAN,MAP,WSTAR,IFV,DISCRM,JSZ
     2AL,CUTOFW,CUTOFC,INK
  202 FORMAT(F3.0,2F2.0,F4.0,F2.0,F4.0,3F3.0,F5.3,F3.0,1X,2F1.0,I2,I1,I2
     1,F6.2,I1,F6.3,I2,2F3.0,1A1)
      IF(CDELT)251,251,253                                                  00210
  253 CDEL2=CDELT                                                           00220
      CBEG=24.0*CDAY*60.0+CHOUR*60.0+CMIN                                   00230
      CEND=CBEG+CDELT                                                       00240
      IVCT=IFITGO-IFIPR                                                     00250
      IFIPR=IFITGO                                                          00260
      CALL MOVFIL(TEST,IVCT)                                                00270
      CALL INIT(CNADR,CON1,CATN,CATS,SESH,DNBR,CUTOFC,CUTOFW,DISCRM,MAP,
     1INK)
      CALL RDOC(TDAYA,THRA,TMINA,TDAYB,THRB,TMINB,XMRR,FREQ,BLOCK,SWREC,    00290
     1ANPT)                                                                 00300
      TBEG=24.0*TDAYA*60.0+THRA*60.0+TMINA                                  00310
      TEND=24.0*TDAYB*60.0+THRB*60.0+TMINB                                  00320
      KDAYA = TDAYA                                                         00330
      KHRA = THRA                                                           00340
      KMINA = TMINA                                                         00350
      KDAYB = TDAYB                                                         00360
      KHRB=THRB                                                             00370
      KMINB = TMINB                                                         00380
      KCDAY = CDAY                                                          00390
      KCHOUR = CHOUR                                                        00400
      KCMIN = CMIN                                                          00410
      KCDEL=CDELT                                                           00420
      IF(CBEG-TEND)10,12,12                                                 00430
   10 IF(CEEG-TBEG)14,13,13                                                 00440
   13 IF(CEND-TEND)201,201,15                                               00450
   14 IF(CEND-TEND)18,18,17                                                 00460
   18 IF(CEND-TBEG)19,19,20                                                 00470
```

```
  12 WRITE OUTPUT TAPE 3,203
 203 FORMAT(78H0   MAP TIME INTERVAL REQUESTED BEGINS LATER THAN FINAL     00490
    1TIME OF THIS FMRT-MRIR/ 19H    NO MAP PRODUCED)                      00500
     NN=5                                                                 00510
     GO TO 199                                                            00520
  19 WRITE OUTPUT TAPE 3,204
 204 FORMAT( 80H0   MAP TIME INTERVAL REQUESTED TERMINATES BEFORE INITI   00570
    1AL TIME OF THIS FMRT-MRIR/ 19H    NO MAP PRODUCED)                   00580
     NN=1                                                                 00590
     GO TO 199                                                            00600
  15 WRITE OUTPUT TAPE 3,6
   6 FORMAT( 77H0   MAP TIME INTERVAL REQUESTED TERMINATES AFTER FINAL     00650
    1TIME OF THIS FMRT-MRIR/ 58H    MAP FOR THE PART OF TIME INTERVAL C    00660
    2OVERED WAS PRODUCED)                                                 00670
     NN=4                                                                 00680
     GO TO 199                                                            00690
  17 WRITE OUTPUT TAPE 3,7
   7 FORMAT( 90H0   MAP TIME INTERVAL REQUESTED BEGINS BEFORE AND ENDS     00730
    1AFTER TIME PERIOD OF THIS FMRT-MRIR/ 54H    MAP FOR PART OF TIME I   00740
    2NTERVAL COVERED WAS PRODUCED)                                        00750
     NN=3                                                                 00760
     GO TO 199                                                            00770
  20 WRITE OUTPUT TAPE 3,8
   8 FORMAT( 82H0   MAP TIME INTERVAL REQUESTED BEGINS EARLIER THAN INI    00810
    1TIAL TIME OF THIS FMRT-MRIR/ 54H    MAP FOR PART OF TIME INTERVAL    00820
    2COVERED WAS PRODUCED)                                                00830
     NN= 2                                                                00840
     GO TO 199                                                            00850
 201 NN=6                                                                 00880
 199 WRITE OUTPUT TAPE 3,9,KDAYA,KHRA,KMINA,KDAYB,KHRB,KMINB,KCDAY,
    1KCHOUR,KCMIN,KCDEL,CPASS
   9 FORMAT( 32H0    TIME INTERVAL OF FMRT-MRIR I4,5HDAYS I2,4HHRS I2,1   00900
    13HMIN    TO    I4,5HDAYS I2,4HHRS I2,3HMIN/ 32H0   TIME INTERVAL R   00910
    2EQUESTED     I4,5HDAYS I2,4HHRS I2,15HMIN    PLUS    I4,3HMIN,8H
    3  PASS,F5.0)
     GO TO (620,200,200,200,620,200),NN
 200 CALL RRKD(TEST,RDAY,RHR,RMIN)                                        00940
C                                                                         00950
C                TEST=0 IS NORMAL RETURN AFTER SUCCESSFULLY READING A     00960
C                DATA RECORD FROM FMRT-MRIR                               00970
C                TEST IS NEGATIVE WHEN TAPE ERROR DETECTED                00980
C                TEST IS POSITIVE WHEN EOF DETECTED                       00990
     IF(TEST) 225,250,620
 225 PRINT 205                                                            01010
 205 FORMAT(13H   TAPE ERROR)                                             01020
     IF(PARITY) 200,250,200                                               01030
 250 RTIME=24.0*RDAY*60.0+RHR*60.0+RMIN                                   01040
     IF(CEEG-RTIME) 300,300,200                                           01050
 300 IF(CTREC   )301,301,302                                              01060
 301 RTIMES=RTIME                                                         01070
 302 RTINT=RTIME-RTIMES                                                   01080
     CDELT=CDELT-RTINT                                                    01090
     RTINTS=RTINTS+RTINT                                                  01100
     IF(CDELT) 620,303,303
 303 CALL INTERP(XMRR,FREQ,BLOCK,SWREC,ANPT,LOCPT,WRDAT,KCHAN,WSTAR,
    1IFV,JSZAL)
```

```
      RTIMES=RTIME                                                      01130
      CTREC=CTREC+1.                                                    01140
      GO TO 200                                                         01150
620   CONTINUE
      IF(MAP)630,630,1030
1030  WRITE OUTPUT TAPE 8,444,CPASS
      WRITE OUTPUT TAPE 3,444,CPASS
 444  FORMAT(7H  BEGIN,F5.0)
      CALL OUTPUT
      WRITE OUTPUT TAPE 8,445,CPASS
 445  FORMAT(5H  END,F5.0)
      WRITE OUTPUT TAPE 3,445,CPASS
      CALL WIPE
630   CONTINUE
      REWIND 19
      GO TO 45
1020  CONTINUE
1000  CALL OUTPUT
      GO TO 49
 251  PAUSE 77777                                                       01200
      CALL EXIT                                                         01210
      END(0,1,0,1,0,0,1,1,0,1,0,0,0,0,0)
```

```
      SUBROUTINE HEAD                                                   01260
      WRITE OUTPUT TAPE 3,10                                            01270
   10 FORMAT(1H1,58X40HLATITUDE OF     LONGITUDE OF         MRIR/27X86HSP 01280
     1OT NUMBER     NADIR ANGLE     VIEWED POINT    VIEWED POINT     DAT 01290
     2A VALUE     ALBEDO)
      RETURN                                                            01310
      END(0,1,0,1,0,0,1,1,0,1,0,0,0,0,0)
```

```
      SUBROUTINE WRITE(SPOTK,XNADA,XLATX,XLONX,DATA,DATA2)
      ISPTK=SPOTK                                                       01370
      WRITE OUTPUT TAPE 3,1,ISPTK,XNADA,XLATX,XLONX,DATA,DATA2
    1 FORMAT(3IX13,11XF7.3,9XF7.3,9XF7.3,9XF7.3,9XF7.3)
      RETURN                                                            01400
      END(0,1,0,1,0,0,1,1,0,1,0,0,0,0,0)
```

```
        ENTRY  RDOC
        ENTRY  SKIP
        ENTRY  SVSKP
        ENTRY  RFIL
        ENTRY  FREQ

FXFLC
FLOFX

 RDOC   TRA    *+5
        AXT    0,4
        AXT    0,2
        AXT    0,1
        TRA    12,4
        SXA    *-4,4
        SXA    *-4,2
        SXA    *-4,1
        AXT    10,2
 RDOC1  RTBB   9
        RCHB   GETDC
        CLA    1,4
        STA    TDAYA
        CLA    2,4
        STA    THRA
        CLA    3,4
        STA    TMINA
        CLA    4,4
        STA    TDAYB
        CLA    5,4
        STA    THRB
        CLA    6,4
        STA    TMINB
        CLA    7,4
        STA    MFR
        CLA    8,4
        STA    FREQ
        CLA    9,4
        STA    BLOCK
        CLA    10,4
        STA    SWREC
        CLA    11,4
        STA    ANPT
        TCCB   *
        TEFB   DONE
        TRCB   TRY
        CLA    TDCC
        CALL   FXFLO
        PZE    35
        HTR    *
        STO*   TDAYA
        CLA    TDCC+1
        CALL   FXFLO
        PZE    35
        HTR    *
        STO*   THRA
```

```
        CLA     TDCC+2
        CALL    FXFLO
        PZE     35
        HTR     *
        STO*    TMINA
        CLA     TDCC+4
        CALL    FXFLO
        PZE     35
        HTR     *
        STO*    TDAYB
        CLA     TDCC+5
        CALL    FXFLO
        PZE     35
        HTR     *
        STO*    THRB
        CLA     TDCC+6
        CALL    FXFLO
        PZE     35
        HTR     *
        STO*    TMINB
        CLA     TDCC+8
        CALL    FXFLO
        PZE     26
        HTR     *
        STO*    MRR
        CLA     TDCC+9
        CALL    FXFLO
        PZE     23
        HTR     *
        STO*    FREQ
        CLA     TDCC+12
        STO*    BLOCK
        CLA     TDOC+13
        STO*    SWREC
        CLA     TDOC+14
        STO*    ANPT
        TRA     RDOC+1
FIX1    DEC     1835
TDAYA   PZE
THRA    PZE
TMINA   PZE
TDAYB   PZE
THRB    PZE
TMINB   PZE
MRR     PZE     0
FREQ    PZE     0
BLOCK   PZE     0
SWREC   PZE     0
ANPT    PZE     0
LOOPT   PZE     0
TRY     BSRB    9
        TIX     RDOC1,2,1
        HTR     *
GETDC   IORP    TDOC,0,-1
        IOCP    0,0,0
DONE    HTR     *
```

```
SKIP   SXA      SVSKP,4
       CLA*     1,4
       CALL     FLOFX
       PZE      35
       HTR      *
       PAX      0,2
       TRA      *+4
       RTEB     9
       RCHB     SKIPR
       TCCB     *
       TIX      *-3,2,1
SVSKP  AXT      0,4
       TRA      2,4
SKIPR  IORTN    TDOC,0,-1
RFIL   SXA      *+6,4
       RTBB     9
       RCHB     COMB
       TCCB     *
       TEFB     *+2
       TRA      RFIL+1
       AXT      0,4
       TRA      1,4
COMB   IORTN    TDOC,0,-1
TDOC   BSS      50
       END
```

```
        ENTRY WIPE
        ENTRY INIT
        ENTRY INTERP
        ENTRY OUTPUT
        ENTRY IBLK

MGRID
SST
LIFFN
FXFLO
HEAD
COMFA
TIN1
N2CSR
WRITE

 INIT   TRA     *+5          PLACE READ-IN DATA IN LOCS FOR THIS SUB
        AXT     0,4
        AXT     0,2
        AXT     0,1
        TRA     12,4
        SXA     *-4,4
        SXA     *-4,2
        SXA     *-4,1
        CLA*    1,4
        STO     NADR
        CLA*    2,4
        STO     CON1
        STO     CON
        CLA*    3,4
        STO     CATN
        STO     CATNN
        CLA*    4,4
        STO     CATS
        STO     CAT
        CLA*    5,4
        STO     D
        STO     DD
        CLA*    6,4
        FSB     =1.
        STO     E
        CLA*    7,4
        STO     CUTOFC
        CLA*    8,4
        STO     CUTOFW
        CLA*    9,4
        STO     DISCRM
        CLA*    10,4
        STO     MAP
        CLA*    11,4
        STO     INK
        CALL    MGRID,CON1,CON,CATN,CATS,CAT,D,E,XI,YJ,ZERO
        CLA     YJ
        FAD     =.5
        STO     GRIDI
        TRA     INIT+1
```

```
 WIPE   TRA      *+5
        AXT      0,4
        AXT      0,2
        AXT      0,1
        TRA      1,4
        SXA      *-4,4
        SXA      *-4,2
        SXA      *-4,1
        CLA      =1817
        STO      NGATE
        CALL     SST,XI,YJ,E,DATA,GRIDI,NGATE
        TRA      WIPE+1
*       SUBROUTINE TO INTERPRET DATA  CALLS FOR MERCATOR I,J POINTS
 INTERP TRA      *+5
        AXT      0,4
        AXT      0,2
        AXT      0,1
        TRA      12,4
        SXA      *-4,4
        SXA      *-4,2
        SXA      *-4,1
        CLA      =2817
        STO      NGATE
        CLA*     $LIRPN          PICK-UP LOC WHERE 1ST WORD OF REC IS STORED
        STA      LOC
        STA      LOC1
        ADD      =8
        STA      RDATA           PUT LOC OF 1ST WORD,1ST SWATH IN LOC RDATA
        CLA      LOC              LOCATION OF 1ST WORD IN THE RECORD,1
        ANA      MASKB            KEEP ONLY THE ADDRESS
        ADD      =3835            LOCATION OF HEIGHT
        STA      *+1
        CLA      **               HEIGHT IS IN THE ADDRESS
        ANA      MASKB            MASK OUT YAW ERROR
        ALS      18               SCALE IT B17
        STO      JHITE            HEIGHT IN KILOMETERS
        CLA      LOC              1-27-67 RAS
        ANA      =0000000077777   1-27-67 RAS
        ADD      =7835            1-27-67 RAS
        STA      *+1              1-27-67 RAS
        CLA      **               1-27-67 RAS
        ARS      18               1-27-67 RAS
        ORA      =0230000000000   1-27-67 RAS
        FAD*     *-1              1-27-67 RAS
        STO      GHA              1-27-67 RAS
        CLA      LOC              1-27-67 RAS
        ANA      =0000000077777   1-27-67 RAS
        ADD      =7835            1-27-67 RAS
        STA      *+1              1-27-67 RAS
        CLA      **               1-27-67 RAS
        ANA      =0000000077777   1-27-67 RAS
        ORA      =0230000000000   1-27-67 RAS
        FAD*     *-1              1-27-67 RAS
        FSB      =90.             1-27-67 RAS
        STO      SDEC             1-27-67 RAS
        CLA*     1,4               WHICH IS TAGGED WITH XR1
        STO      MRATE           PUT INPUTS TO SUB IN PROPER LOCS
        CLA*     2,4
        STO      FREQ
        CLA*     3,4
```

```
         STC     BLCCK
         CLA*    4,4
         STC     SWREC
         CLA*    5,4
         STO     ANPT
         ALS     18
         STD     IN2             STORE NO. OF ANCH POINTS IN CALL SEQS BELOW
         STD     IN4
         STD     IN6
         STD     IN8
         CLA     6,4             DET. 1ST LOC OF ANCHOR LONG. TABLE AND
         SUB     =100835            STORE IN CALL SEQS BELOW
         STA     IN3
         STA     IN7
         STA     LONATB          SET LOC OF 1ST ANCHOR NADIR ANGLE IN LONG.
*                                       TABLE
         STA     LONTBL
         ADD     =2835
         STA     LONTBX
         SUB     =1835            2-15-67 RAS
         STA     LONTAB
         STA     LONTST          SAVE 1ST ANCHOR LONG. LOC
         CLA     6,4             DET. 1ST LOC OF ANCHOR LAT. TABLE AND
         SUB     =200835           STORE IN CALL SEQS BELOW
         STA     IN1
         STA     IN5
         STA     LATATB          SET LOC OF 1ST ANCHOR NADIR ANGLE IN LAT.
*                                    TABLE
         ADD     =1835
         STA     LATTAB
         STA     LATST           SAVE 1ST ANCHOR LAT. LOC
         CLA*    7,4
         STO     WRDAT
         CLA*    8,4             STORE CHAN(IE, SENSOR ) NUMBER
         ANA     MASKA
         ARS     18
         STO     KCHAN
         SUB     =1
         STO     KCHAN1          CHAN MINUS 1
         CLA*    9,4              1-27-67 RAS
         STO     WSTAR            1-27-67 RAS
         CLA*    10,4
         ANA     MASKA
         ARS     18
         SUB     =1
         STC     KCHAN2
         CLA*    11,4
         STO     JSZAL
CN       AXT     0,1              1-27-67 RAS
         CLA     ANPT            PUT NO. OF ANCHOR POINTS IN XR2
         PAX     0,2
RDOC2    CLA*    RDATA           BEGIN LOOP TO PUT ANCHOR NADIR ANGLES IN
         CALL    FXFLO
         PZE     29
         HTR     *
         STO*    LONATB
         STO*    LATATB
         CLA     LONATB
         ADD     =2835
         STO     LONATB
```

```
        CLA     LATATB
        ADD     =2835
        STO     LATATB
        TXI     *+1,1,-1
        TIX     RDOC2,2,1       LOOP BACK UNTIL ALL NADIR ANGLES ARE USED
        CLA     RCATA
        ADD     ANPT
        STO     RDATA
        AXT     0,1
BEGIN   CLA     WRDAT
        TZE     NHDR
        CALL    HEAD
NHDR    CLA     ANPT            BEGIN LOOP TO UNPACK NEXT SWATH
        PAX     0,2             PUT NO. OF ANCHOR POINTS IN XR2
        CLA*    RCATA
        ANA     MASKB
        TZE     INTERP+1        RETURN TO MAIN PROG IF LAST FILLED SWATH OF
        STO     POP               LAST REC IS REACHED
        LRS     1               CALCU NO WDS IN SENSOR BLOCK
        RND
        STO     SBLK
        CLA     POP
        CALL    FXFLO
        PZE     35
        HTR     *
        FAD     =1.0
        STO     SN1
        TXI     *+1,1,-2        SKIP ONE SWATH WORD
MKTAB   CLA*    RDATA           BEGIN LOOP TO FORM ANCH LAT AND LONG TABLE
        ANA     MASKA
        CALL    FXFLO
        PZE     11
        HTR     *
        STO*    LATTAB
        CLA     LATTAB
        ADD     =2835
        STO     LATTAB
        CLA*    RCATA
        ANA     MASKB
        CALL    FXFLO
        PZE     29
        HTR     *
        STO*    LONTAB
        CLA     LCNTAB
        ADD     =2835
        STO     LONTAB
        TXI     *+1,1,-1
        TIX     MKTAB,2,1       LOOP BACK UNTIL ANCH LAT AND LONG TAB. DONE
        SXA     SAVE,1
        OCT     076000000016    2-13-67 RAS
        AXT     1,1             2-13-67 RAS
        CLA     RDATA
        STA     RCATA2
        CLA     ANPT            2-13-67 RAS
        STA     GCAT            2-13-67 RAS
GCAT    AXT     **,7            2-13-67 RAS
GCPHER  TNX     MK7,7,1         2-13-67 RAS
        TXI     *+1,1,-2        2-13-67 RAS
GNU     CLA*    LONTBL          2-13-67 RAS
        FSB*    LCNTBX          2-13-67 RAS
```

```
        LAS     =180.           2-13-67 RAS
        TRA     HOUND           2-13-67 RAS
        TRA     HOUND           2-13-67 RAS
        TRA     GOPHER          2-13-67 RAS
HOUND   TMI     HORSE           2-13-67 RAS
        CLA*    LONTBX          2-13-67 RAS
        FAD     =360.           2-13-67 RAS
        STO*    LONTBX          2-13-67 RAS
        TRA     GNU             2-13-67 RAS
HORSE   SCD     *+2,7           2-13-67 RAS
        LXA     GOAT,5          2-13-67 RAS
        TXI     *+1,5,**        2-13-67 RAS
        SXA     IMPALA,1        2-13-67 RAS
APE     CLA*    LONTBL          2-13-67 RAS
        FAD     =360.           2-13-67 RAS
        STO*    LONTBL          2-13-67 RAS
        TXI     *+1,1,2         2-13-67 RAS
        TIX     APE,5,1         2-13-67 RAS
IMPALA  AXT     **,1            2-13-67 RAS
        TRA     GNU             2-13-67 RAS
 MK7    NOP
        LXA     SAVE,1          2-13-67 RAS
        LXA     SAVE,7
        LDQ     SBLK
        MPY     KCHAN1
        STO     TEMP1
        PCA     ,1
        ADD     TEMP1
        PAC     ,1
        STZ     SPOTK     INITIALIZE SWATH POINT
        CLA     POP             PUT DATA POPULATION FOR SWATH IN XR2
        PAX     0,2
        LDQ     SBLK
        MPY     KCHAN2
        STO     TEMP1
        PCA     ,7
        ADD     TEMP1
        PAC     ,7
 INTR   CLA     SPOTK           BEGIN LOOP TO ACCUM. PHYS DATA ACC. SWATH
        FAD     =1.0              POINT GEOG. LOCATION
        STO     SPOTK           SELECT NEXT SWATH POINT
        CALL    COMPA,MRATE,FREQ,SPOTK,SN1,NADA   CALC SWATH POINT NADIR
        CLA     NADA
        SSP
        CAS     NADR
        TRA     JUMA
        TRA     INO1
        TRA     INO1
 INO1   CLA*    RDATA
        ANA     =077777000000 11-15-67 R.A.S.
        TMI     JUMA
        CALL    FXFLO
        PZE     14
        PXD     ,0
        STO     DATA
        CAS     =171.
        TRA     *+3
        TRA     JUMA
        TRA     JUMA
        CLA*    RDATA2
```

```
        ANA     =0777777000000 11-15-67 R.A.S.
        TMI     JUMA
        TZE     JUMA
        CALL    FXFLO
        PZE     14
        PXD     ,0
        STO     DATA2
        CLA     NADA
        CALL    TIN1            CALC. LAT. OF SWATH POINT
IN1     PZE     **
IN2     PZE     3,0,**
        FSB     =90.0           SUBTRACT 90 DEG FROM LAT.
        STO     LATX
        CLA     NADA
        CALL    TIN1            CALC. LONG. OF SWATH POINT
IN3     PZE     **
IN4     PZE     1,0,**
        CAS     =360.0          CORRECT LONG. IF OVER 360 DEG
        TRA     IN4A
        TRA     IN4B
        TRA     IN4B
IN4A    FSB     =360.0
        TRA     IN4+1
IN4B    STO     LONX
        TPL     *+3
        FAD     K360
        STO     LONX
        CLA     KCHAN2
        CAS     =4835
        HTR
        TRA     *+2
        TRA     NOT5
        CALL    N2C5R,WSTAR,C5K,DATA2,LATX,LONX,SDEC,GHA,JSZAL
        CLA     DATA2
        CAS     DISCRM
        TRA     JUMA
        TRA     JUMA
        TRA     Z1
NOT5    CLA     DATA2
        CAS     DISCRM
        TRA     Z1
        TRA     JUMA
        TRA     JUMA
Z1      TZE     JUMA
        CLA     WRDAT
        TZE     JUM1
        CALL    WRITE,SPOTK,NADA,LATX,LONX,DATA,DATA2
JUM1    CLA     CATNN
        STO     CATN
        CLA     DD
        STO     D
        CALL    MGRID,CON1,LONX,CATN,CATS,LATX,D,E,XI,YJ,ZERO
        CLA     ZERO
        TNZ     JUMA
        CALL    SST,XI,YJ,E,DATA,GRIDI,NGATE
JUMA    TIX     *+2,2,1
        TRA     IN9
        CLA     SPOTK           SELECT NEXT SWATH POINT AND ACCUM. AS ABOVE
```

```
        FAD     =1.
        STO     SPCTK
        CALL    COMPA,MRATE,FREQ,SPOTK,SN1,NADA
        CLA     NADA
        SSP
        CAS     NADR
        TRA     JUMB
        TRA     IN02
        TRA     IN02
IN02    CLA*    RDATA
        ALS     18                  11-15-67 R.A.S.
        ANA     =C777777000000 11-15-67 R.A.S.
        TMI     JUMB
        CALL    FXFLO
        PZE     14                  11-15-67 R.A.S.
        PXD     ,0
        STO     DATA
        CAS     =171.
        TRA     *+3
        TRA     JUMB
        TRA     JUMB
        CLA*    RDATA2
        ALS     18
        ANA     =0777777000000 11-15-67 R.A.S.
        TMI     JUMB
        TZE     JUMB
        CALL    FXFLO
        PZE     14
        PXD     ,0
        STO     DATA2
        CLA     NADA
        CALL    TIN1
IN5     PZE     **
IN6     PZE     3,0,**
        FSB     =90.0
        STO     LATX
        CLA     NADA
        CALL    TIN1
IN7     PZE     **
IN8     PZE     1,0,**
        CAS     =360.0
        TRA     IN8A
        TRA     IN8B
        TRA     IN8B
IN8A    FSB     =360.0
        TRA     IN8+1
IN8B    STO     LONX
        TPL     *+2
        FAD     K360
        STO     LONX
        CLA     KCHAN2
        CAS     =4835
        HTR
        TRA     *+2
        TRA     NOTSB
        CALL    N2C5R,WSTAR,C5K,DATA2,LATX,LONX,SDEC,GHA,JSZAL
        CLA     DATA2
        CAS     DISCRM
        TRA     JUMB
        TRA     JUMB
        TRA     Z2
```

```
NOTSE  CLA     DATA2
       CAS     DISCRM
       TRA     Z2
       TRA     JUMB
       TRA     JUMB
Z2     TZE     JUMB
       CLA     WRCAT
       TZE     JUM2
       CALL    WRITE,SPCTK,NADA,LATX,LONX,DATA,DATA2
JUM2   CLA     CATNN
       STO     CATN
       CLA     DD
       STO     D
       CALL    MGRID,CON1,LONX,CATN,CATS,LATX,D,E,XI,YJ,ZERO
       CLA     ZERO
       TNZ     JUMB
       CALL    SST,XI,YJ,E,DATA,GRIDI,NGATE
JUMB   TXI     *+1,7,-1
       TXI     *+1,1,-1        MOVE TO NEXT WORD OF SWATH
       TIX     INTR,2,1        RETURN TILL ALL POINTS IN SENSOR GROUP DONE
IN9    OCT     -076000000016
       CLA     SWREC           COUNT ONE SWATH COMPLETED AT LOOP FINISH
       SUB     =1835
       STO     SWREC
       TZE     INTERP+1        RETURN TO MAIN PR. IF ALL SWATHS DONE
       CLA     RDATA           PUT LOC OF 1ST WORD OF NEXT SWATH IN LOC
       ADD     BLOCK             RDATA WHICH IS TAGGED WITH XR1
       STA     RDATA
       AXT     0,1             ZERO XR1
       CLA     LATST           RE-SET LOCS FOR INITIAL ENTRYS IN ANCH LAT
       STA     LATTAB            AND LONG TABLE
       CLA     LONTST
       STA     LONTAB
       TRA     BEGIN           LOOP BACK UNTIL ALL SWATHS OF REC ARE PROC.
LONATB PZE     0
LATATB PZE     0
 WRCAT PZE     0
 LATST PZE     0
LONTST PZE     0
 MRATE PZE     0
 FREQ  PZE     0
 BLOCK PZE     0
 SWREC PZE     0
 ANPT  PZE     0
 KCHAN PZE     0          CHAN NO 1-5
KCHAN1 PZE     0
KCHAN2 PZE     0
 SBLK  PZE     0               WORD SIZE OF SENSOR BLOCK
LONTAB PZE     0
LATTAB PZE     0
 RDATA PZE     0,1
RDATA2 PZE     0,7
 MASKB OCT     000000077777
 SN1   PZE     0
 MASKA OCT     077777000000
 FOF   PZE     0
 SPOTK PZE     0
 DATA  PZE     0
```

```
 DATA2 PZE     0
 LATX  PZE     0
 LCNX  PZE     0
 NADA  PZE     0
 TWO   DEC     2
 IMASK OCT     777777
 LOC   PZE     0,1
 LOC1  PZE     0,1
 ONEF  DEC     1.0
 TEMP1 BSS     1
 TEMP2 BSS     1
LONTEL PZE     0,1
LONTBX PZE     0,1
 SAVE  PZE     0
JSZAL  PZE     0                2-6-67 RAS
CSK    DEC     1.               1-27-67 RAS
WSTAR  PZE     0                1-27-67 RAS
SDEC   PZE     0                1-27-67 RAS
GHA    PZE     0                1-27-67 RAS
 CON1  PZE     0
 CON   PZE     0
 CATN  PZE     0
 CATNN PZE     0
 CATS  PZE     0
 CAT   PZE     0
 C     PZE     0
 CD    PZE     0
 E     PZE     0
 XI    PZE     0
 YJ    PZE     0
 ZERO  PZE     0
 K360  DEC     360.
 NADR  BSS     1
 JHITE PZE     0
DISCRM PZE     0
CUTOFW PZE     0
CUTOFC PZE     0
 MAP   PZE     0
 GRIDI PZE     0
 NGATE PZE     0
 INK   BSS     1
OUTPUT TRA     *+5
        AXT    0,4
        AXT    0,2
        AXT    0,1
        TRA    1,4
        SXA    *-4,4
        SXA    *-4,2
        SXA    *-4,1
        CLA    =3817
        STO    NGATE
        CALL   SST,XI,YJ,E,DATA,GRIDI,NGATE
        CLA    MAP
        CAS    =2817
        TRA    *+3
        TRA    *+2
        TRA    JHW
        CLA    =4817
        STO    NGATE
```

```
      CALL    SST,XI,YJ,E,DATA,GRIDI,NGATE
JHW   CLA     =5B17
      STC     NGATE
      CLA     CUTOFW
      STO     XI
      CLA     CUTOFC
      STC     YJ
      CALL    SST,XI,YJ,E,DATA,GRIDI,NGATE
      TRA     OUTPUT+1
IBLK  TRA     *+5
      AXT     0,4
      AXT     0,2
      AXT     0,1
      TRA     2,4
      SXA     *-4,4
      SXA     *-4,2
      SXA     *-4,1
      XEC     IBLK+1
      CLA     INK
      STO*    1,4
      TRA     IBLK+1
      END
```

SUBROUTINE TO COMPUTE CHANNEL 5 REFLECTANCE FOR NIMBUS

```
      SUBROUTINE N2C5R(WSTAR,C5K,DATA,PLAT,PLON,SDEC,SLON,JSZAL)
      DIMENSION CLIM(15)
      SZAL=JSZAL
      CLIM(15)=COSF(SZAL*.01745329)
      COSZEN=COSF(PLAT*0.01745329)*COSF(SDEC*0.01745329)*COSF((SLON-PLON
     1)*0.01745329)+SINF(PLAT*0.01745329)*SINF(SDEC*0.01745329)
      IF(COSZEN-CLIM(15))10,20,20
   10 DATA=0.
      RETURN
   20 REFL=(C5K*DATA)/(WSTAR*COSZEN)
      DATA=REFL*100.
      RETURN
      END(0,1,0,1,0,0,1,1,0,1,0,0,0,0,0)
```

A.3 Subroutines Common To HRIR and MRIR

```
      SUBROUTINE SST(XJJ,YII,BRL,DATA,GRIDI,NGATE)

      SUBROUTINE SST(XJJ,YII,BRL,DATA,GRIDI,NGATE)
      DIMENSION ITABZ(3),NCODE(13),IOUT(26),NCARD(77),ARAMAP(104,77),ARA
     1POP(104,77)
      NBRL=BRL+1.
      GO TO(71,72,73,74,75),NGATE
C                ZERO OUT MAPS
   71 DO 3 I=1,104
      DO 3 J=1,77
      ARAMAP(I,J)=0.
    3 ARAPOP(I,J)=0.
      RETURN
C                ADD DATA TO MAP
   72 J=0
      IF(XJJ)56,57,53
   53 J=(XJJ+.5)
   57 J=NBRL-J
      IF(J)56,54,55
   54 J=1
   55 I=YII+1.5
      IF(I)56,1,2
    1 I=1
    2 ARAMAP(I,J)=ARAMAP(I,J)+DATA
      ARAPOP(I,J)=ARAPOP(I,J)+1.0
   56 RETURN
C                DIVIDE DATA FOR AVERAGE
   73 IGRID=GRIDI+1.
      IF(IGRID-104)556,556,555
  555 IGRID = 104
  556 DO 6 I=1,IGRID
      DO 6 J=1,NBRL
      IF(ARAPOP(I,J))6,6,5
    5 ARAMAP(I,J)=ARAMAP(I,J)/ARAPOP(I,J)+.5
    6 CONTINUE
      RETURN
C                OUTPUT MAPS ON PRINTER PAPER
   74 II=1
      IF(NBRL-26)7,7,8
    7 ITABZ(1)=NBRL
      GO TO 11
    8 II=II+1
      ITABZ(1)=26
      IF(NBRL-52)9,9,10
    9 ITABZ(2)=NBRL
      GO TO 11
   10 II=II+1
      ITABZ(2)=52
      ITABZ(3)=NBRL
   11 DO 17 II2=1,2
      N=-25
      DO 17 III=1,II
      WRITE OUTPUT TAPE 3,300
  300 FORMAT(1H1)
      N=N+26
      M=ITABZ(III)
      DO 16 I=1,IGRID
      IJ=0
```

```
      SUBROUTINE SST(XJJ,YII,ERL,DATA,GRIDI,NGATE)

      DO 15 J=N,M
      IJ=IJ+1
      IF(II2-1)13,13,14
   13 IOUT(IJ)=ARAMAP(I,J)
      GO TO 15
   14 IOUT(IJ)=ARAPOP(I,J)
   15 CONTINUE
      WRITE OUTPUT TAPE 3,3301
 3301 FORMAT(1H )
   16 WRITE OUTPUT TAPE 3,301,(IOUT(J),J=1,IJ)
  301 FORMAT(1H0,26(1H+,I4))
   17 CONTINUE
      RETURN
C                OUTPUT MAP CARDS
C                WARMEST TEMP IS IN XJJ-COLDEST IN YII
   75 NCODE(1)=-1
      NCODE(2)=0
      NCODE(3)=4096
      NCODE(4)=8192
      NCODE(5)=12288
      NCODE(6)=16384
      NCODE(7)=20480
      NCODE(8)=24576
      NCODE(9)=28672
      NCODE(10)=32768
      NCODE(11)=36864
      NCODE(12)=65536
      CALL IBLK(ICODE)
      NCODE(13)=ICODE
      SM=10./(XJJ-YII)
      E=-SM*YII
      DO 30 I=1,IGRID
      DO 20 J=1,77
   20 NCARD(J)=NCODE(13)
      DO 27 J=1,77
      IF(ARAMAP(I,J))27,27,21
   21 IF(ARAMAP(I,J)-YII)24,24,22
   22 IF(ARAMAP(I,J)-XJJ)23,25,25
   23 IY=(SM*ARAMAP(I,J)+E)+1.
      GO TO 26
   24 IY=12
      GO TO 26
   25 IY=11
   26 NCARD(J)=NCODE(IY)
   27 CONTINUE
      II=I
      IF(II-99)558,558,557
  557 II=-II+99
  558 WRITE OUTPUT TAPE 3,302,(NCARD(J),J=1,77),II
  302 FORMAT(1X,77A1,1H+,I2)
      WRITE OUTPUT TAPE 8,303,(NCARD(J),J=1,77),II
  303 FORMAT(77A1,1H+,I2)
   30 CONTINUE
      ARAMAP(1,1)=YII
      DO 559 I=2,12
      C=I-2
```

```
      SUBROUTINE SST(XJJ,YII,BRL,DATA,GRIDI,NGATE)

  559 ARAMAP(1,I)=(C-B)/SN
      WRITE OUTPUT TAPE 3,560
      WRITE OUTPUT TAPE 8,560
  560 FORMAT(70H   R12    R11    R0     R1     R2     R3     R4     R5     R6
     1R7     R8     R9)
      WRITE OUTPUT TAPE 3,561,(ARAMAP(1,J),J=1,12)
      WRITE OUTPUT TAPE 8,561,(ARAMAP(1,J),J=1,12)
  561 FORMAT(1H ,12F6.1/)
      RETURN
      END(0,1,0,1,0,0,1,1,0,1,0,0,0,0,0)



      SUBROUTINE COMPA(XMRATE,FREQ,SPCTK,SN1,XNADA)

      SUBROUTINE COMPA(XMRATE,FREQ,SPCTK,SN1,XNADA)
      XNADA=(XMRATE/FREQ)*(SPCTK-SN1/2.)
      RETURN
      END(0,1,0,1,0,0,1,1,0,1,0,0,0,0,0)
```

```
        ENTRY  RRKC
        ENTRY  RRKD1
        ENTRY  LIRPN

FXFLO

 RRKD   TRA    *+5             SUB. TO READ NEXT DATA REC
        AXT    0,4
        AXT    0,2
        AXT    0,1
        TRA    5,4
        SXA    *-4,4
        SXA    *-4,2
        SXA    *-4,1
        TCCB   *
        RTBB   9
        RCHB   GETDA
        TCOB   *
        XEC    RRKD+1
        STZ*   1,4             SET PARAMETER (TEST) TO ZERO IF DATA RECORD
        TRCB   RKD3            READ NORMALLY     TEST FOR TAPE ERROR
        TEFB   RKD4            TEST FOR END OF FILE
 RRKDA  CLA    IRINP           UNPACK RECORD DAY
        ANA    MASKA
        CALL   FXFLO
        PZE    17
        HTR    *
        XEC    RRKD+1
        STO*   2,4
        CLA    IRINP           UNPACK RECORD HOUR
        ANA    MASKB
        CALL   FXFLO
        PZE    35
        HTR    *
        XEC    RRKD+1
        STO*   3,4
        CLA    IRINP+1         UNPACK RECORD MINUTES
        ANA    MASKA
        CALL   FXFLO
        PZE    17
        HTR    *
        XEC    RRKD+1
        STO*   4,4
        TRA    RRKD+1          RETURN TO MAIN PROGRAM
 RKD3   AXT    10,4
        BSRB   9
        RTBB   9
        RCHB   GETDA
        TCOB   *
        TRCB   *+2
        TRA    RRKDA-1
        TIX    RKD3+1,4,1
        XEC    RRKD+1
        CLA    MINUS           SET PARAMETER (TEST) NEGATIVE IF TAPE ERROR
        STO*   1,4             CONTINUES
```

```
        TRA     RRKDA-1         CHECK FOR E O F AND BRING IN REC-MESS. PRIN
RKD4    XEC     RRKD+1          SET PARAMETER (TEST) POS IF END OF FILE
        CLA     L5
        STC*    1,4
        TRA     RRKD+1          RETURN TC MAIN PROGRAM
RRKD1   TRCB    *+1             SUB. TO TURN OFF END OF FILE AND PARITY IN-
        TEFB    *+1             DICATOR
        TRA     1,4             RETURN TC MAIN PROGRAM
LIRPN   PZE     IRINP
MINUS   DEC     -5.0
GETDA   ICRT    IRINP,0,2500
MASKA   OCT     077777000000
MASKE   OCT     000000077777
L5      DEC     5.0
IRINP   BSS     2500
        END
```

```
        ENTRY  MOVFIL
MOVFIL  TRA    *+5
        AXT    **,4
        AXT    **,2
        AXT    **,1
        TRA    3,4
        SXA    *-4,4
        SXA    *-4,2
        SXA    *-4,1
        CLA*   1,4
        TMI    *+8
        TZE    *+7
        CLA*   2,4
        SUB    =1B17
        TRCB   *+1
        TEFB   *+1
        TZE    MOVFIL+1
        TRA    *+2
        CLA*   2,4
        TZE    BACK
        TPL    FWD-1
BACK    SSP
        ADD    =1E17
        PDX    ,2
        BSFB   9
        TIX    BACK+3,2,1
        RTBB   9
        TCOB   *
        TRCB   *+1
        TEFB   *+1
        TRA    MOVFIL+1
        PDX    ,2
FWD     TEFB   *+1
        RTBB   9
        TCOB   *
        TEFB   *+2
        TRA    FWD+1
        TIX    FWD,2,1
        TRCB   *+1
        TEFB   *+1
        TRA    MOVFIL+1
        END
```

```
*       INTERPØLATIØN SUBRØUTINE    TIN1
*       FAP
        CØUNT   101
*       LIST    8
*       SUBRØUTINE TIN1
        ENTRY TIN1
 TIN1   STØ     TIN1+98
        SXD     TIN1+87,1
        SXD     TIN1+88,2
        SXD     TIN1+89,4
        CLA     2,4
        STØ     TIN1+94
        ADD     TIN1+91
        PAX     0,1
        SXD     TIN1+29,1
        ALS     1
        STA     TIN1+95
        CLA     TIN1+94
        ARS     17
        SUB     TIN1+95
        PAX     0,1
        SXD     TIN1+31,1
        ADD     TIN1+95
        PAX     0,1
        ADD     1,4
        STA     TIN1+23
        STA     TIN1+41
        STA     TIN1+43
        CLA     TIN1+98
        CAS     0,1
        TIX     *-1,1,2
        TRA     TIN1+26
        CLA     TIN1+94
        LBT
        TRA     TIN1+41
        TIX     TIN1+31,1,0
        LXD     TIN1+90,1
        TXL.    TIN1+33,1,0
        LXD     TIN1+31,1
        PXD     0,1
        ARS     18
        CHS
        ADD     TIN1+23
        STA     TIN1+54
        ADD     TIN1+91
        STA     TIN1+52
        TRA     TIN1+50
        CLA     0,1
        TXI     TIN1+43,1,2
        FAD     0,1
        LRS     35
        FMP     TIN1+92
        CAS     TIN1+98
        TXI     TIN1+29,1,-1
        TXI     TIN1+29,1,-1
        TXI     TIN1+29,1,-3
        LXD     TIN1+90,2
        LXA     TIN1+95,1
        CLA     0,1
        STØ     CØM+1,2
```

```
        CLA     0,1
        FSB     TIN1+98
        STØ     CØM,2
        TXI     TIN1+58,2,-2
        TIX     TIN1+52,1,2
        CLA     CØM
        STØ     CØM,2
        LXA     TIN1+94,4
        LXD     TIN1+93,2
        TXI     TIN1+64,2,-2
        PXD     0,2
        PDX     0,1
        CLA     CØM+2,1
        FSB     CØM,2
        TZE     TIN1+79
        STØ     TIN1+97
        LDQ     CØM,2
        FMP     CØM+3,1
        STØ     TIN1+96
        LDQ     CØM+2,1
        FMP     CØM+1,2
        FSB     TIN1+96
        FDP     TIN1+97
        STQ     CØM+3,1
        TXI     TIN1+66,1,-2
        CLA     CØM+2,2
        STØ     CØM+2,1
        TIX     TIN1+63,4,1
        CLA     CØM+1,1
        LXD     TIN1+87,1
        LXD     TIN1+88,2
        LXD     TIN1+89,4
        TRA     3,4
        HTR
        HTR
        HTR
        HTR
        HTR     1,0,0
        DEC     .5
        HTR     0,0,2
        HTR
        HTR
        HTR
        HTR
        HTR
        HTR
        PZE
        PZE
CØM     BSS     40
        END
```

```
*       CALLICØTT  FLØFX ANF FXFLØ SUBRØUTINE
*       LIST    8
*       FAP
        CØUNT   43
*       SUBRØUTINE FLØFX AND FXFLØ
        ENTRY FLØFX
        ENTRY FXFLØ
FLØFX   TZE     3,4
        STØ     ARGU
        XCA
        LLS     8
        SSP
        SUB     KØ1
        SUB     1,4
        STA     A
        CLM
        TMI     3,4
        TØV     *+1
A       LLS     **
        TNØ     3,4
        TRA     2,4
FXFLØ   TZE     3,4
        TØV     *+1
        STØ     ARGU
        CLA     KØ2
        ADD     1,4
        STØ     TEMP
        TMI     2,4
        CLA     ARGU
        LRS     27
        TZE     B
        LRS     8
        CLA     TEMP
        ADD     KØ4
        LLS     8
        ALS     19
        TRA     *+3
B       CLA     TEMP
        ALS     27
        STØ     TEMP+1
        TØV     2,4
        CLA     TEMP
        LLS     27
        FAD     TEMP+1
        TNØ     3,4
        TRA     2,4
ARGU    PZE
KØ1     ØCT     135
KØ2     ØCT     170
KØ4     ØCT     10
TEMP    BSS     2
        END
```

```
      SUBROUTINE MGRID(CON1,CON,CATN,CATS,CAT,D,E,XI,YJ,ZERO)
      TRIGF(X,Z)=SINF(X+(Z/2.))/COSF(X+(Z/2.))
      AN=0.01745329*45.0
      CON2=D*E
      IF(CON2-360.)4,2,2
    2 CON=CCN-CON1
      IF(CCN)3,12,12
    3 CON=360.+CON
      GO TO 12
    4 CON2=CCN2+CCN1
    5 IF(CCN2-360.)8,8,6
    6 CON2=CON2-360.
      IF(CON2-CON)7,10,10
    7 IF(CON-CCN1)78,11,11
    8 IF(CON2-CON)78,11,9
    9 IF(CON-CON1)78,11,11
   10 CON=(360.0-CON1)+CON
      GO TO 12
   11 CON=CCN-CON1
   12 XI=CON/D
   13 IF(CATN)58,46,14
   14 IF(CATS)28,26,15
   15 IF(CAT)78,78,16
   16 IF(CATN-CAT)78,18,17
   17 IF(CAT-CATS)78,18,18
   18 CATN=(0.01745329*CATN)
   19 CAT=(0.01745329*CAT)
   20 YN=LOGF(TRIGF(AN,CATN))
   21 Y=LOGF(TRIGF(AN,CAT))
   22 YJ=YN-Y
   24 GO TO 88
   26 IF(CAT)78,18,16
   28 IF(CAT)32,18,30
   30 IF(CATN-CAT)78,18,18
   32 IF(CAT-CATS)78,34,34
   34 CATN=(0.01745329*CATN)
   36 CAT=-1.0*(0.01745329*CAT)
   38 YN=LOGF(TRIGF(AN,CATN))
   40 Y=LOGF(TRIGF(AN,CAT))
   42 YJ=YN+Y
   44 GO TO 88
   46 IF(CATS)48,82,82
   48 IF(CAT)50,96,78
   50 IF(CAT-CATS)78,52,52
   52 CAT=-1.0*(0.01745329*CAT)
   54 YJ=LOGF(TRIGF(AN,CAT))
   56 GO TO 88
   58 IF(CATS)60,82,82
   60 IF(CAT)62,78,78
   62 IF(CATN-CAT)78,66,64
   64 IF(CAT-CATS)78,66,66
   66 CATN=-1.0*(0.01745329*CATN)
   68 CAT=-1.0*(0.01745329*CAT)
   70 YN=LOGF(TRIGF(AN,CATN))
   72 Y=LOGF(TRIGF(AN,CAT))
```

```
74 YJ=Y-YN
76 GO TO 88
78 ZERO=1.0
   RETURN
82 ZERO=1.0
   RETURN
88 D=0.01745329*D
90 YJ=YJ/D
92 ZERO=0.0
94 RETURN
96 YJ=0.0
   GO TO 92
   END(1,1,0,0,1,0,1,1,0,1,0,0,0,0,0)
```